Bimodality in Damped Lyα Systems

Art Wolfe

Collaborators: Hsiao-Wen Chen,

Jason Prochaska & Regina Jorgenson

Lyman Break Galaxies Properties (Stars)

Comoving SFR Density (z=3)

$$\dot{\rho}_* = 10^{-1.5} - 10^{-0.8} M_\odot yr^{-1} Mpc^{-3}$$

Covering Factor (z=[2.5,3.5])

$$f_A \ < \ 10^{-3} \text{ for } R < 27.5$$

Damped Lyα Systems (Neutral Gas)

$$f_A \ = \ 0.33 \text{ for } \mathrm{N(HI)} \geq 2 \times 10^{20} \mathrm{cm}^{-2}$$

Damped Lyα Systems (Neutral Gas)

Comoving SFR Density (z=3)

$$\dot{\rho}_* < \; 10^{-2.7}\ \mathbf{M_{\odot}yr^{-1}Mpc^{-3}}$$

Limit on *in situ* Star Formation from HUDF Survey
(Wolfe & Chen ‘06)

Astrophysical Consequences of upper limit $d\rho^*/dt < 10^{-2.7} M_\odot yr^{-1} Mpc^{-3}$

1. Limit on Metal Production

2. Limit on Gas Heating Rate

Cooling Rates from HIRES profiles

○

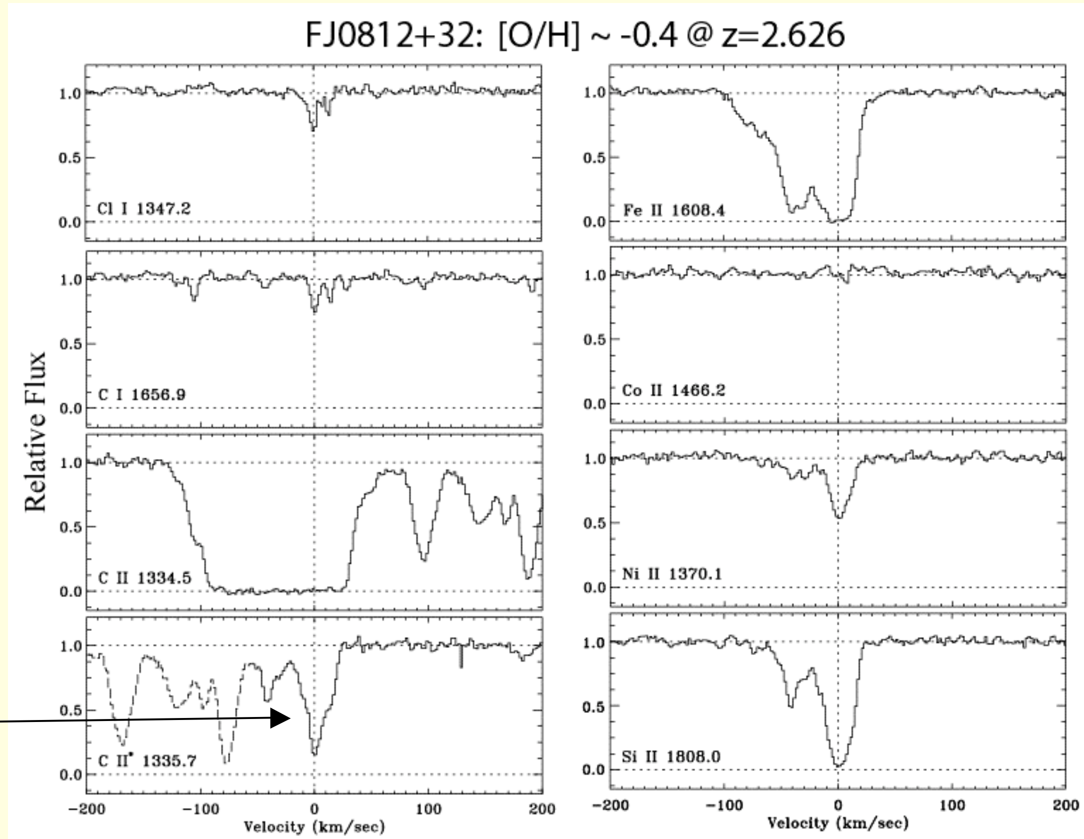

Cooling Rate Indicator

Obtaining Cooling Rates from CII* Absorption

- [C II] 158 micron transition dominates cooling of neutral gas in Galaxy ISM

- Spontaneous emission rate per atom $l_c = n\Lambda_{[CII]}$ obtained from strength of 1335.7 absorption and Lyman alpha absorption

- Thermal balance condition $l_c = \Gamma_{pe}$ gives heating rate per atom

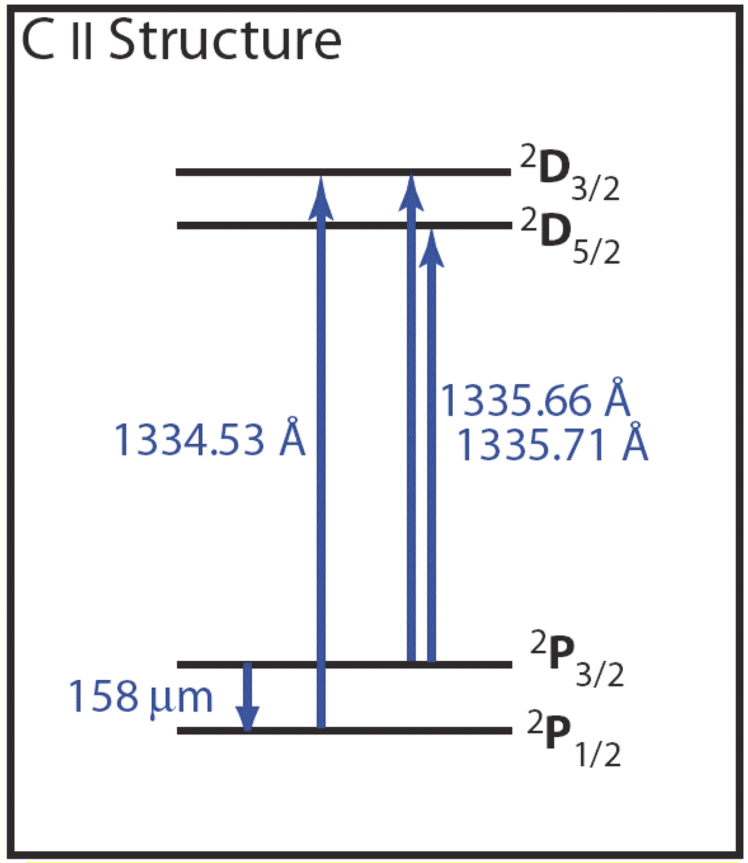

$$l_c = n\Lambda_{[CII]} \sim \frac{N(\mathrm{CII}^*)}{N(\mathrm{HI})} h\nu_{21} A_{21}$$

Two Types of DLAs?

Frequency Distribution of [C II] 158 μm Cooling Rates

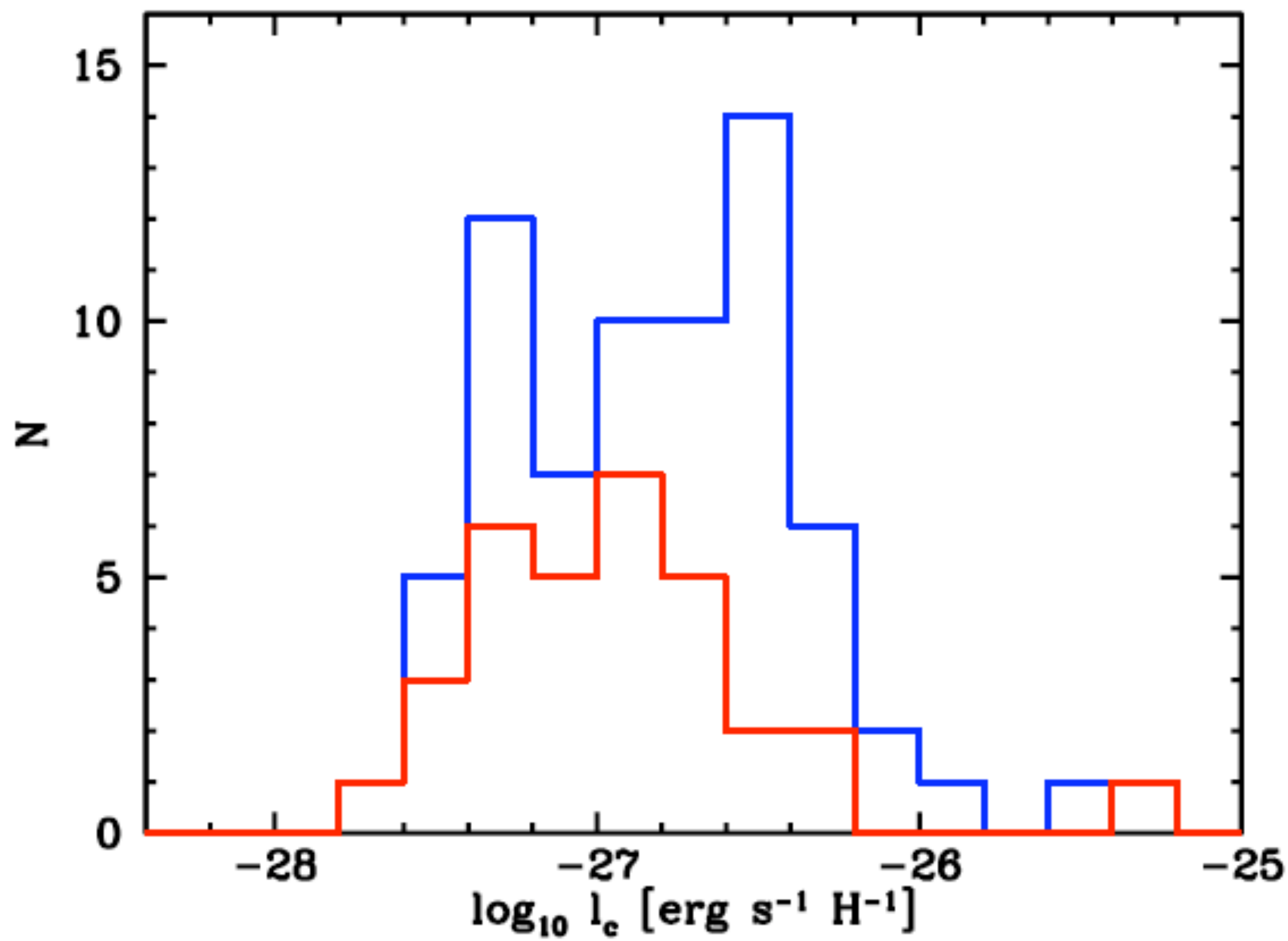

Frequency Distribution of [C II] 158 μm Cooling Rates

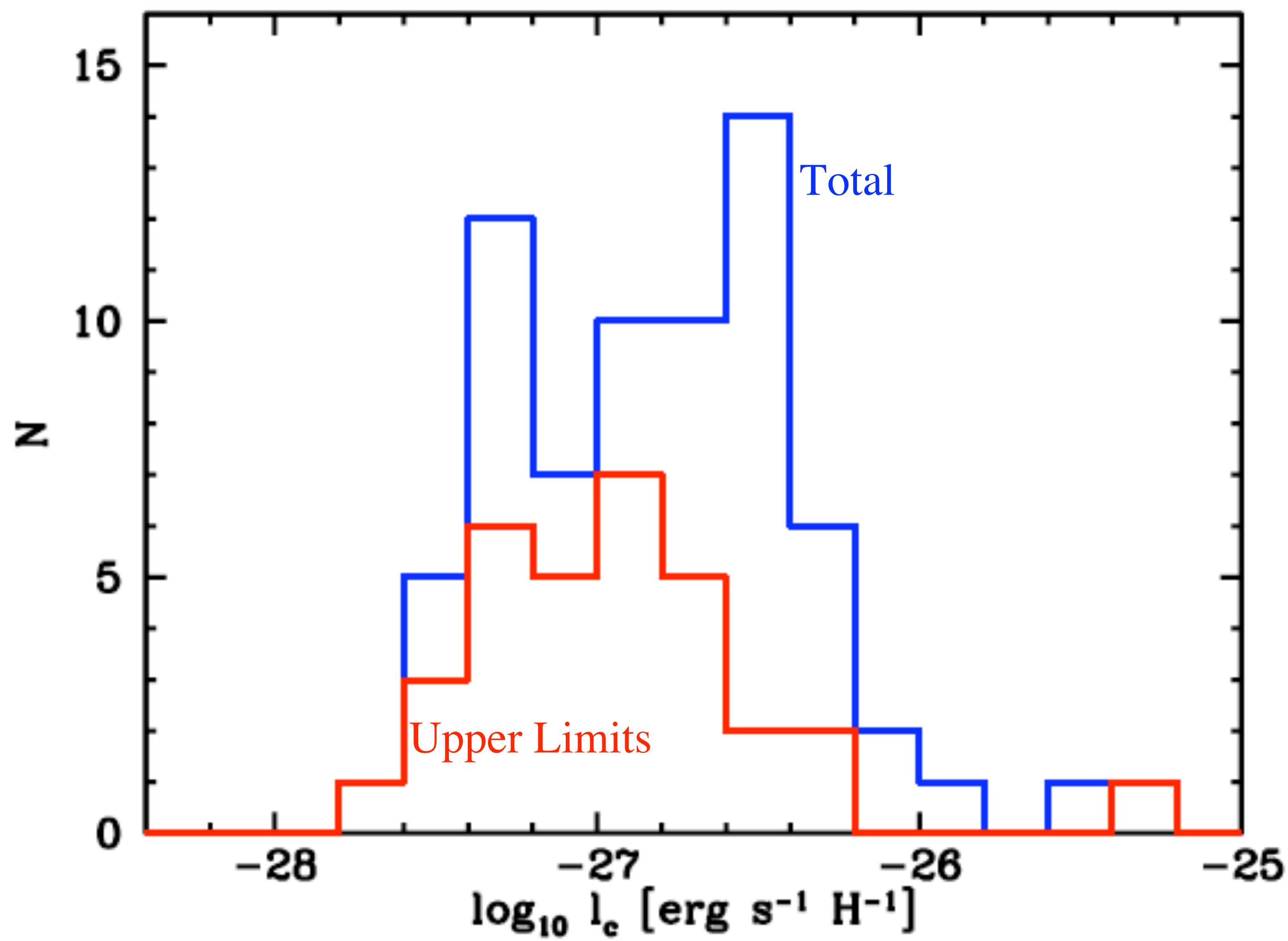

Frequency Distribution of [C II] 158 μm Cooling Rates

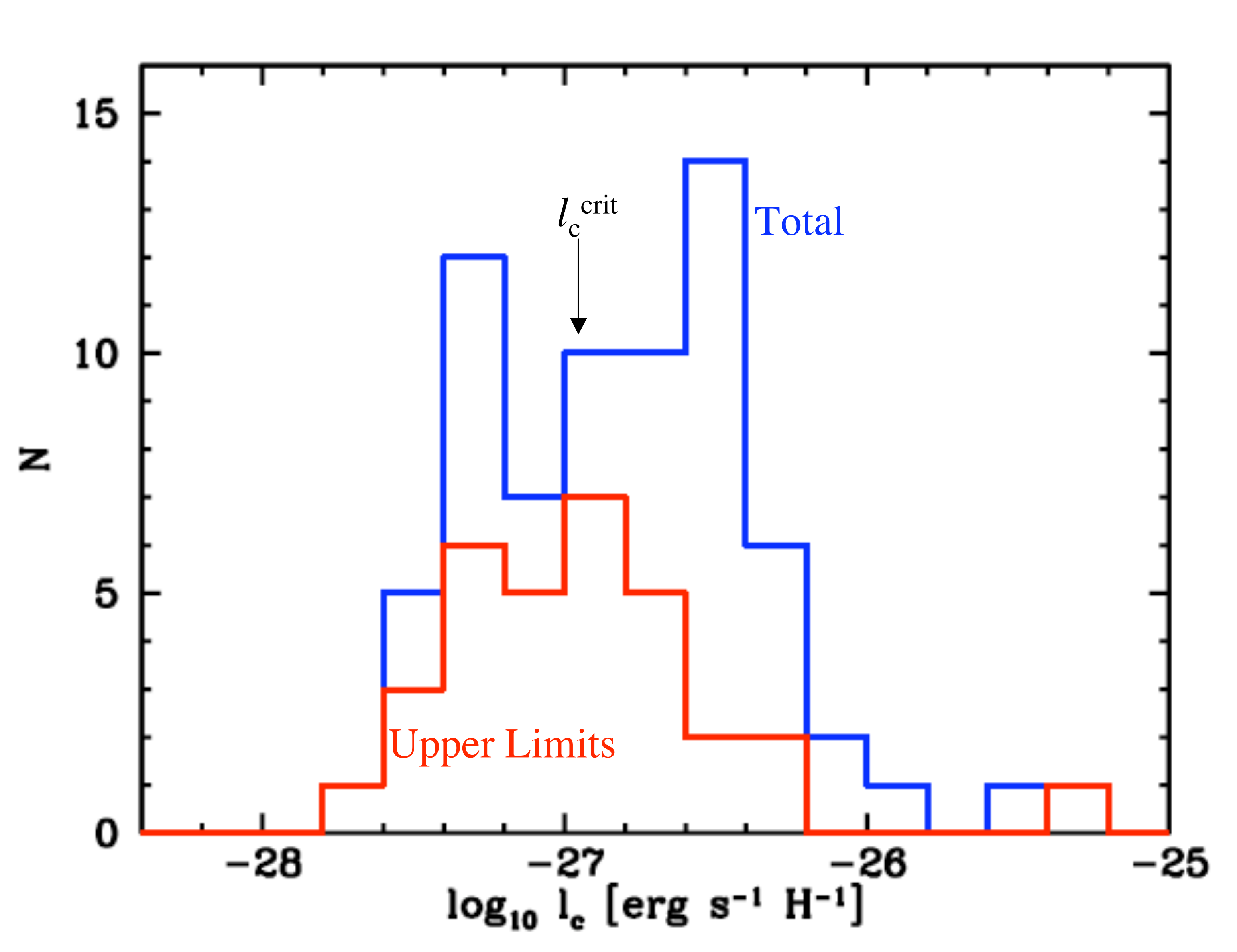

Velocity Interval Distribution

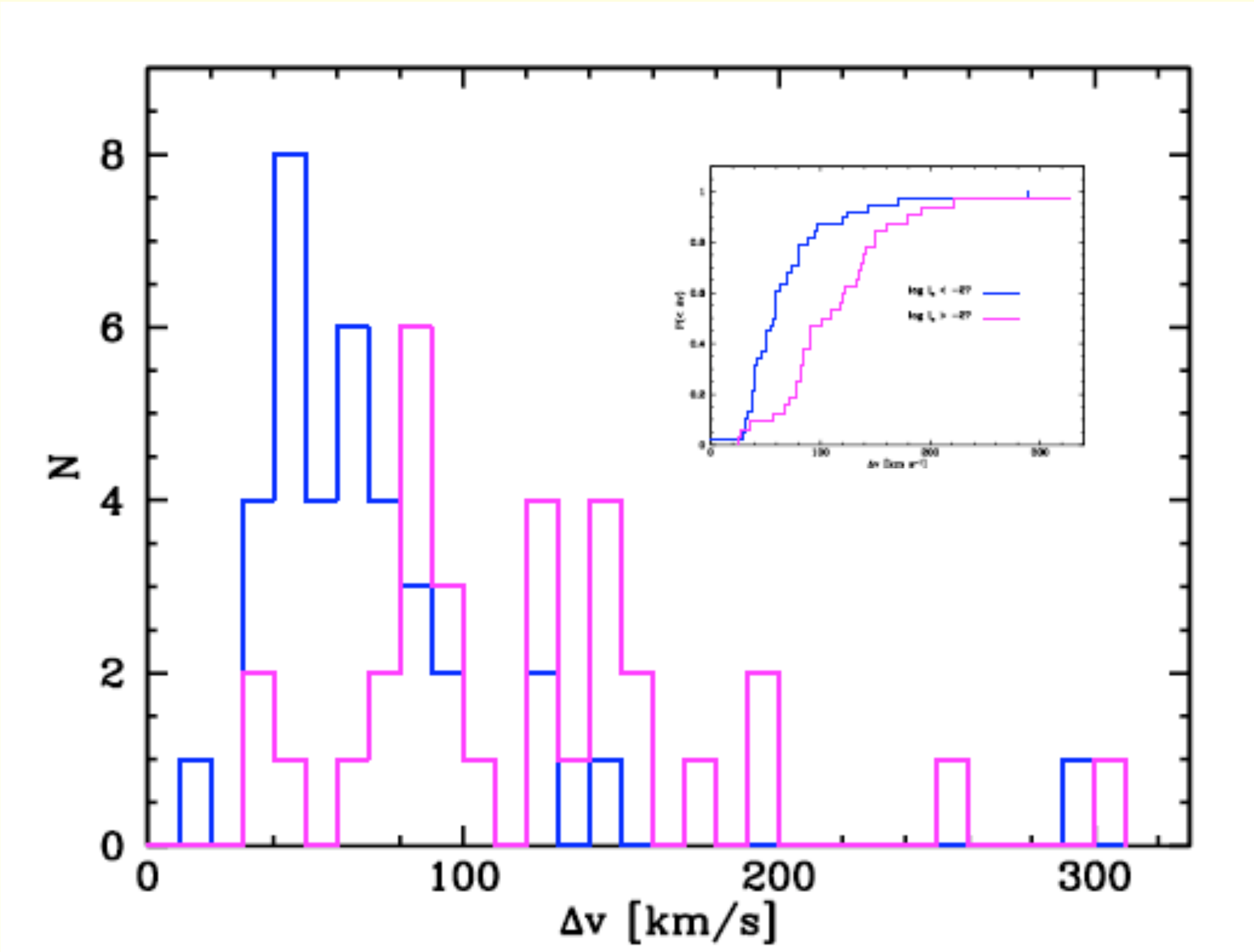

Distribution of Metalicities

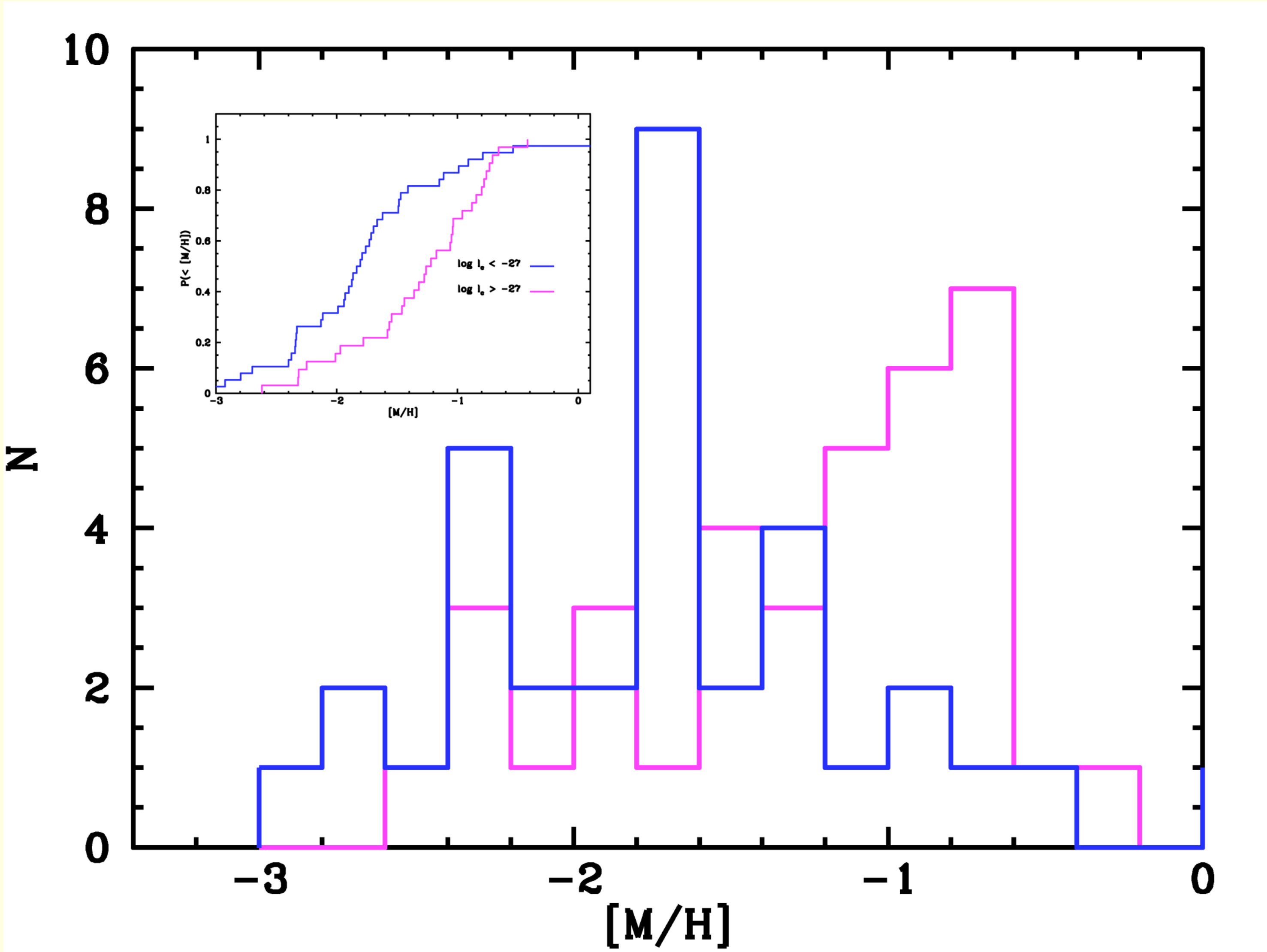

Distribution of Dust-to-Gas Ratios

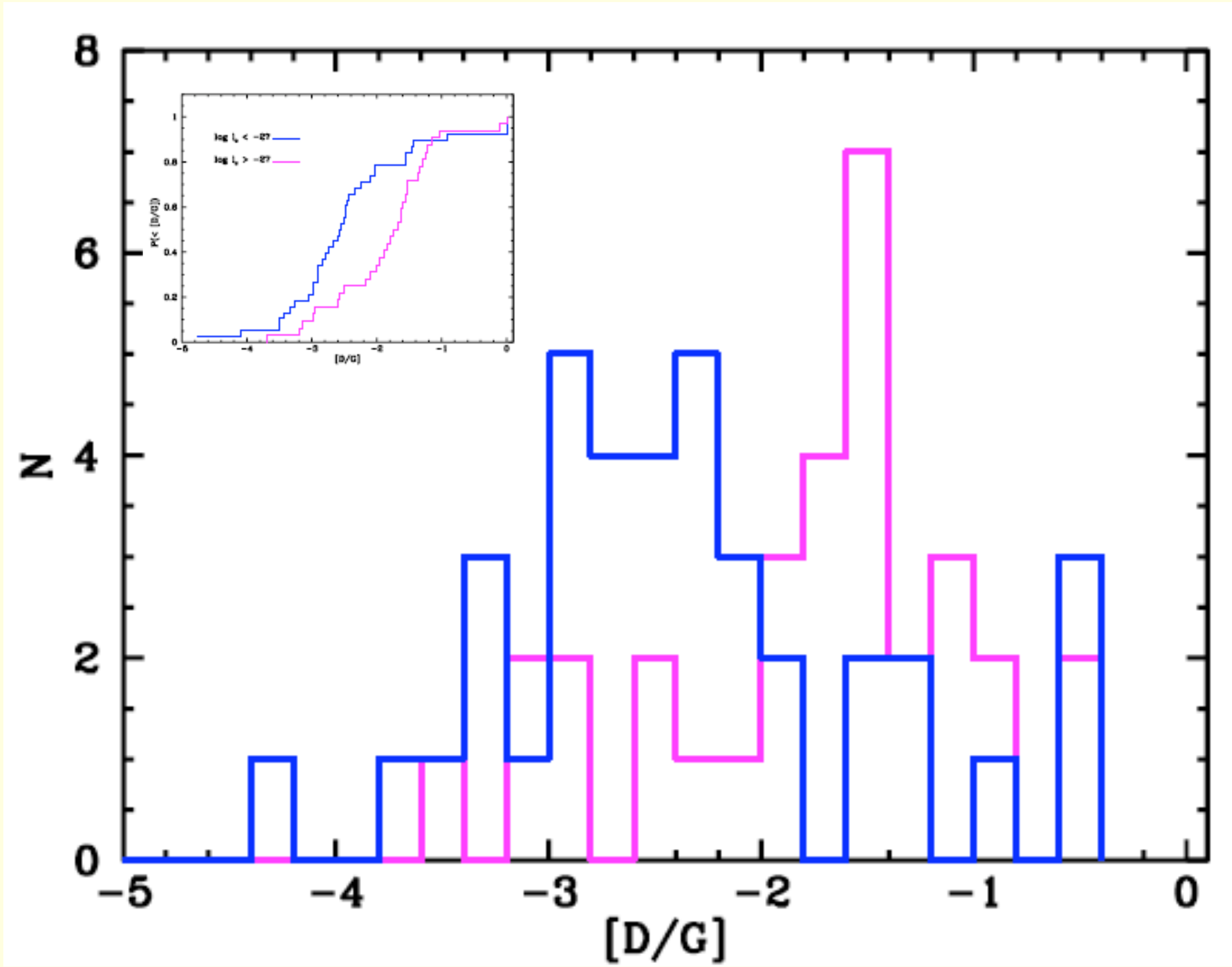

Distribution of H I Column Densities

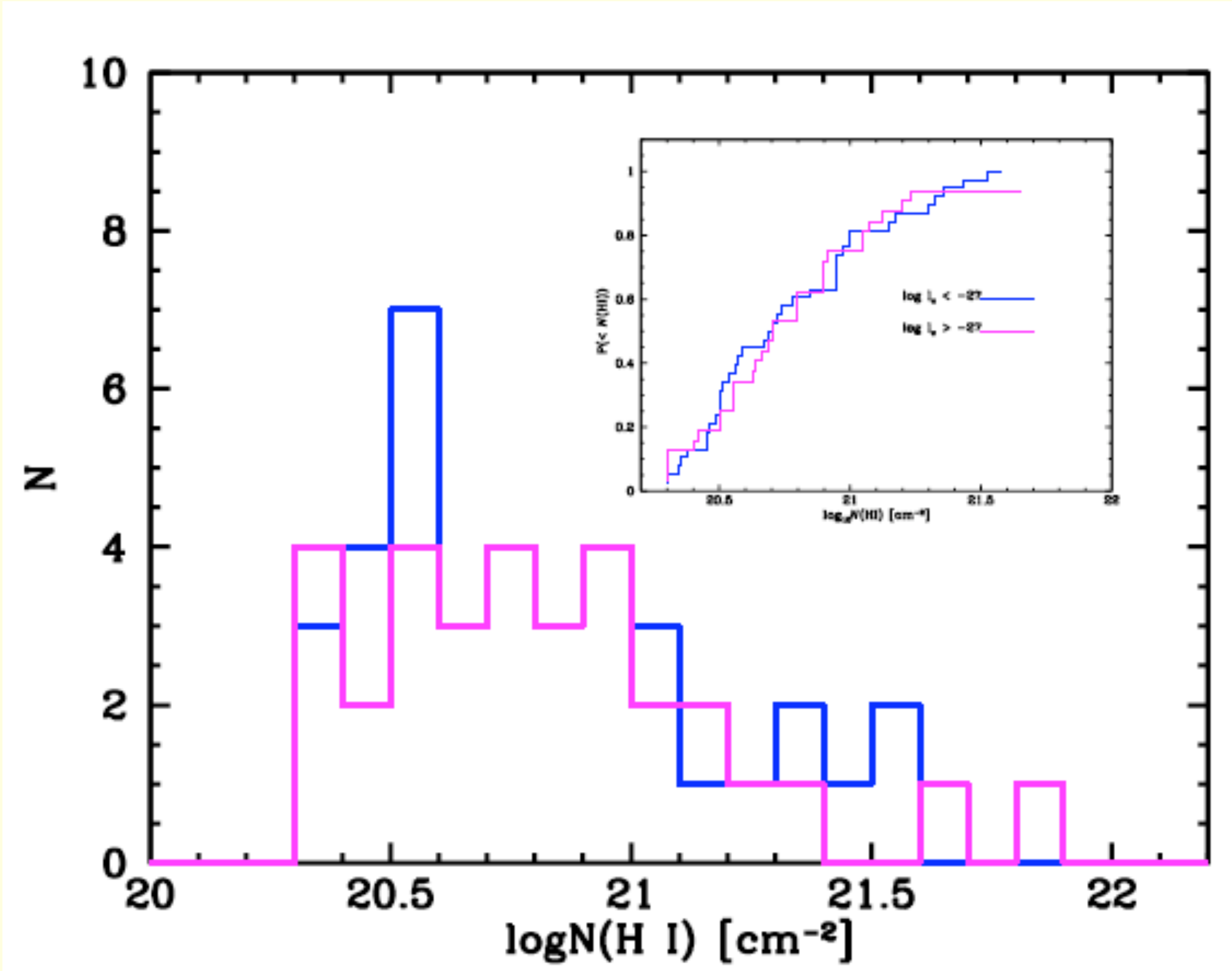

Physical Interpretation of two DLA populations

1. DLAs with $l_c \leq 10^{-27}$ ergs $s^{-1}H^{-1}$

WNM gas heated by X-ray and
FUV Background Radiation

Frequency Distribution of [C II] 158 μm Cooling Rates

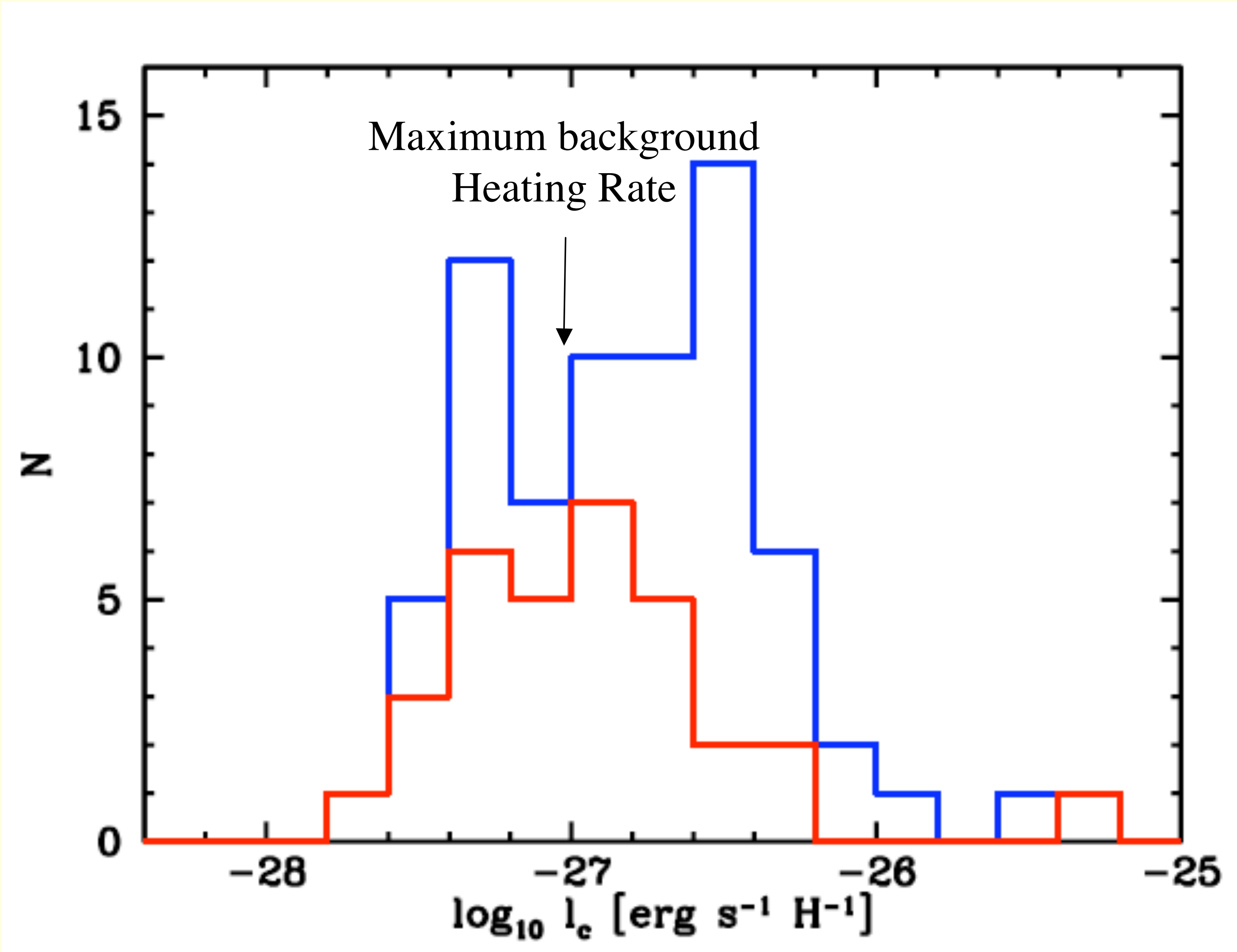

Physical Interpretation of two DLA populations

2. DLAs with $l_c > 10^{-27}$ ergs $s^{-1}H^{-1}$

CNM gas heated by FUV Radiation
Emitted by LBGs embedded in
DLAs

Can *in situ* star formation in DLAs balance cooling in DLAs with $l_c > 10^{-27}$ ergs s^{-1}H^{-1} ?

-[C II] 158 μm cooling rate $\mathcal{C}=(2.0\pm0.5)\times10^{38}$ ergs s^{-1} Mpc^{-3}

-Grain photoelectric heating $\propto d\rho_*/dt$

-Predicted comoving heating rate: $\mathcal{H}_{DLA}<2\times10^{37}$ergs s^{-1} Mpc^{-3}

-External energy input required

LBG-DLA Configuration for $l_c > 10^{-27}$ ergs s^{-1} H^{-1}

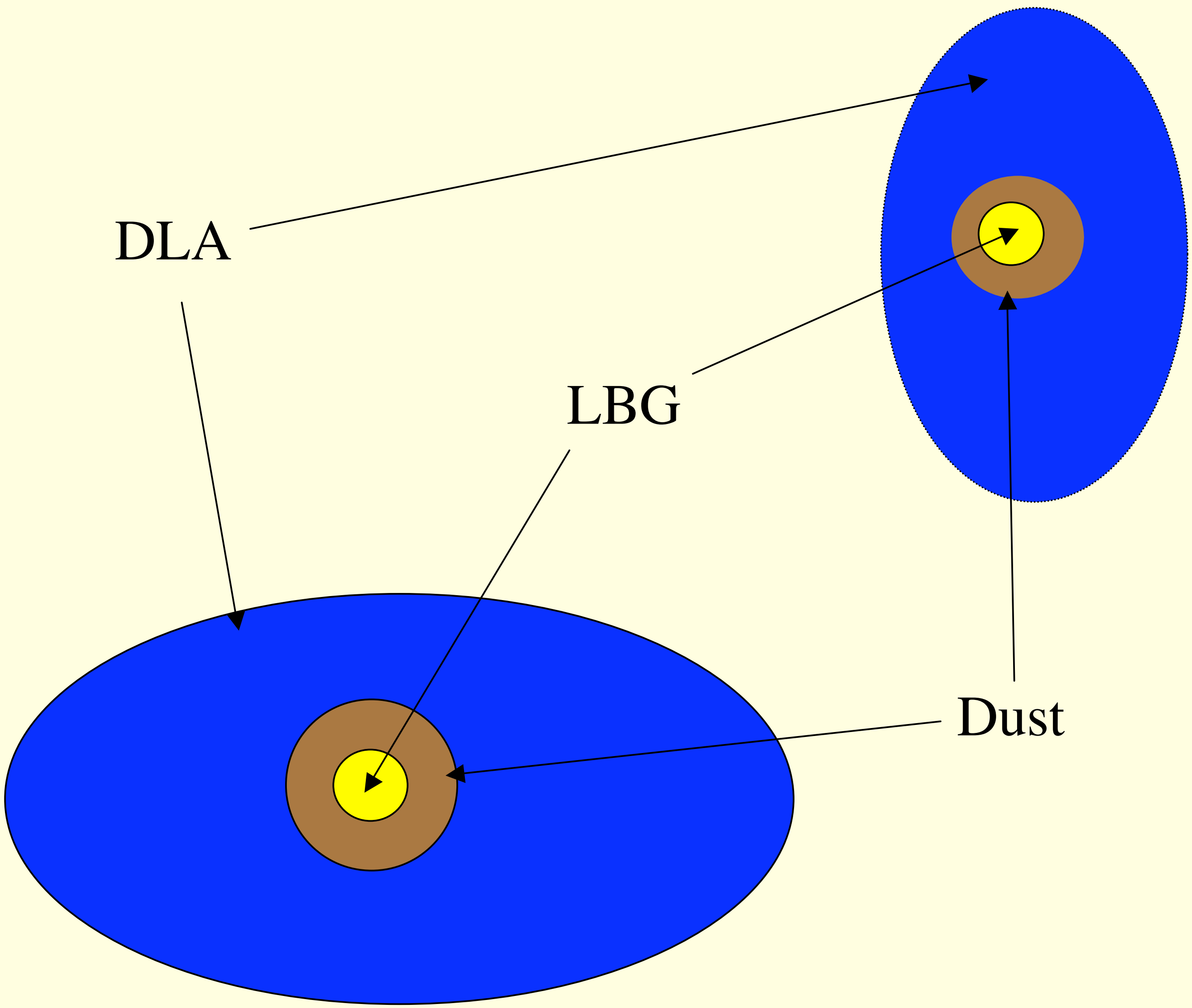

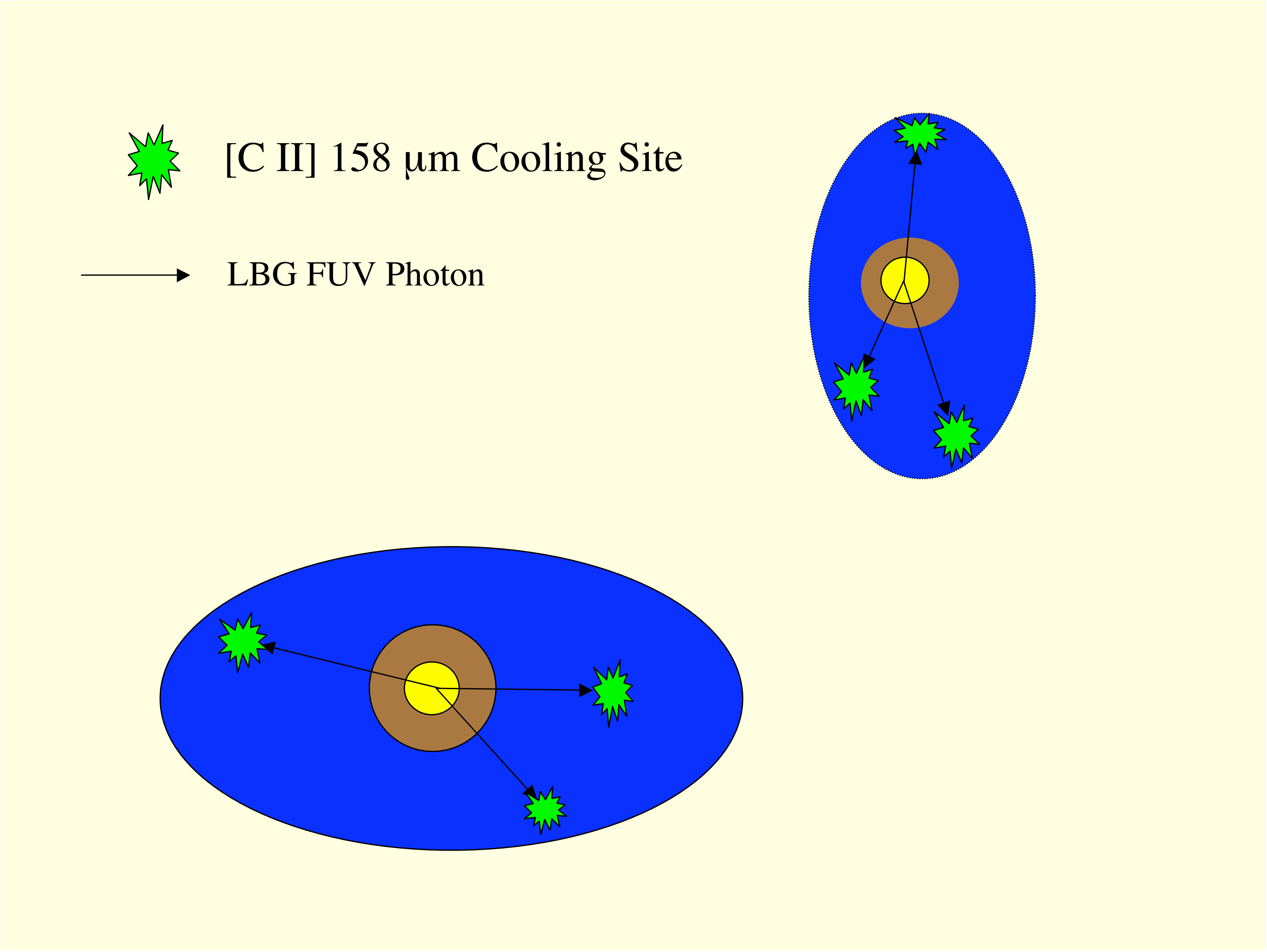
[C II] 158 μm Cooling Site
LBG FUV Photon

An LBG associated with a DLA (Moller etal ‘02)

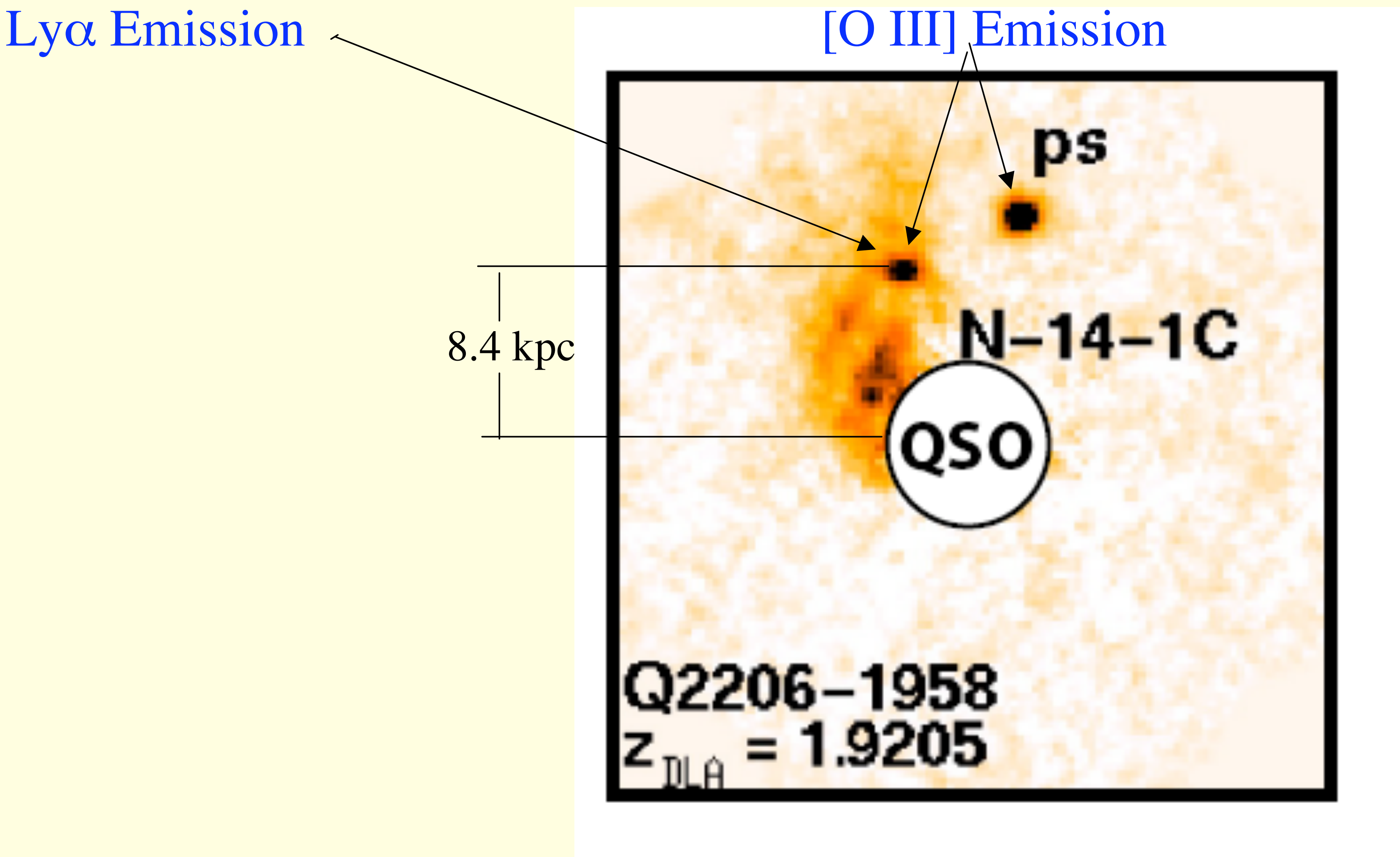

Solution: Energy and Metal Input from LBGs ($l_c > 10^{-27}$)

-Comoving Heating Rate from attenuated FUV LBG radiation:
$\boldsymbol{H_{LBG}}$=(3.0 ±1.5)x10^{38} ergs s^{-1} Mpc^{-3}

-Metal input due to P-Cygni winds emitted by LBGs a possibility

Solution does not apply to 50% of DLA population
Heated by background radiation alone ($l_c \leq 10^{-27}$)

-Embedded LBGs not present in these cases

-Source of metals?

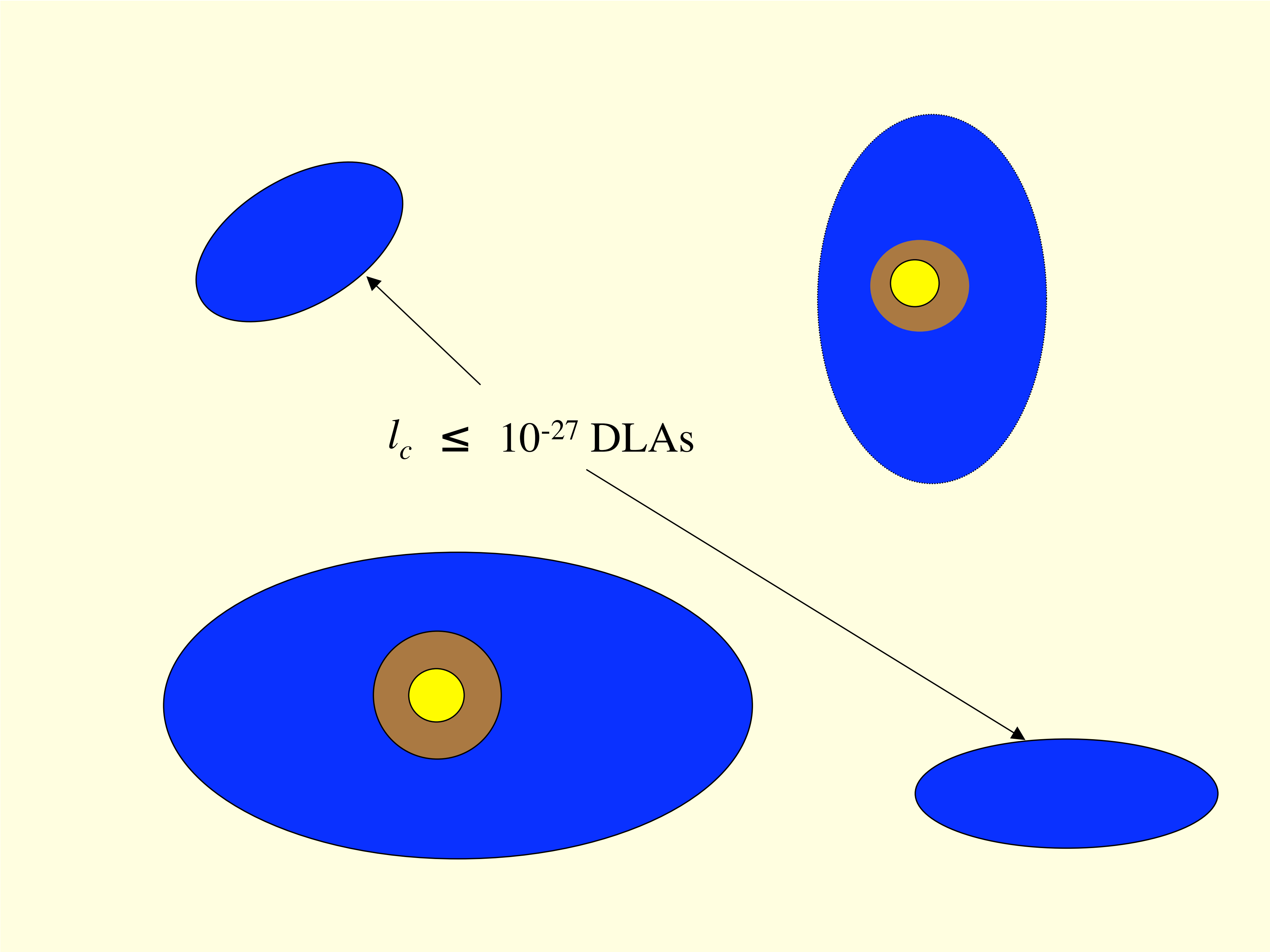
$l_c \leq 10^{-27}$ DLAs

Is l_c a mass indicator?

low l_c	high l_c
$\Delta v=50$ km s^{-1}	$\Delta v=102$ km s^{-1}
[M/H]=-1.81	[M/H]=-1.25
N(HI)=$10^{20.7}$ cm^{-2}	N(HI)=$10^{20.7}$ cm^{-2}

Origin of Bimodality

- Presence of hot (T>3x10^5K) gas in significant fraction of DLAs inferred from OVI absorption (Fox *etal* '07)

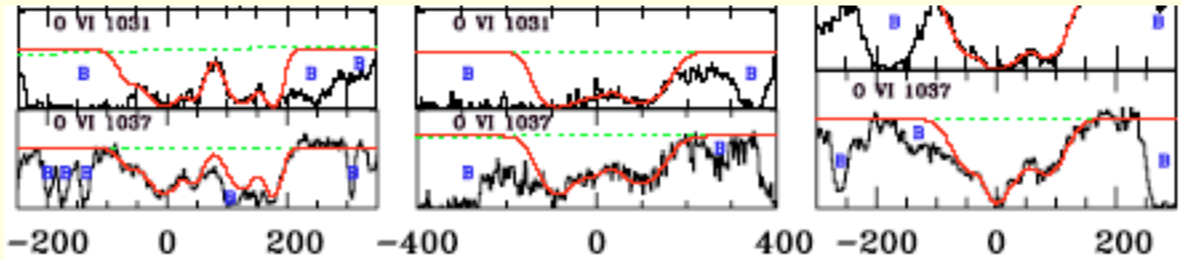

- Hot halo gas predicted **only** for DM halos with $M_{DM}>10^{11.5\text{-}12}M_{\odot}$

Hot Mode

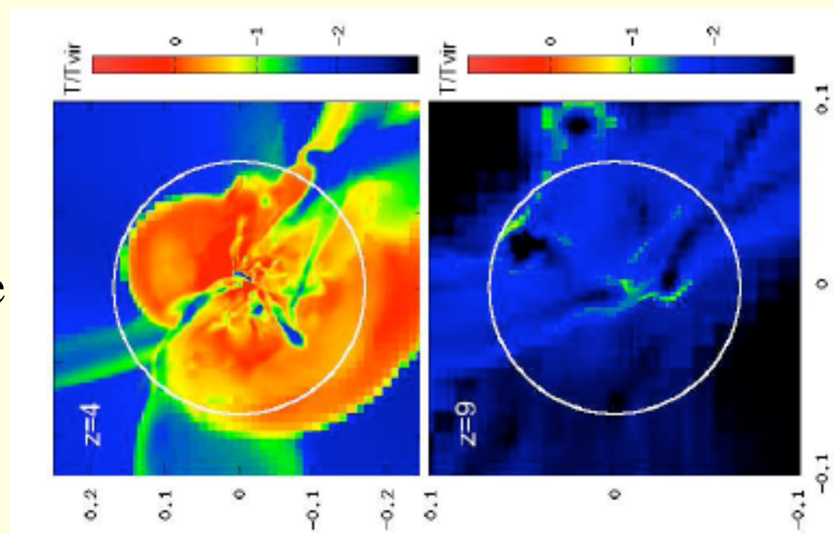

Cold Mode

Origin of Bimodality

- Presence of hot (T>3x10^5K) gas in significant fraction of DLAs inferred from OVI absorption (Fox *etal* '07)

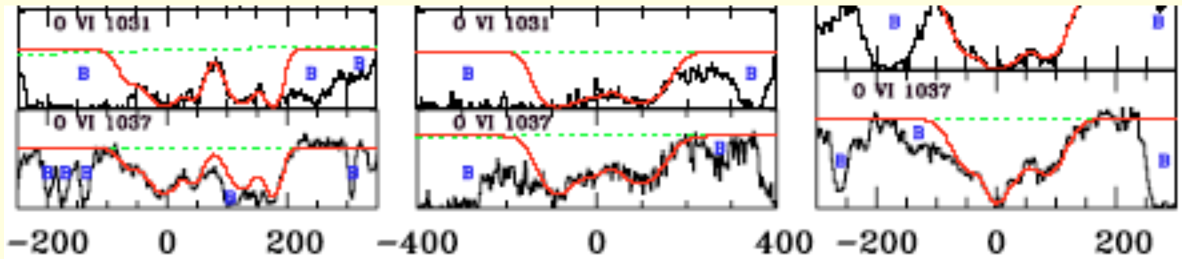

- Hot halo gas predicted **only** for DM halos with M_{DM}>$10^{11.5\text{-}12}M_\odot$

Hot Mode

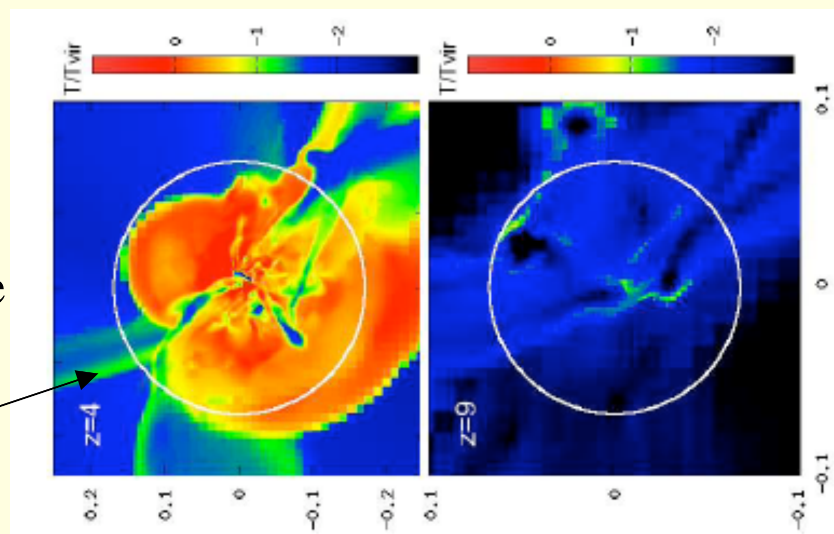

Cold Mode

Cold streams

Origin of Bimodality (cont.)

•Fraction of DLAs with $M_{DM}>10^{11.5}\,M_{\odot}$ can be large

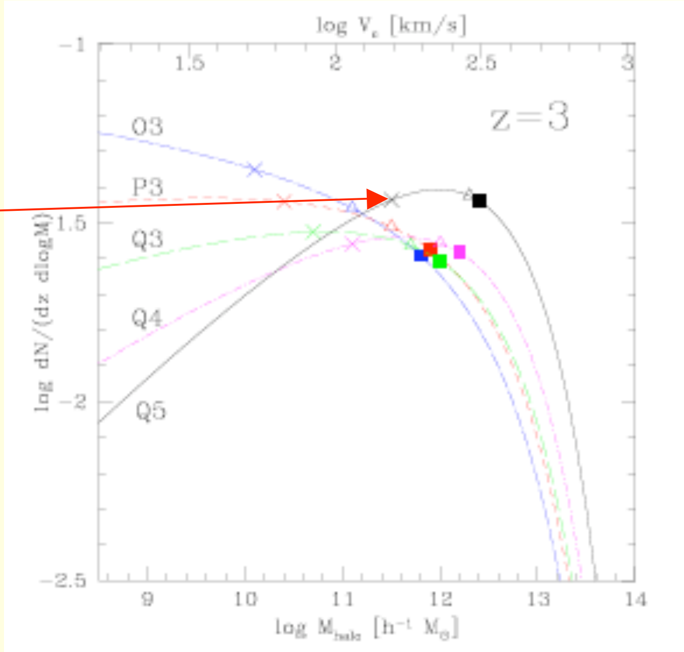

Two Modes of DLA Formation

1. High Mass: Hot mode (OVI), spherical accretion leads to star-forming bulge .

   --Neutral DLA gas accreted along filaments

   --Result is LBG-DLA configuration with high l_c

2. Low Mass: Cold mode accretion leads to neutral 'disk' formation

   --Result is pure DLA configuration with low l_c

   --UDF data require low SFRs in DLA gas

Test: Metallicity Distribution of DLAs with OVI should Resemble that of high l_c DLAs

Results: Inconclusive

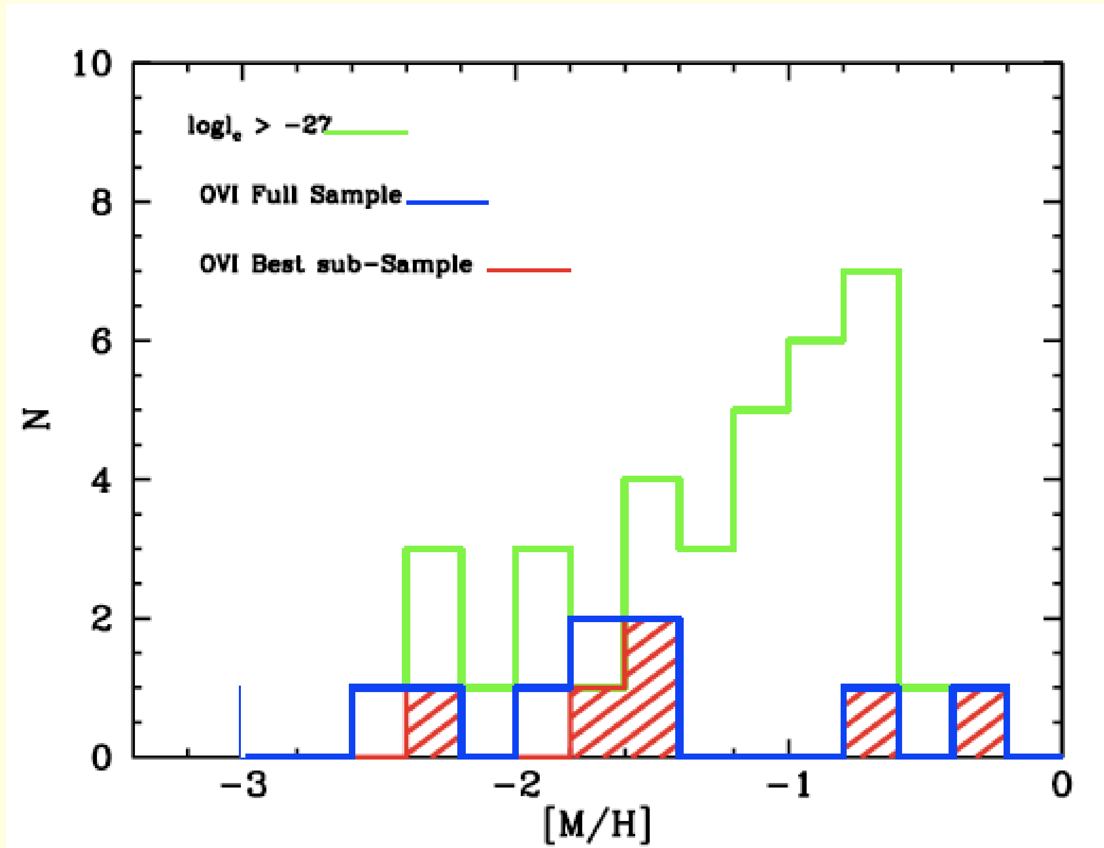

Summary of Results

• Star-forming Galaxies at high z:
  - **--**low area covering factor
  - **--**high comoving SFR density

•Damped Lyα Systems
  - **--**large area covering factor
  - **--**low comoving SFR density

Summary of Results

- Star-forming Galaxies at high z:
  - **--**low area covering factor
  - **--**high comoving SFR density
- Damped Lyα Systems
  - **--**large area covering factor
  - **--**low comoving SFR density

- Bimodality in Damped Lyα Systems
  - **--**Evidence from two peaks in l_c distribution divided by l_c^{crit}
  - **--**Support from disjoint Δv, [M/H], [D/G] distributions

Summary of Results

- Star-forming Galaxies at high z:
  - **--**low area covering factor
  - **--**high comoving SFR density
- Damped Lyα Systems
  - **--**large area covering factor
  - **--**low comoving SFR density

- Bimodality in Damped Lyα Systems
  - **--**Evidence from two peaks in l_c distribution divided by l_c^{crit}
  - **--**Support from disjoint Δv, [M/H], [D/G] distributions

- Interpretation
  - **--**DLAs with $l_c \leq l_c^{crit}$: WNM gas in low-mass halos heated by X-ray and FUV backgrounds.
  - **--**DLAs with $l_c > l_c^{crit}$: CNM gas in high-mass halos heated by central 'bulge' sources (LBGs).

Summary of Results

• Star-forming Galaxies at high z:
 --low area covering factor
 --high comoving SFR density

•Damped Lyα Systems
 --large area covering factor
 --low comoving SFR density

•Bimodality in Damped Lyα Systems
 --Evidence from two peaks in l_c distribution divided by l_c^{crit}
 --Support from disjoint Δv, [M/H], [D/G] distributions

•Interpretation
 --DLAs with $l_c \leq l_c^{crit}$: WNM gas in low-mass halos heated by X-ray and FUV backgrounds.
 --DLAs with $l_c > l_c^{crit}$: CNM gas in high-mass halos heated by central 'bulge' sources (LBGs).

• Consequences
 --DLAs $\rightleftarrows$ LBG interaction. DLAs supply gas for star formation and radiative feedback from LBGs heats and chemically enriches DLA gas

Metal Column Densities from HIRES profiles

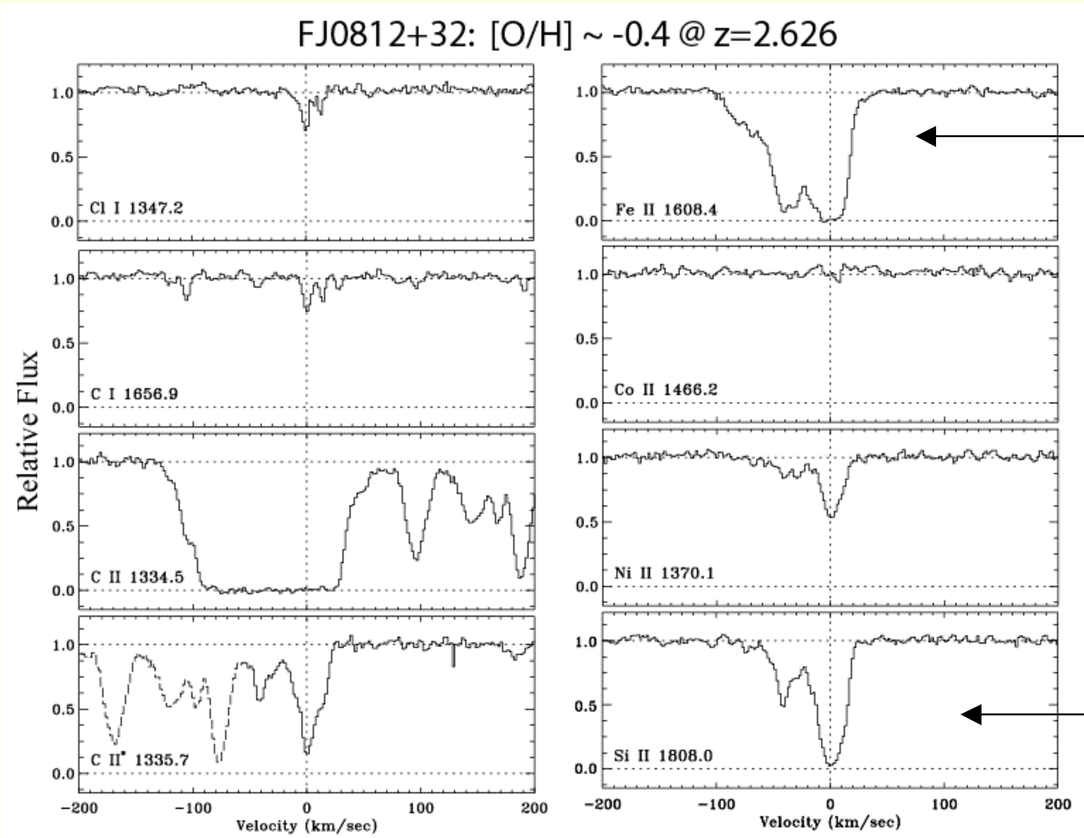

Depletion Indicator

Metallicity Indicator

Comparison between predicted and observed metal abundance

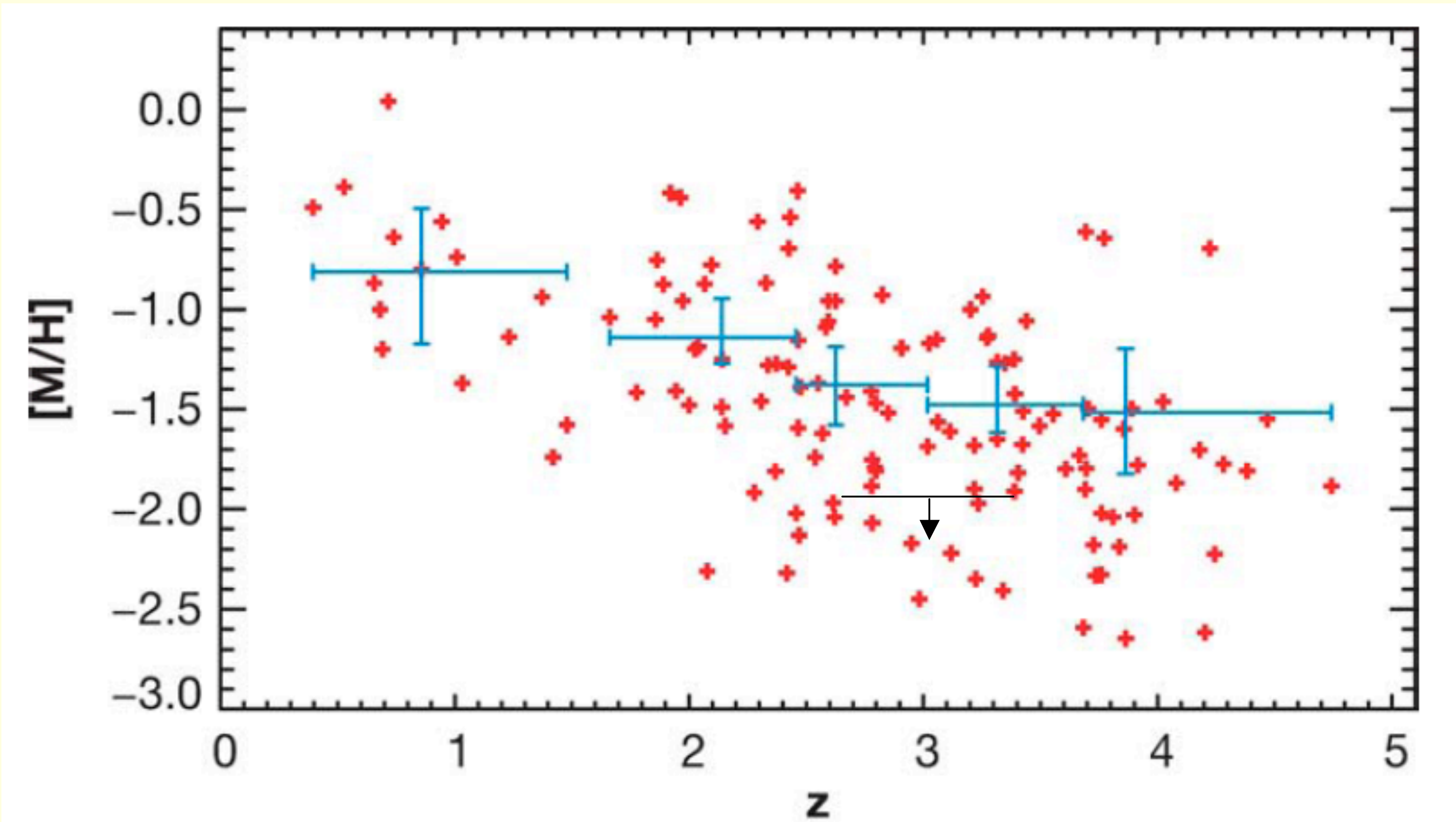

(3) Critical Surface Density larger at high *z*

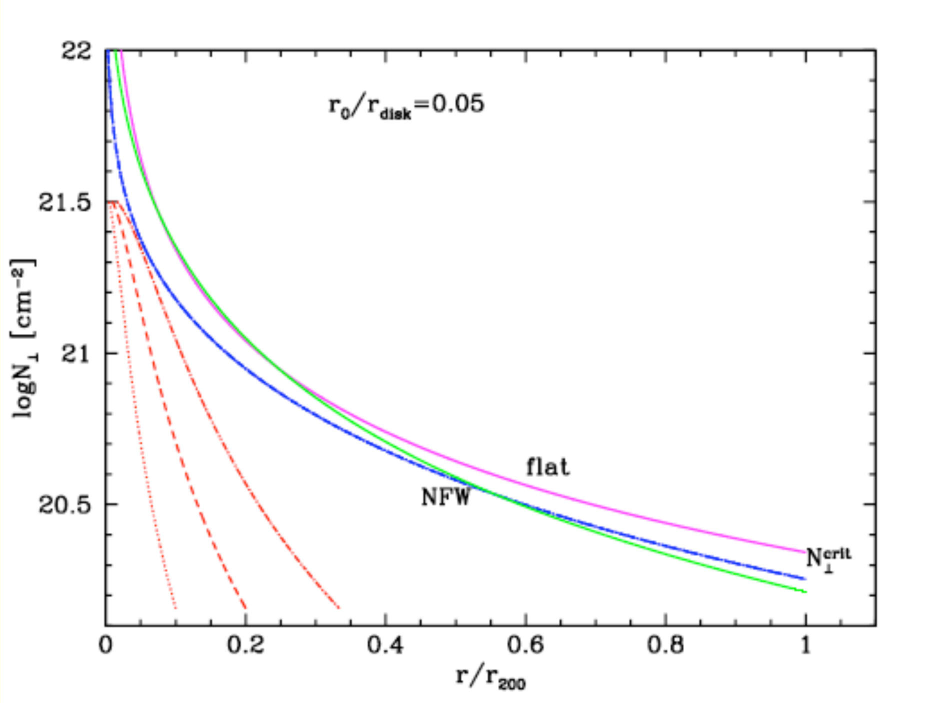

- $N^{crit}_\perp \propto \kappa\sigma$
- $\kappa \propto (G\rho)^{1/2}$ (epicyclic freq.)
- $N^{crit}_\perp \propto (1+z)^{3/2}$
- Neutral Gas Subcritical

l_c versus n for background heating

Empirical Upper Limits on l_c

158 μm emission rate predicted for gas heated by X-ray and FUV background radiation

True l_c intersect background curves In low density WNM

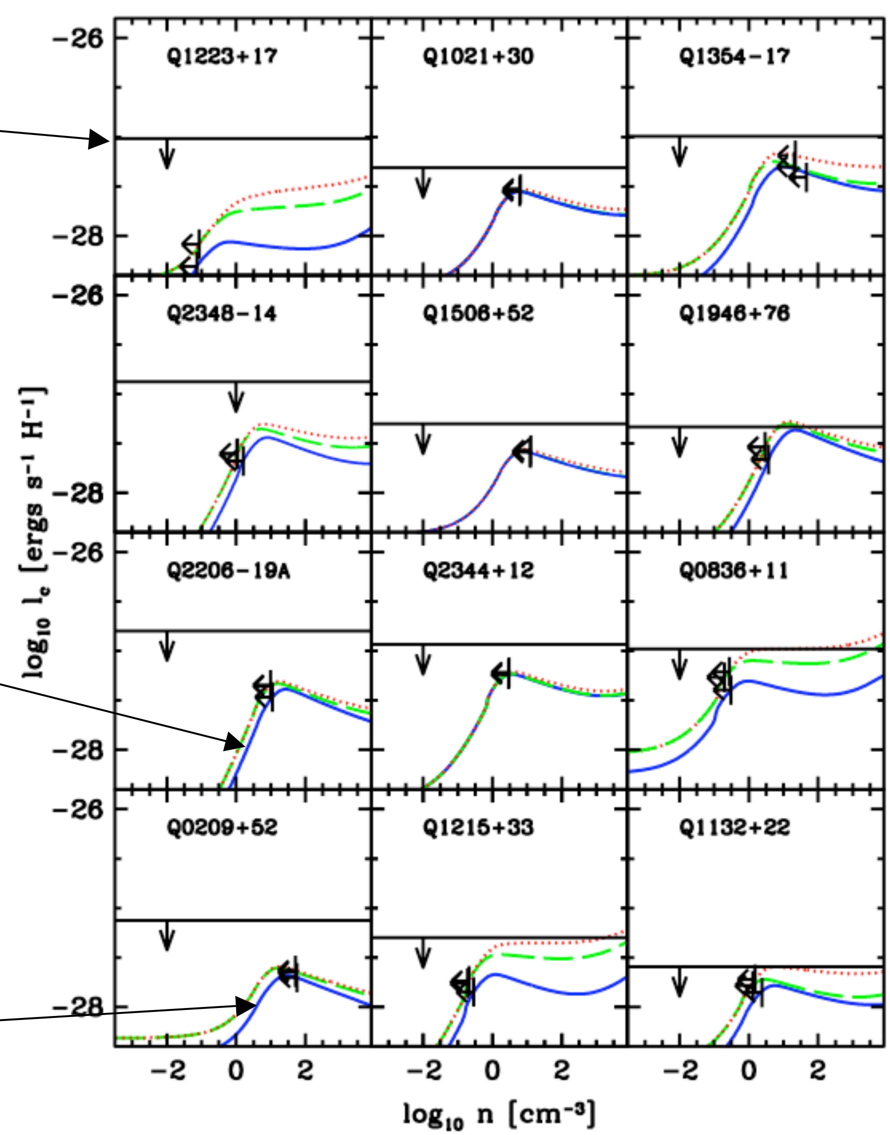

Effect of local heat sources on l_c versus n curves

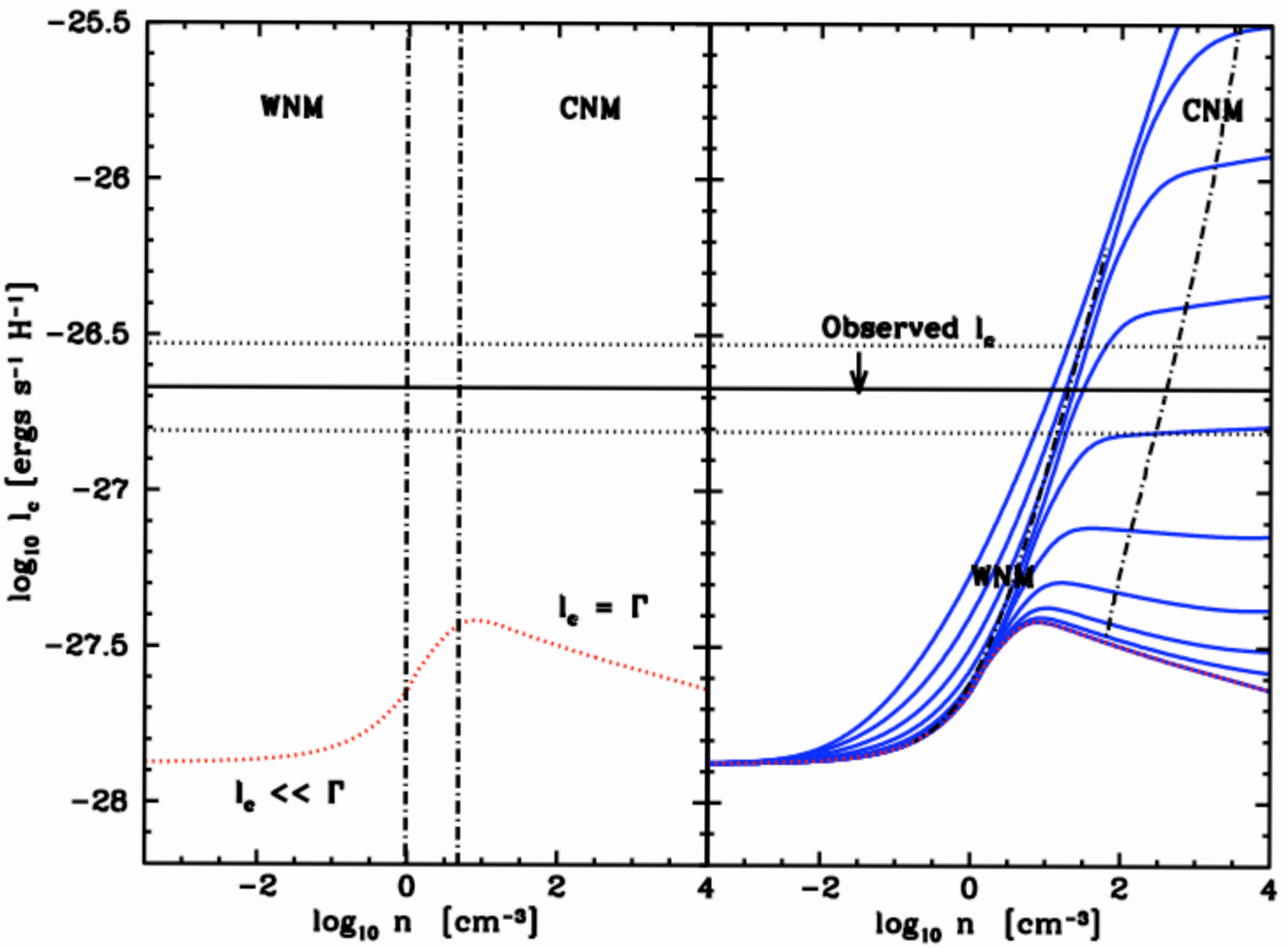

Origin of Bimodality (cont.)

•Fraction of DLAs with DLAs with M_{DM} $>10^{11.5}\,M_{\odot}$ can be large

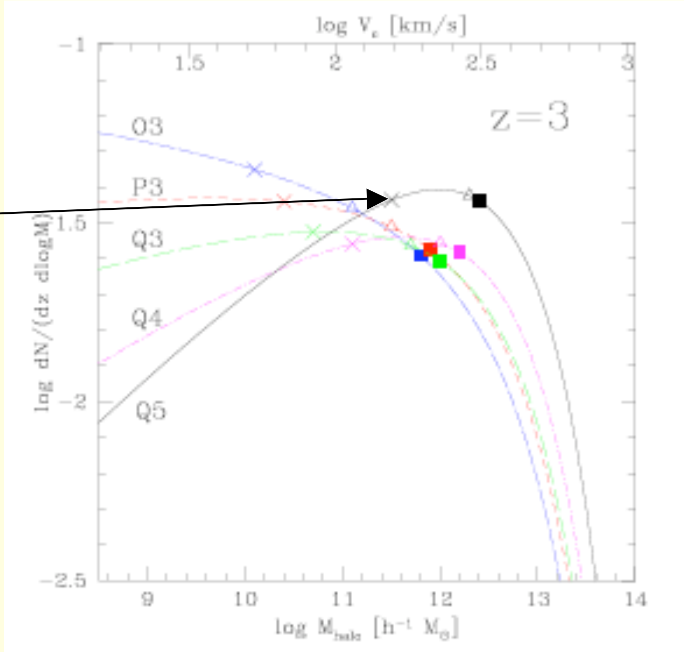

Two Modes of DLA Formation

1. High Mass: Hot mode, spherical accretion leads to star-forming bulge .

   --OVI absorption arises in interfaces between coronal gas and CIV clouds

   --Neutral DLA gas accreted along filaments

   --Result is LBG-DLA configuration with high l_c

2. Low Mass: Cold mode accretion leads to neutral ‘disk’ formation

   --No OVI absorption

   --Pure DLA configuration with low l_c

   --UDF images require low SFRs/Area

Halo Mass Distribution of Comoving SFR Density

- Correlation between disk size and M_{halo}

  $\theta_{dla} \approx (1'')(M_{halo}/10^{11} M_{\odot})^{1/3}$

- Kernel angular bandwidth $\theta_{dla} \approx (0.5 \rightarrow 1.5)\theta_{kern}$

- Kernel with $\theta_{kern} = 2''$ sensitive to halos with $M_{halo} = (10^{11.5 \rightarrow} 10^{12.5}) M_{\odot}$ which contribute ≈ 40% of total SFR density

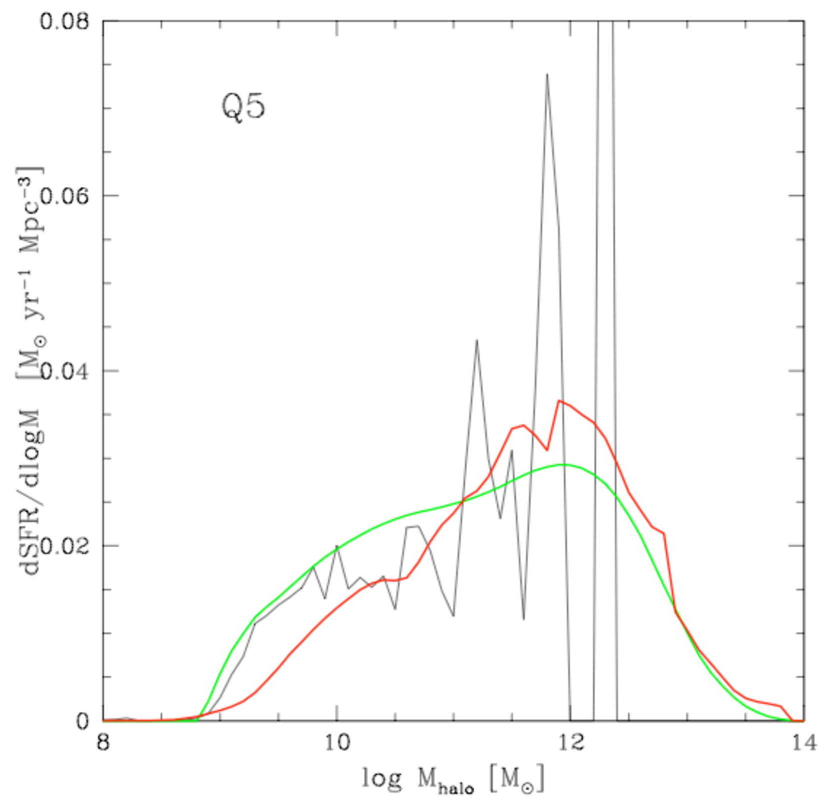

Comoving Density of Neutral Gas versus Redshift

Current Visible Matter

Current Neutral gas

Dwarf Galaxies

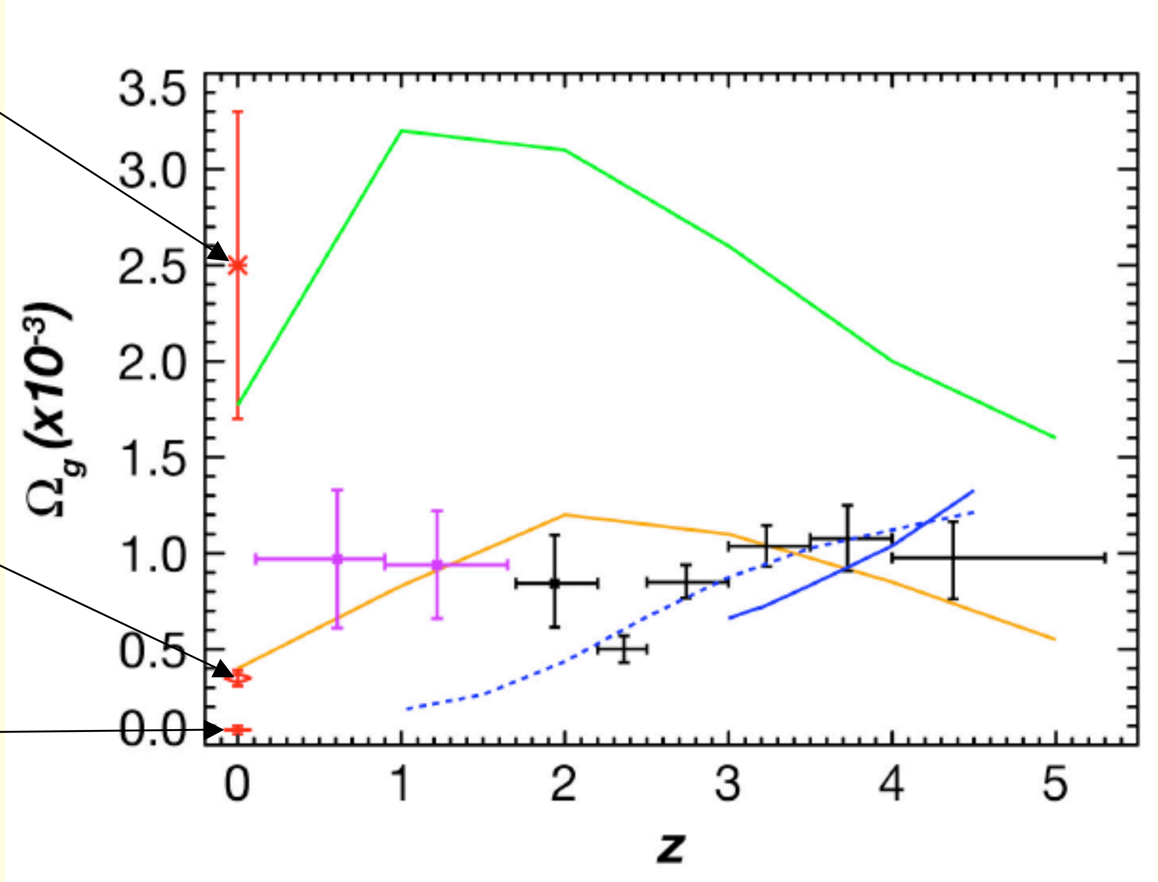

DLA-LBG cross-correlation function and LBG autorcorrelation function (Cooke etal ‘06)

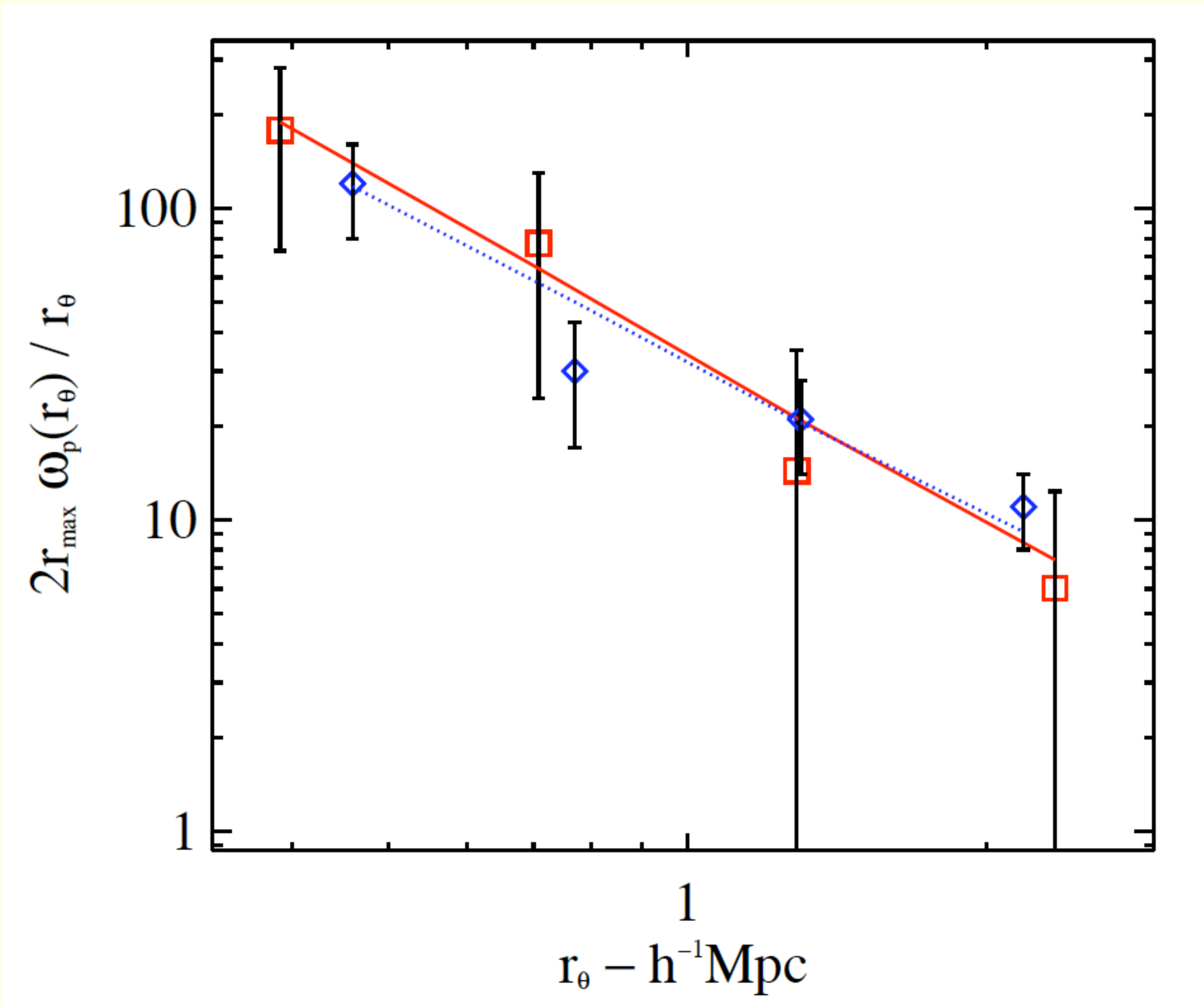

Star Formation in DLAs ?

- Do DLAs undergo *in situ* star formation ?
- If DLAs undergo *in situ* star formation, how does the comoving SFR density compare to that of LBGs?
- Or is star formation at high z confined only to compact objects like LBGs?
- In that case, what is the relationship between LBGs and DLAs? Are DLAs the neutral-gas reservoirs for star formation in LBGs?

Connection between Gas and Stars; Kennicutt-Schmidt Law

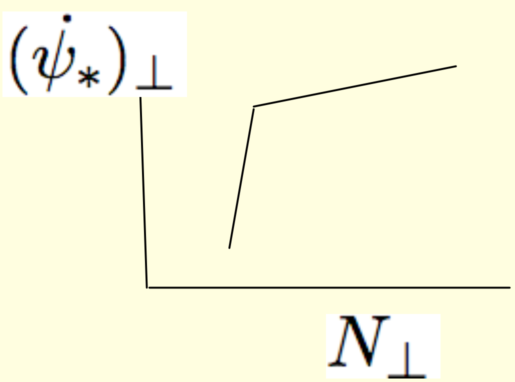

$$(\dot{\psi}_*)_\perp = \begin{cases} 0 \;;\, N_\perp < N_\perp^{crit} \\ K \times [N_\perp / N_c]^\beta \;;\, N_\perp \geq N_\perp^{crit}, \end{cases}$$

$$\dot{\rho}_*(> N) = (H_0/c) \int_N^{N_{max}} dN' f(N', X) \dot{\psi}_*(N')$$

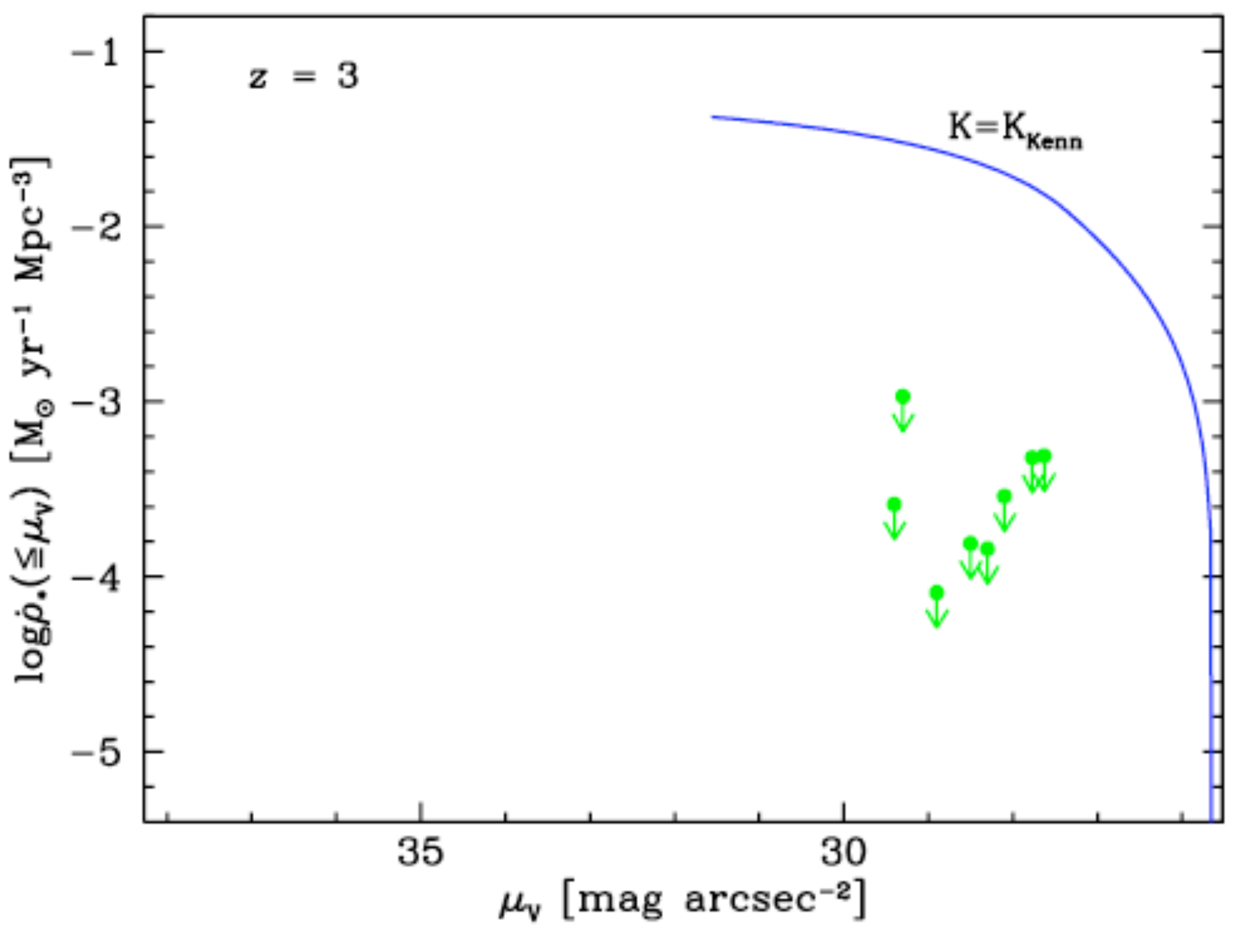

Lower SFR Efficiencies: Effect of Decreasing Normalization K

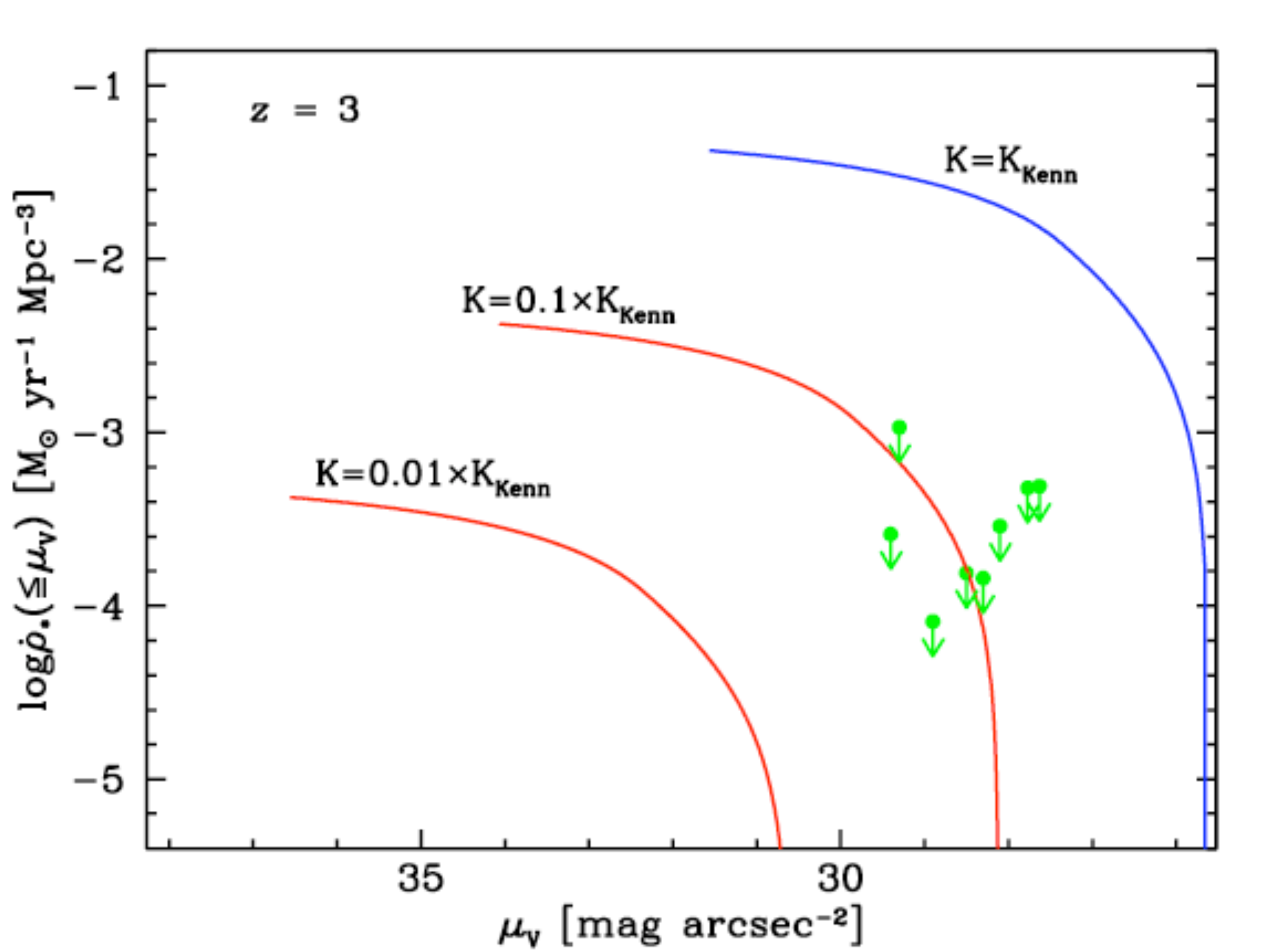

Objects detected in HUDF for θ_{kern}=0.5 arcsec

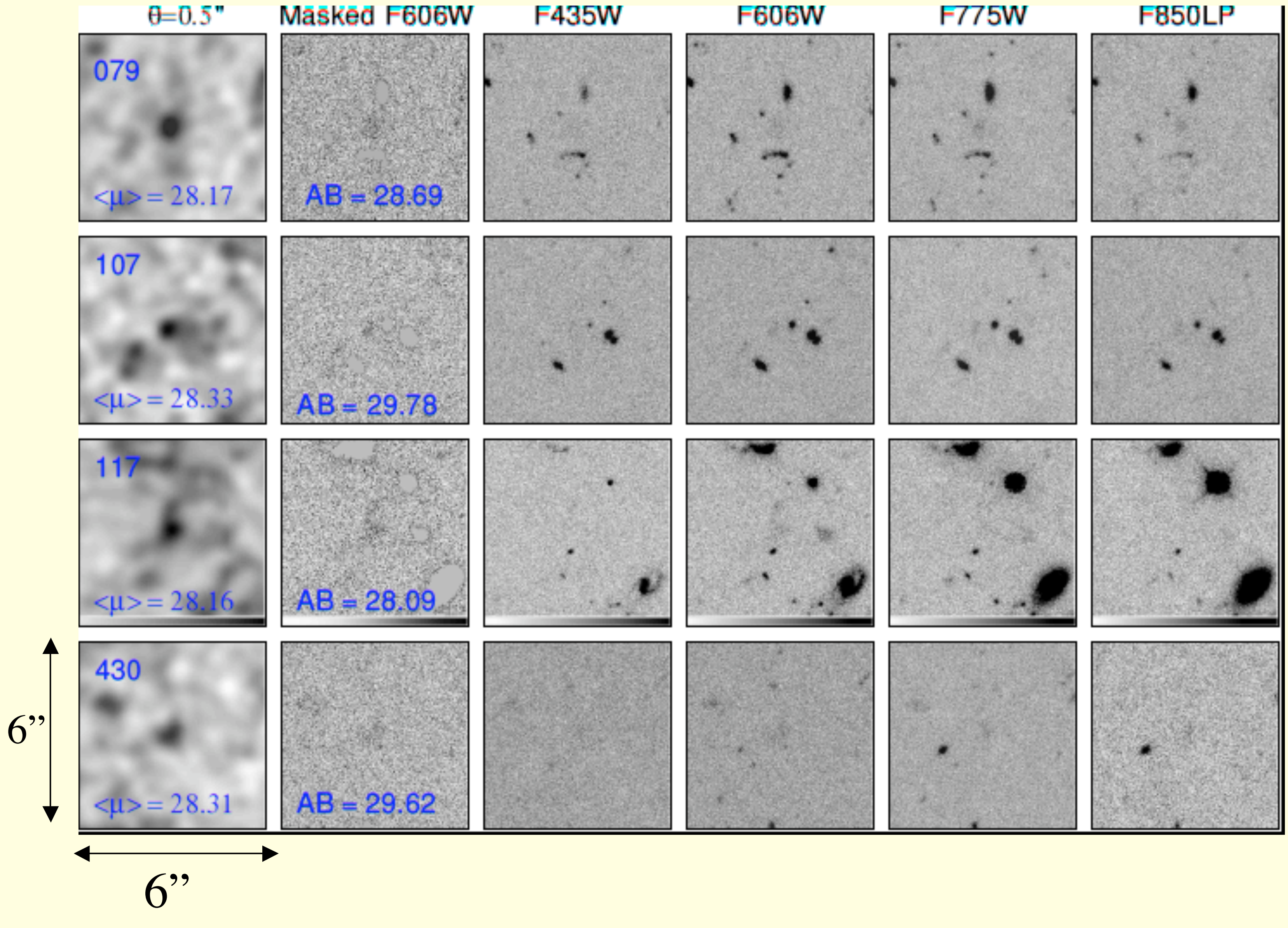

J_ν distribution inferred for $l_c > 10^{-27}$ population

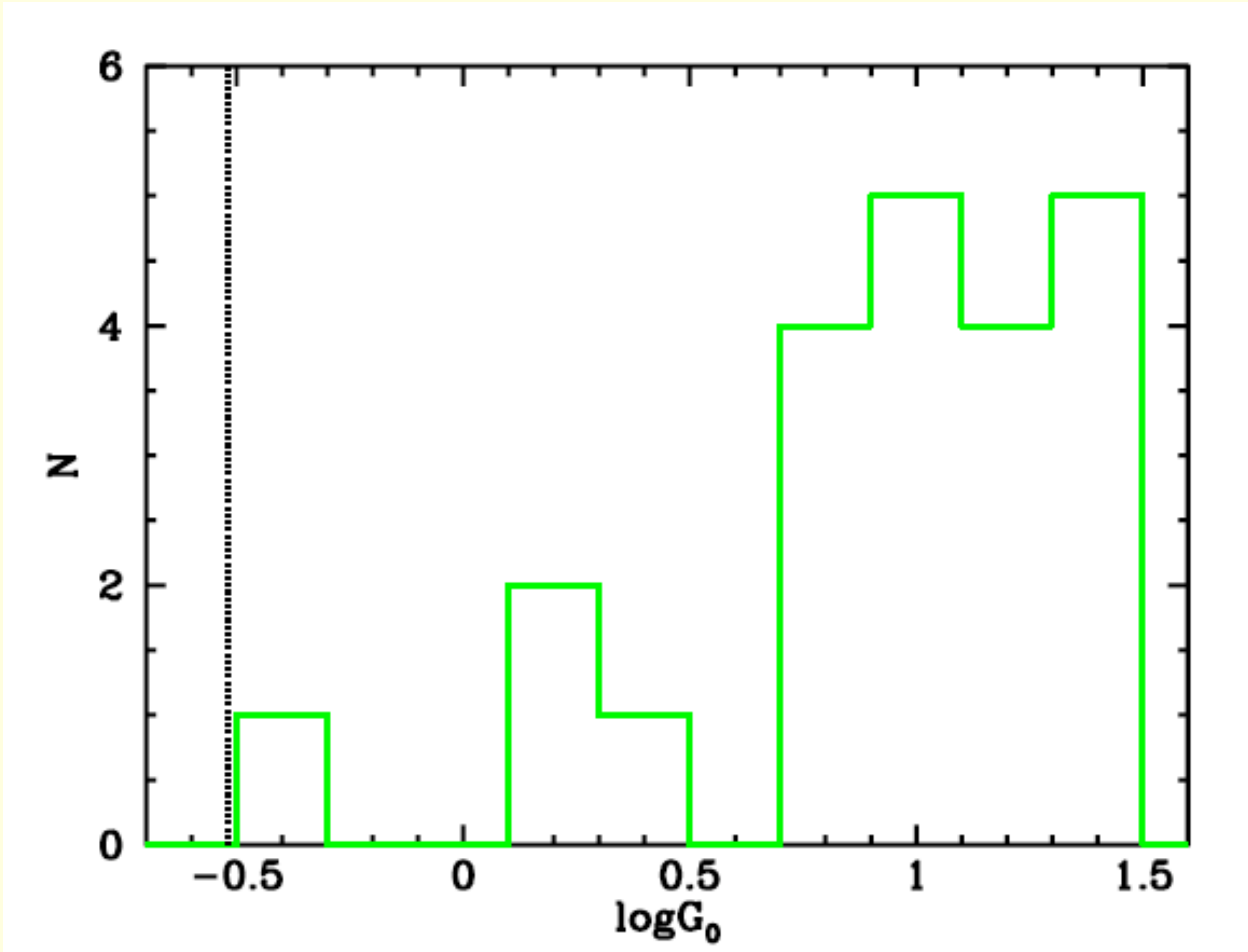

Challenges

- DLA halo mass distribution continuous
- Lack of emission below $20J_\nu^{bkd}$
- Distribution of J_ν predicted for centrally located LBGs
- But relation between local and bkd. implies $\langle J_\nu \rangle \sim 10J_\nu^{bkd}$

Background

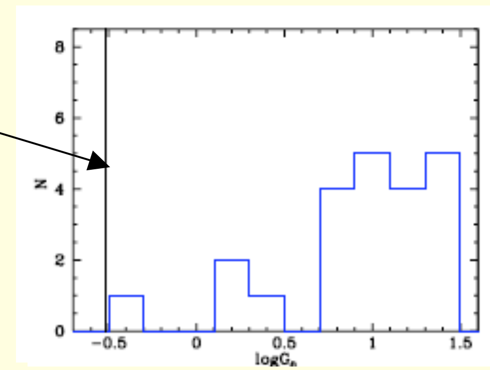

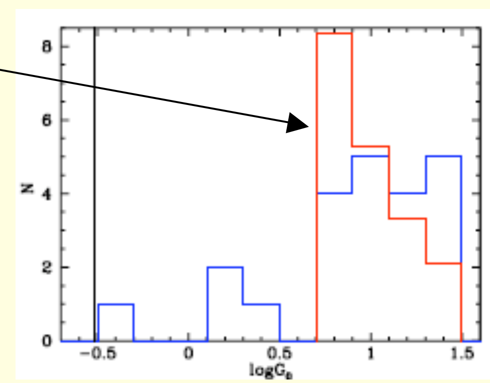

Kennicutt-Schmidt Law for Galaxies

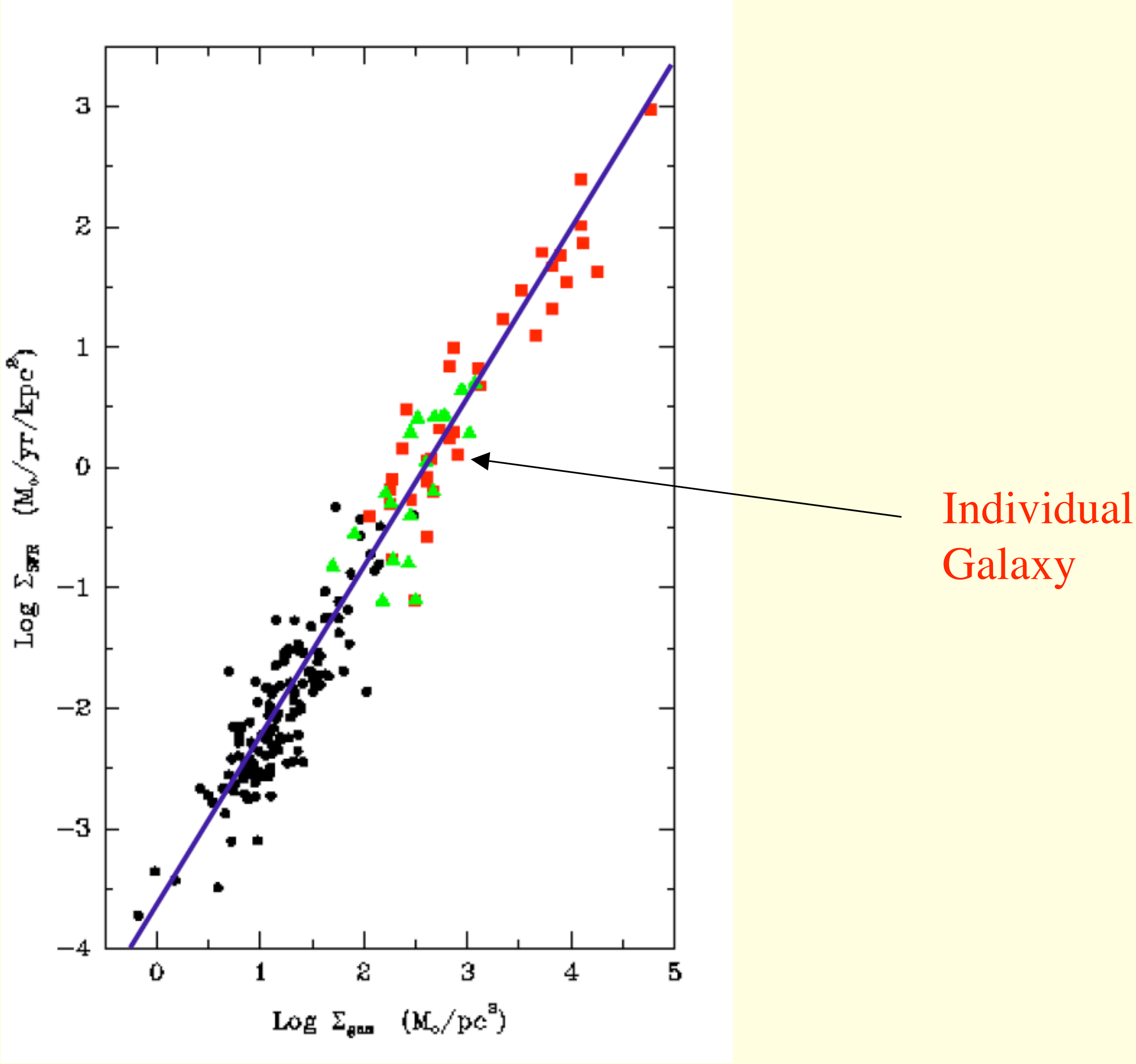

[C II] 158 μm Emission Rate (per atom) vs. *N*(H I)

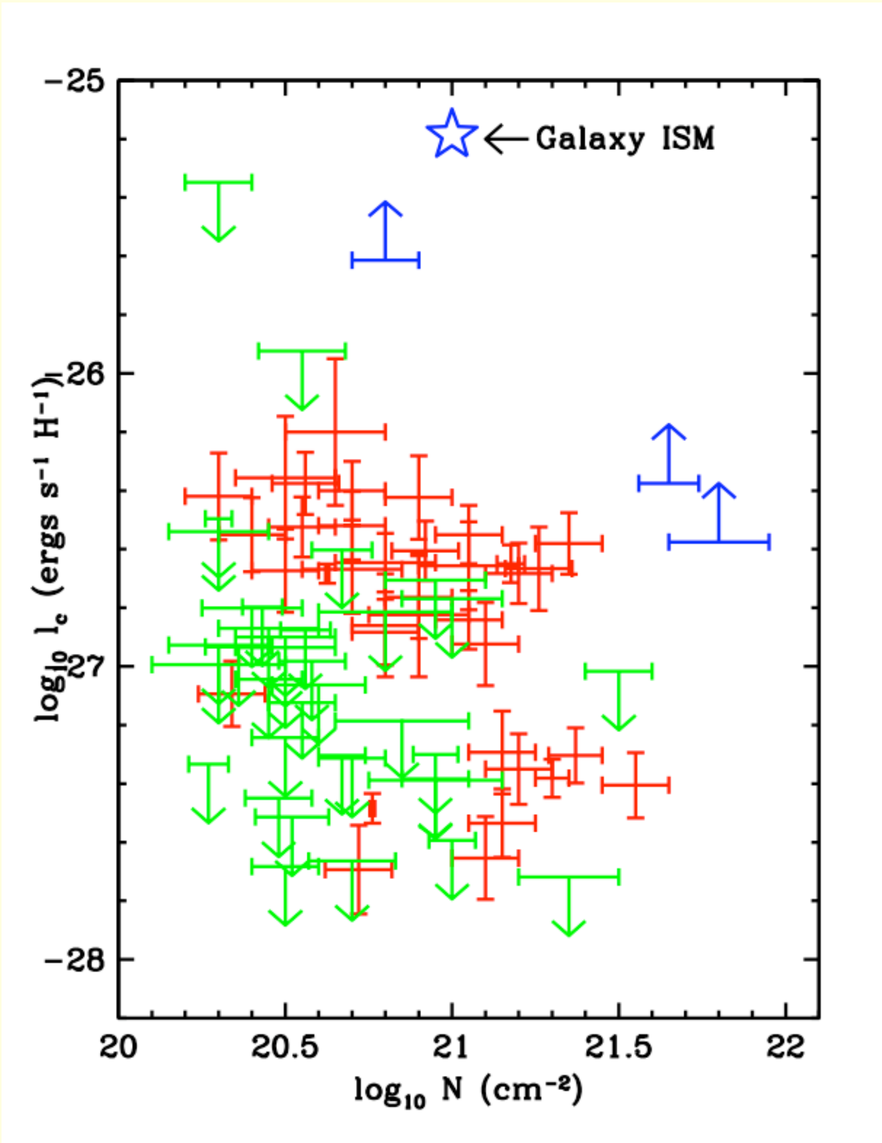

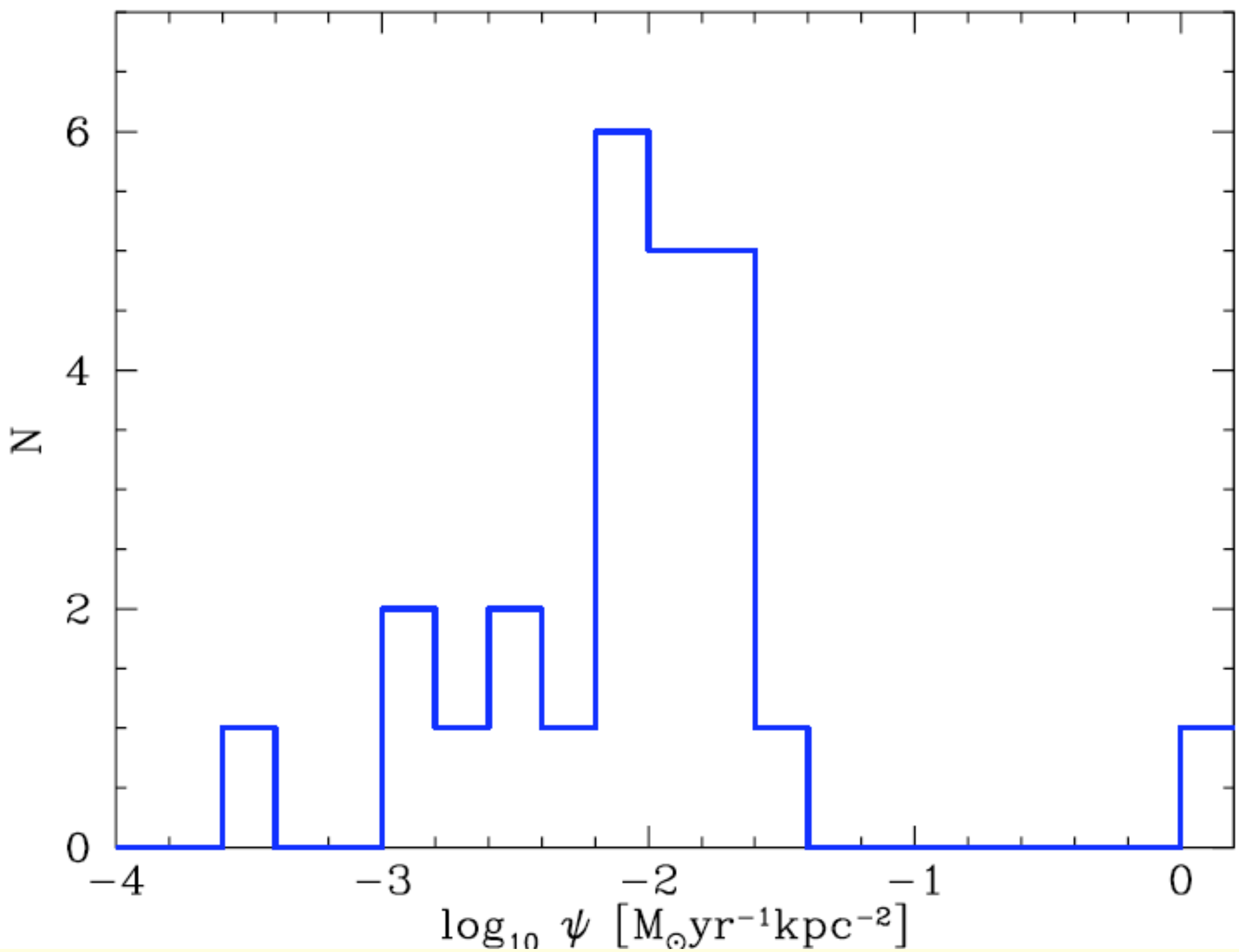

N
0
2
4
6
−4
−3
−2
−1
0
log10 ψ [M⊙yr−1kpc−2]

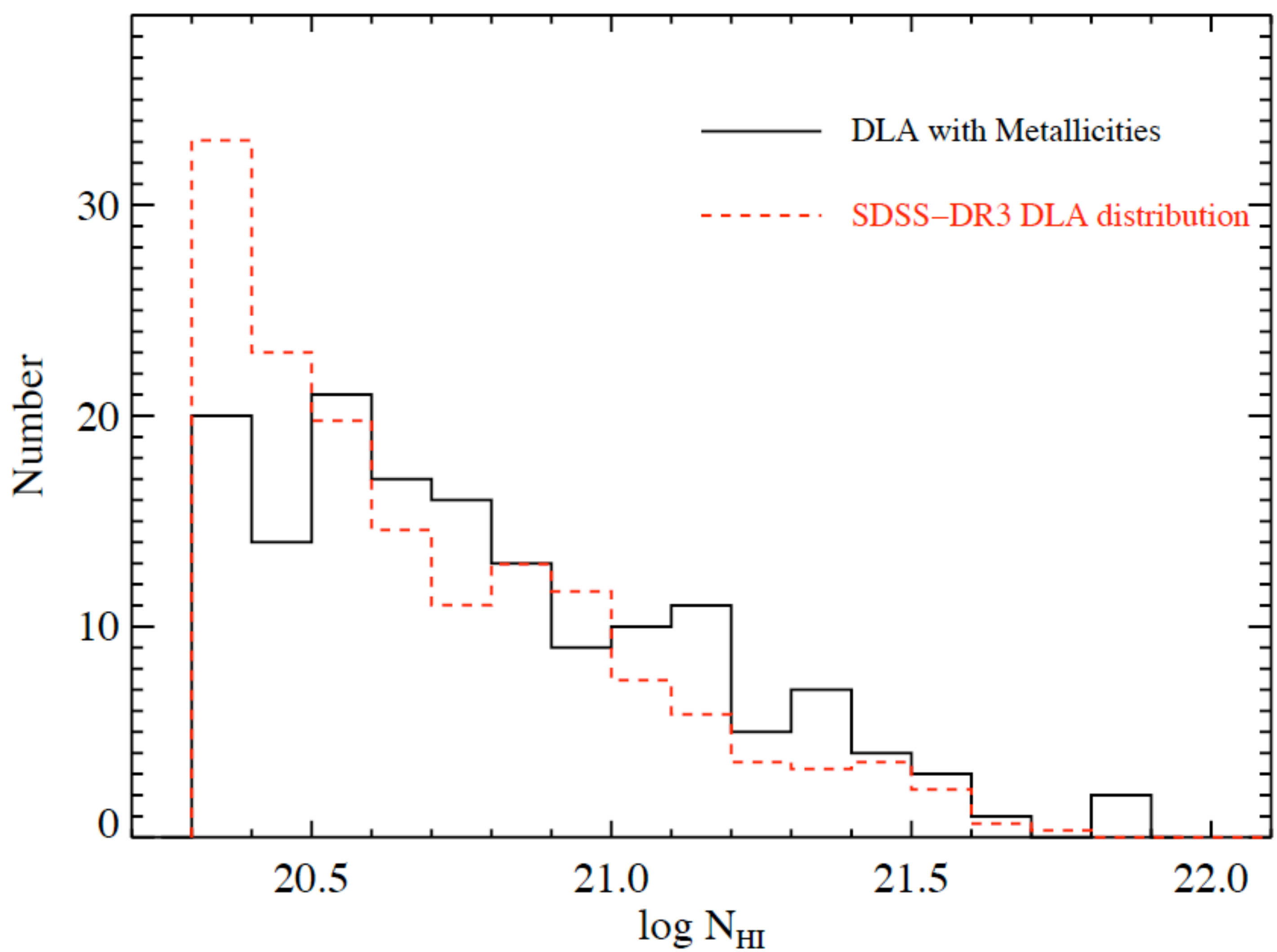

DLA with Metallicities
SDSS–DR3 DLA distribution
Number
30
20
10
0
20.5
21.0
21.5
22.0
log N_{HI}

Lower SFR Efficiencies: Effect of decreasing slope β

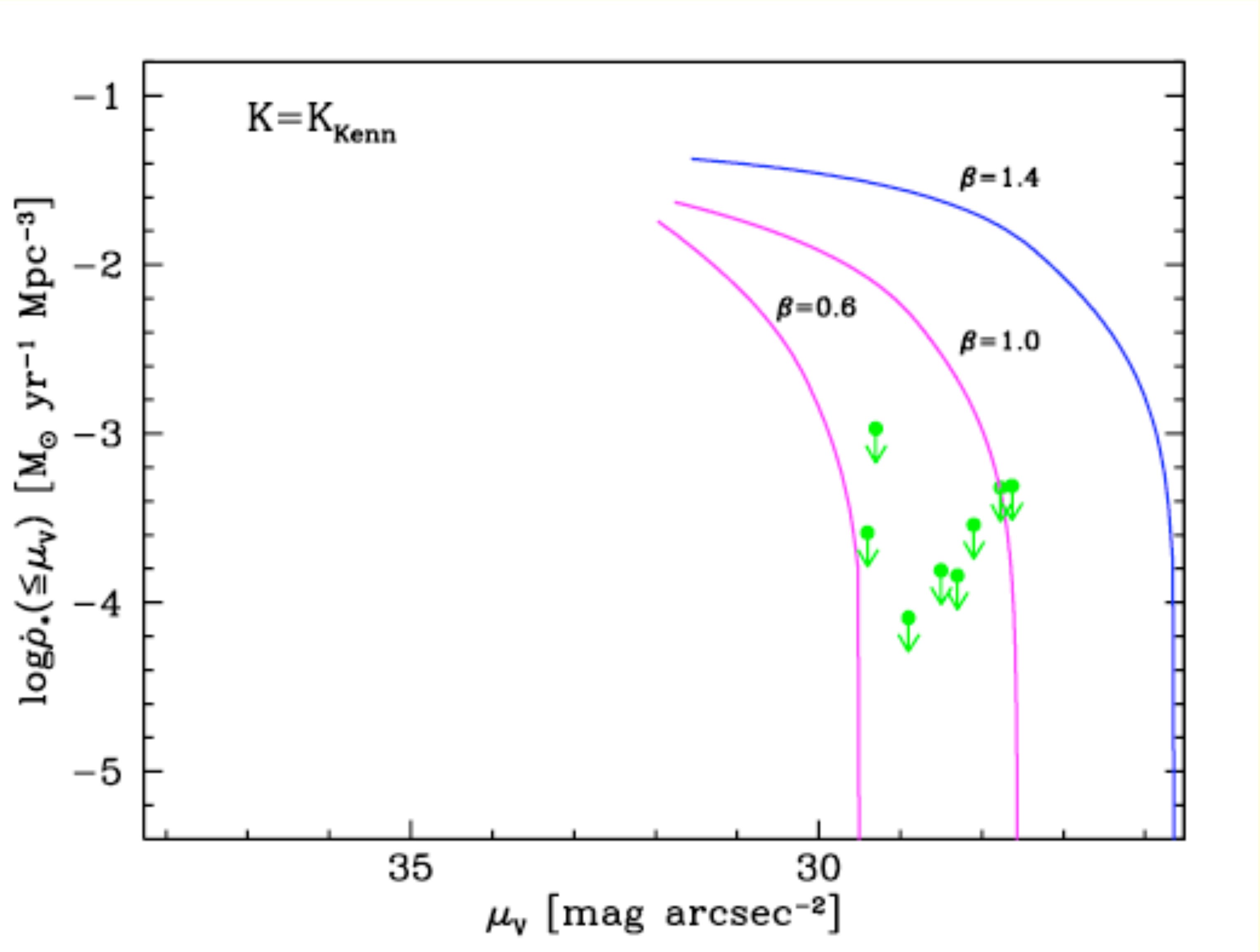

Self regulated *in situ* star formation in DLAs with LBG Cores

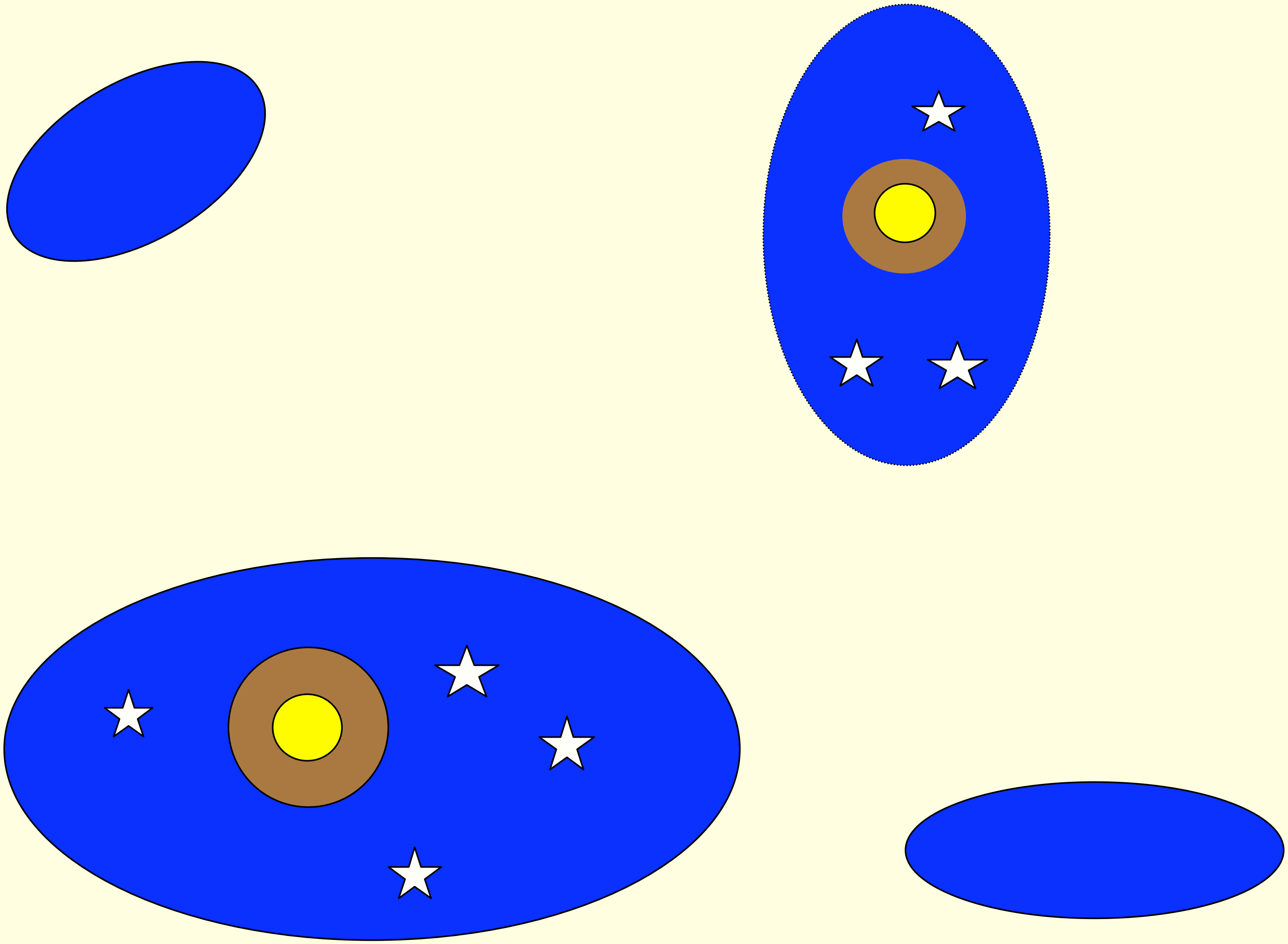

Consquences of upper limit on comoving star formation Density

Upper limit: $d\rho_*/dt < 10^{-2.7}\ M_\odot\ yr^{-1} Mpc^{-3}$

1. ***Limit on Metal Production***

   -Predicted [M/H] <-2.2

   compared to measured [M/H]**=-1.4±0.07**

   -Source of observed metals?

Threshold Determinations from Simulations

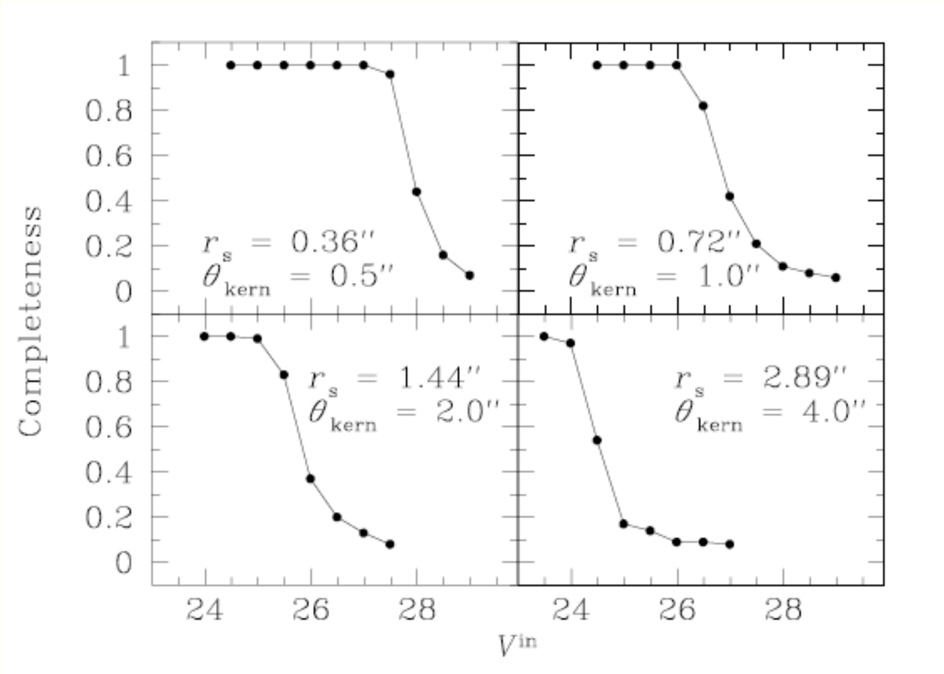

1. **Place 10^3 objects with identical exponential brightness profiles, V magnitudes, θ_{DLA} , on UDF image**
2. **Compute recovery fraction as function of V magnitude**
3. **In principle threshold given by $N_{recover}=N_{95}$**
4. **In practice we used more conservative threshold given by $N_{recover}=200$**

Nature of Reddening in DLAs

Murphy etal 2005

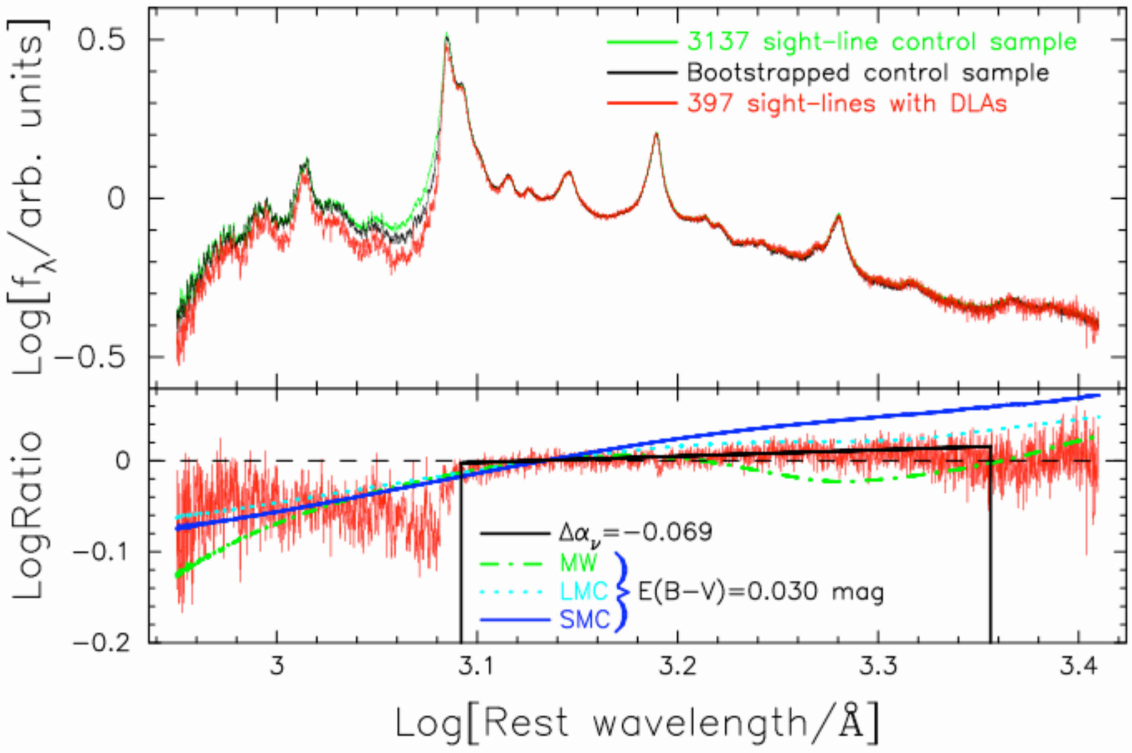

Evidence for Dust Depletion and α Enhancement

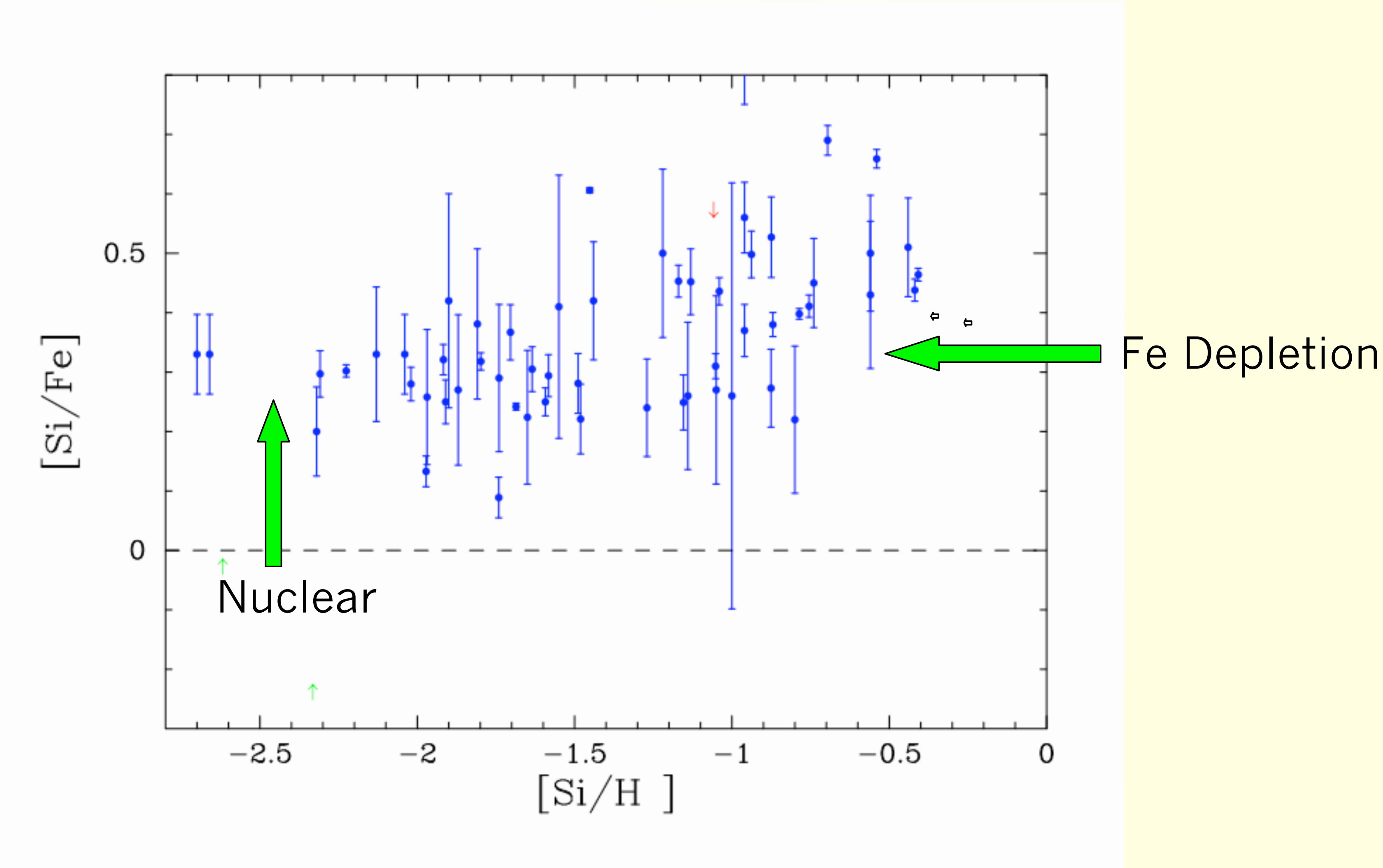

[C II] 158 μm cooling rates versus

Dust-to Gas Ratio

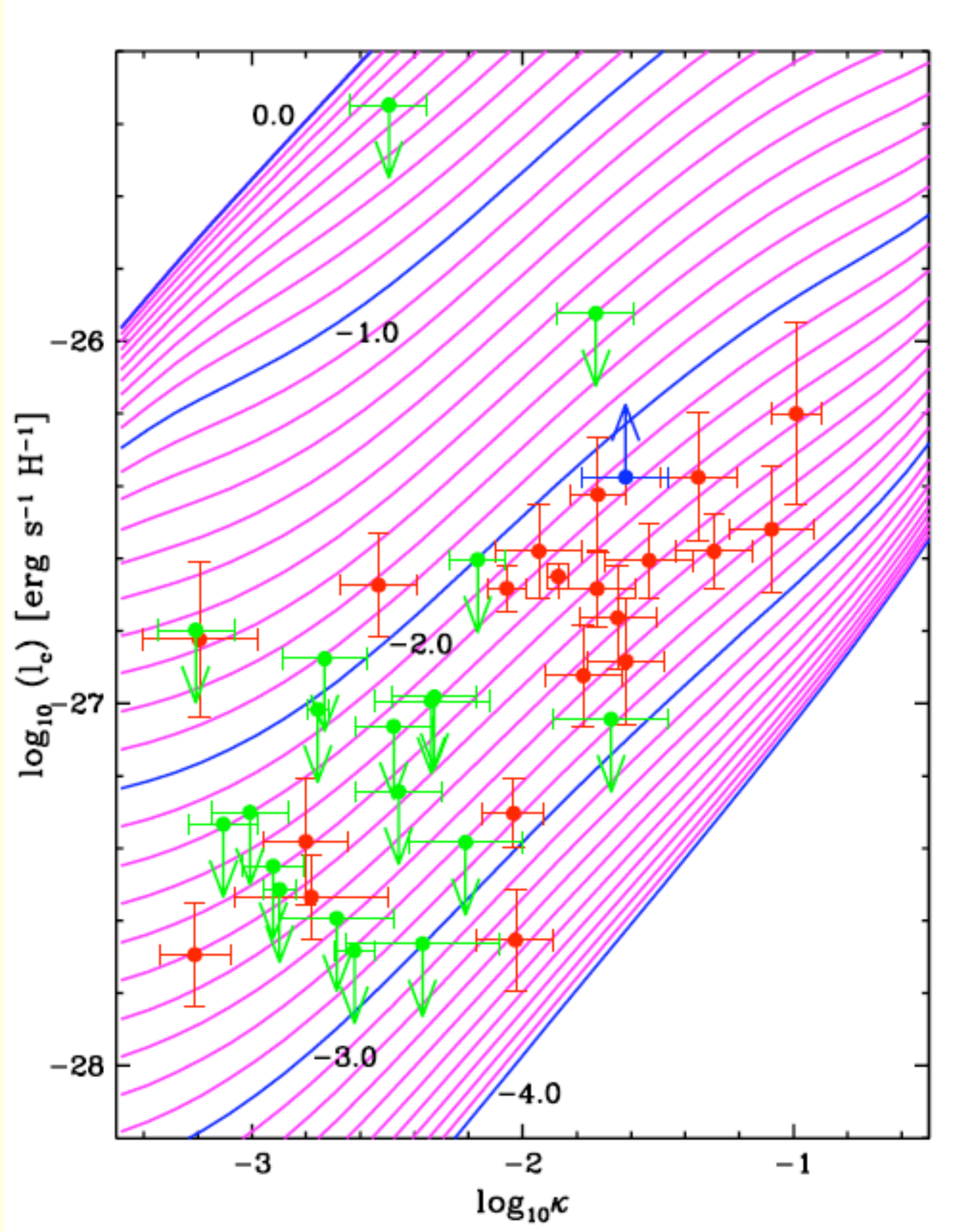

•Star formation in DLAs may be present, but in regions sequestered away from the neutral gas

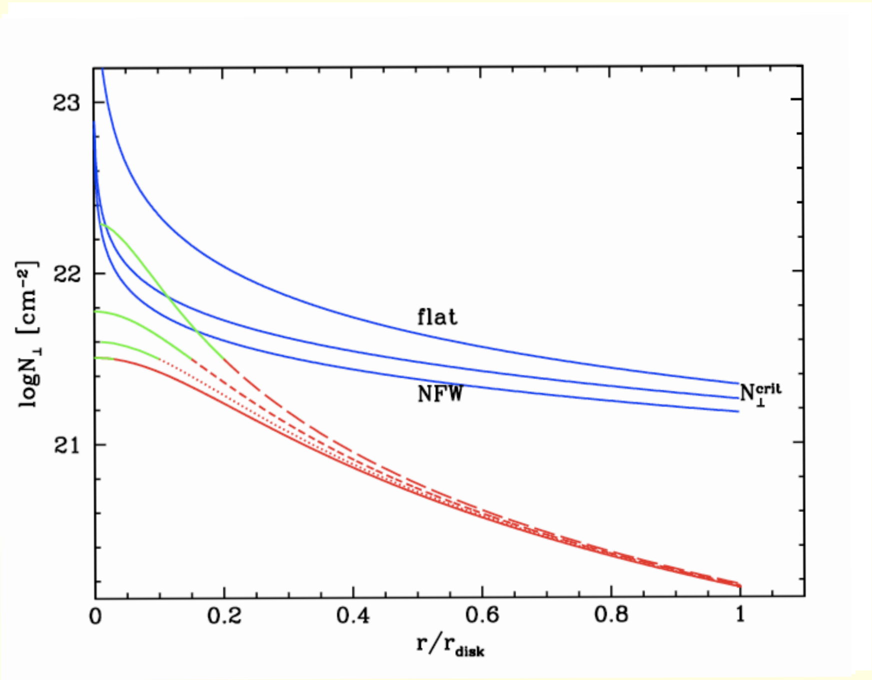

•Molecular gas may be located at $r < r_{\rm break}$

•Extend $N_{\perp}$ to $r < r_{\rm break}$

•Molecular gas may be Toomre unstable

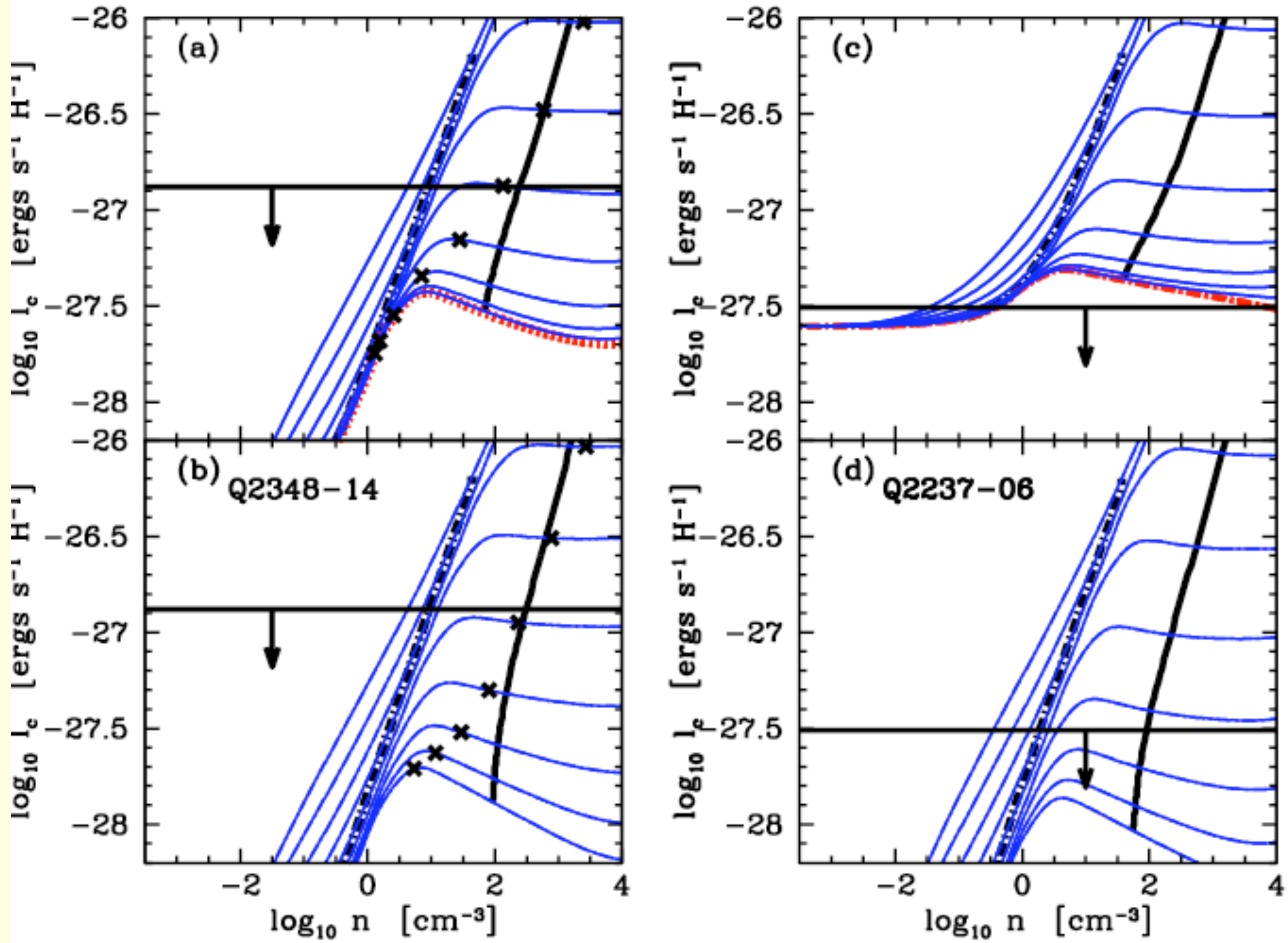

(a)
(b)
Q2348-14
(c)
(d)
Q2237-06
log10 Ic [ergs s-1 H-1]
log10 n [cm-3]
-26
-26.5
-27
-27.5
-28
-2
0
2
4

Magnitude-Size Relation for LBGs (Bouwens etal 2004)

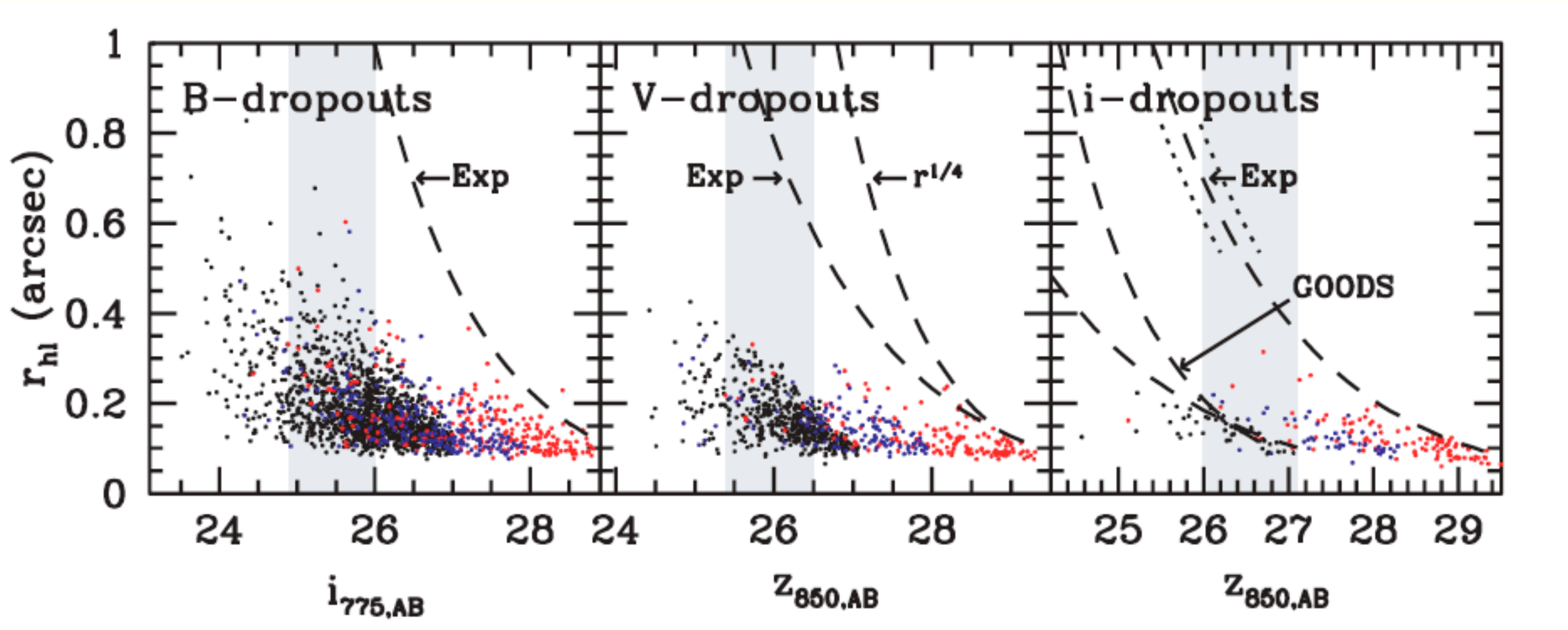

(1) Cumulative Comoving SFR Density Predicted by Kennicutt-Schmidt Relation for z=3

$$\dot{\rho}_*(> N) = (H_0/c) \int_N^{N_{max}} dN' f(N', X) \dot{\psi}_*(N')$$

(2) For Randomly Oriented Disks

$$\dot{\rho}_*(\geq N, X) = (H_0/c) \int_N^{N_{max}} dN K(N/N_c)^\beta \int_{N_{min}}^{\min(N_0,N)} dN_\perp g(N_\perp, X)(N_\perp^2/N^3)(N_\perp/N)^{\beta-1}$$

$$f(N, X) = \int_{N_{min}}^{\min(N_0,N)} dN_\perp g(N_\perp, X)(N_\perp^2/N^3)$$

The Gas Content Predicted for the High-Redshift Universe

O'Shea and Norman 2007

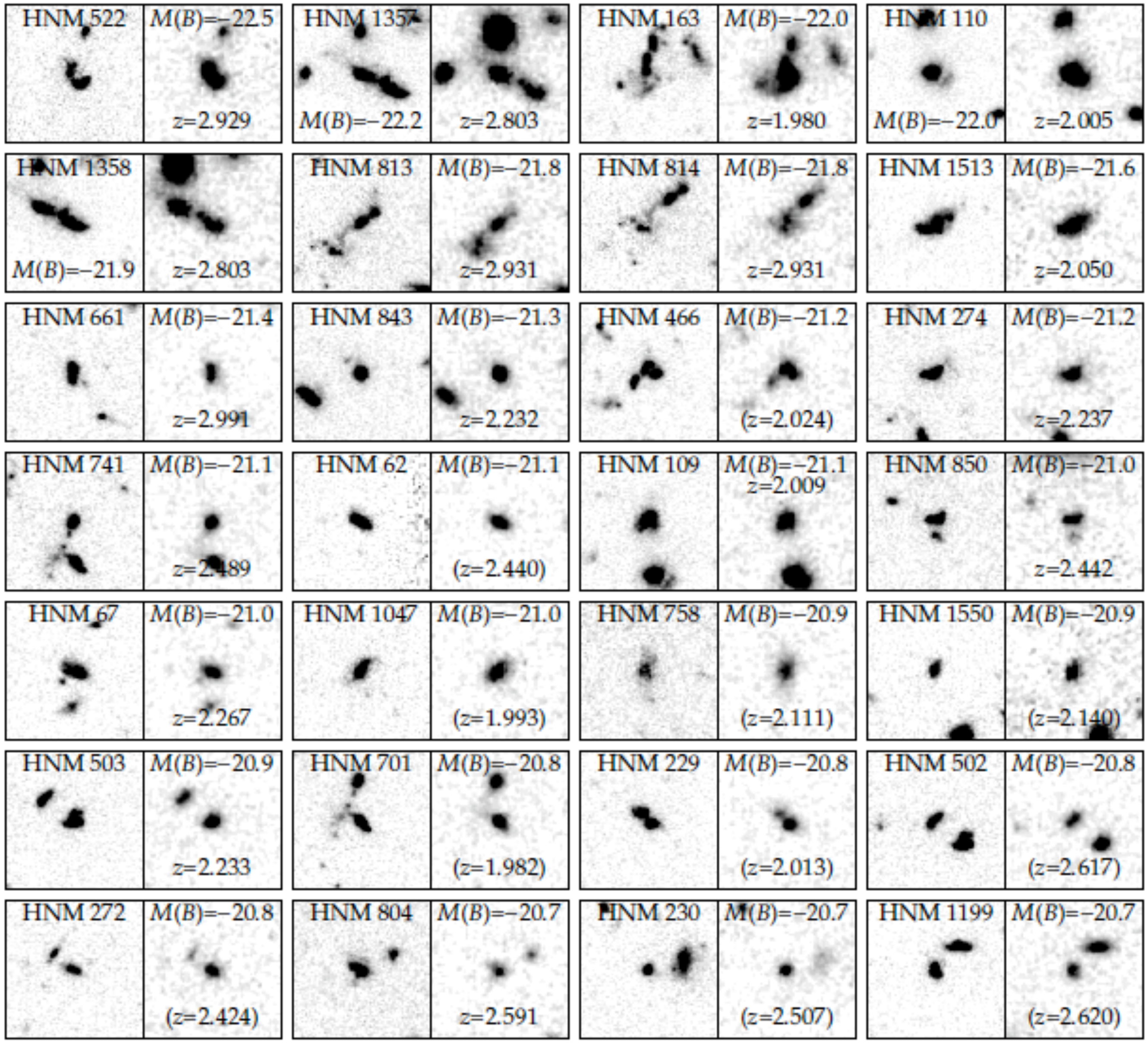

HNM 522
M(B)=−22.5
z=2.929
HNM 1357
M(B)=−22.2
z=2.803
HNM 163
M(B)=−22.0
z=1.980
HNM 110
M(B)=−22.0
z=2.005
HNM 1358
M(B)=−21.9
z=2.803
HNM 813
M(B)=−21.8
z=2.931
HNM 814
M(B)=−21.8
z=2.931
HNM 1513
M(B)=−21.6
z=2.050
HNM 661
M(B)=−21.4
z=2.991
HNM 843
M(B)=−21.3
z=2.232
HNM 466
M(B)=−21.2
(z=2.024)
HNM 274
M(B)=−21.2
z=2.237
HNM 741
M(B)=−21.1
z=2.489
HNM 62
M(B)=−21.1
(z=2.440)
HNM 109
M(B)=−21.1
z=2.009
HNM 850
M(B)=−21.0
z=2.442
HNM 67
M(B)=−21.0
z=2.267
HNM 1047
M(B)=−21.0
(z=1.993)
HNM 758
M(B)=−20.9
(z=2.111)
HNM 1550
M(B)=−20.9
(z=2.140)
HNM 503
M(B)=−20.9
z=2.233
HNM 701
M(B)=−20.8
(z=1.982)
HNM 229
M(B)=−20.8
(z=2.013)
HNM 502
M(B)=−20.8
(z=2.617)
HNM 272
M(B)=−20.8
(z=2.424)
HNM 804
M(B)=−20.7
z=2.591
HNM 230
M(B)=−20.7
(z=2.507)
HNM 1199
M(B)=−20.7
(z=2.620)

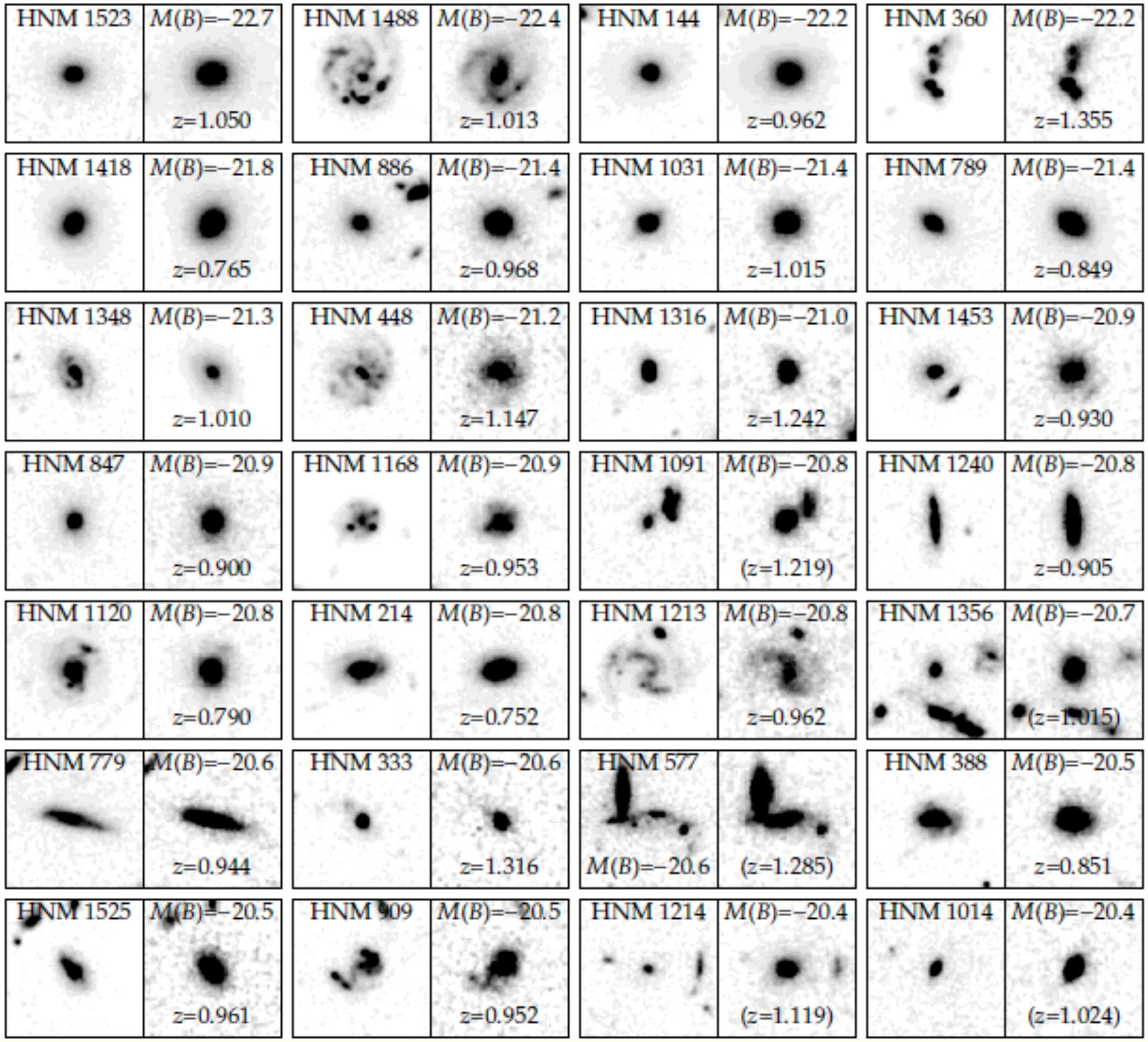
HNM 1523
M(B)=−22.7
z=1.050
HNM 1488
M(B)=−22.4
z=1.013
HNM 144
M(B)=−22.2
z=0.962
HNM 360
M(B)=−22.2
z=1.355
HNM 1418
M(B)=−21.8
z=0.765
HNM 886
M(B)=−21.4
z=0.968
HNM 1031
M(B)=−21.4
z=1.015
HNM 789
M(B)=−21.4
z=0.849
HNM 1348
M(B)=−21.3
z=1.010
HNM 448
M(B)=−21.2
z=1.147
HNM 1316
M(B)=−21.0
z=1.242
HNM 1453
M(B)=−20.9
z=0.930
HNM 847
M(B)=−20.9
z=0.900
HNM 1168
M(B)=−20.9
z=0.953
HNM 1091
M(B)=−20.8
(z=1.219)
HNM 1240
M(B)=−20.8
z=0.905
HNM 1120
M(B)=−20.8
z=0.790
HNM 214
M(B)=−20.8
z=0.752
HNM 1213
M(B)=−20.8
z=0.962
HNM 1356
M(B)=−20.7
(z=1.015)
HNM 779
M(B)=−20.6
z=0.944
HNM 333
M(B)=−20.6
z=1.316
HNM 577
M(B)=−20.6
(z=1.285)
HNM 388
M(B)=−20.5
z=0.851
HNM 1525
M(B)=−20.5
z=0.961
HNM 909
M(B)=−20.5
z=0.952
HNM 1214
M(B)=−20.4
(z=1.119)
HNM 1014
M(B)=−20.4
(z=1.024)

Evidence for Threshold Surface Densities at z=0

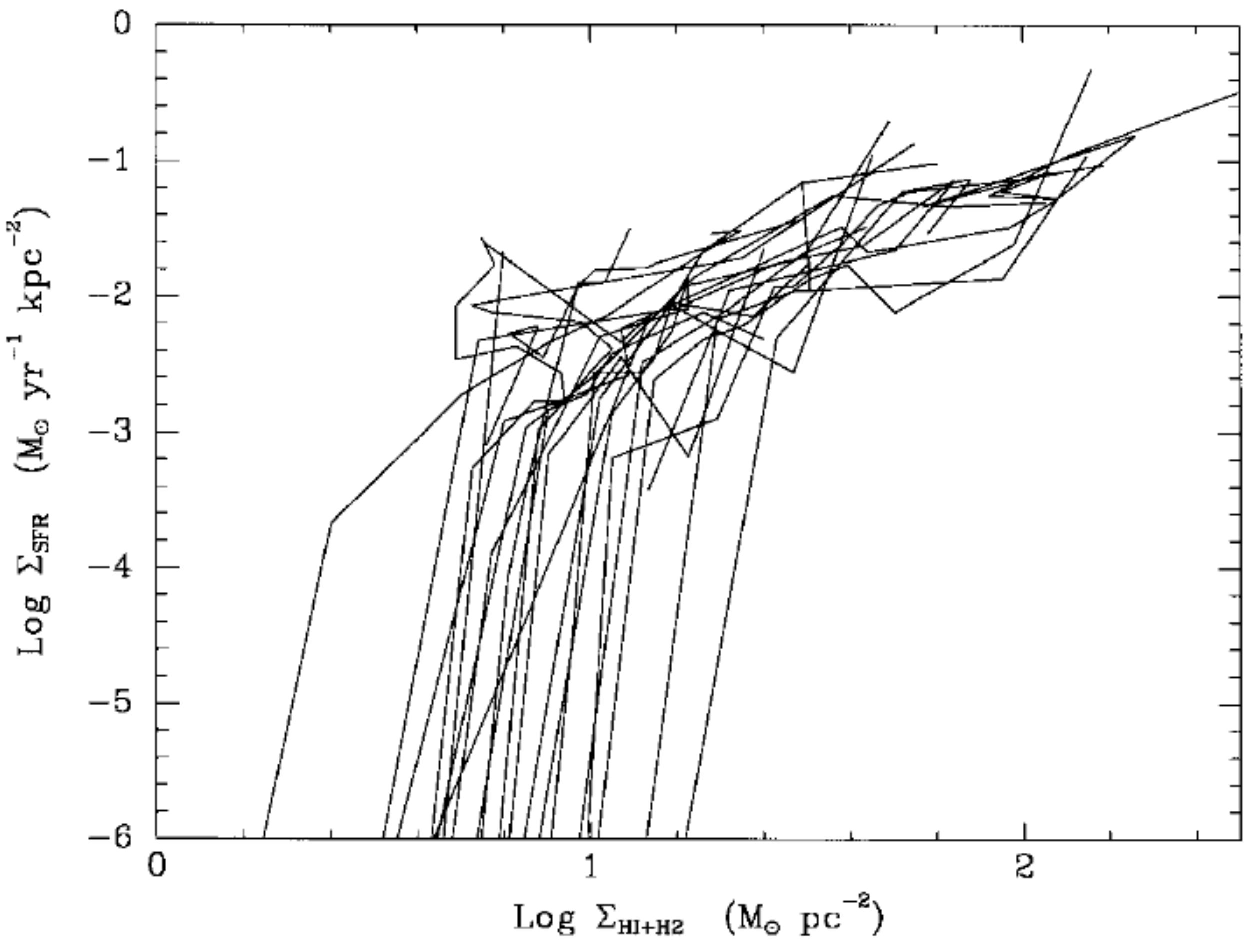

FIG. 3.—Profiles of the azimuthally averaged SFR per unit area as a function of gas density for 21 spirals with spatially resolved Hα data.

Kennicutt-Schmidt Law for Galaxies

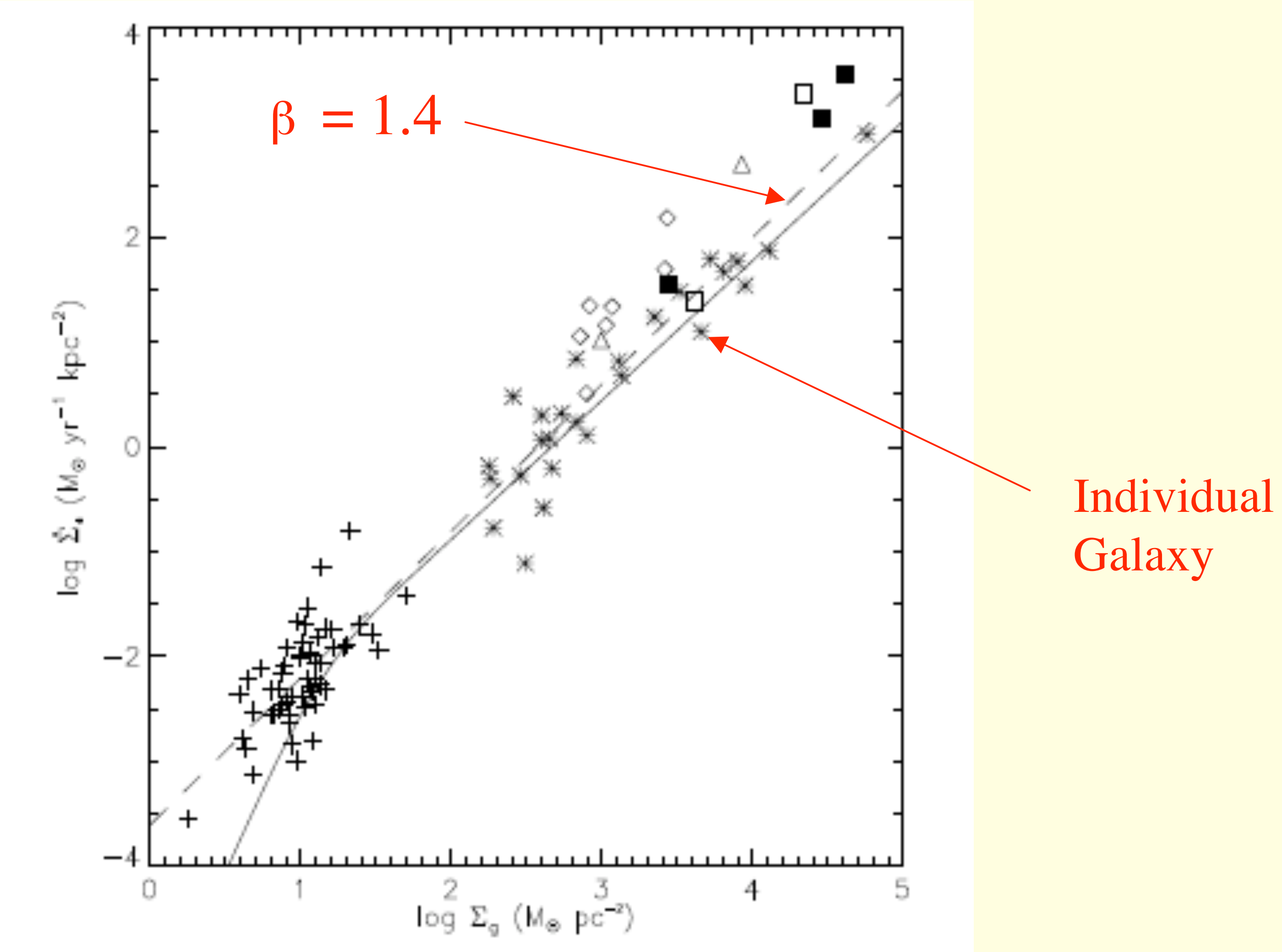

(2) Effects of Low Molecular Content in DLAs

- Median $f_{H2}=10^{-6}$ in DLAs. By comparison, $f_{H2}=10^{-1}$ in MW
- SFR~f_{H2} in most models for star formation

Contrast Between DLAs and MW

•MW: Since $N_{\rm crit}\sim N_{shield}\sim 10^{20.7}$ cm^{-2}, Toomre instability $N>N_{\rm crit}$ leads to significant molecule formation, and to star formation

•DLAs: If $N_{\rm shield}$ ($=10^{22}$) $>$ $N_{\rm crit}$ ($=10^{21.5}$), Toomre instability leads to gravitationally bound *atomic* clouds, hence no star formation.

•Reason for high $N_{\rm shield}$ in DLAs is low dust content ($\kappa=0.025$) and high FUV radiation intensities ($G_0\sim 4$).

Molecular content versus total proton column density

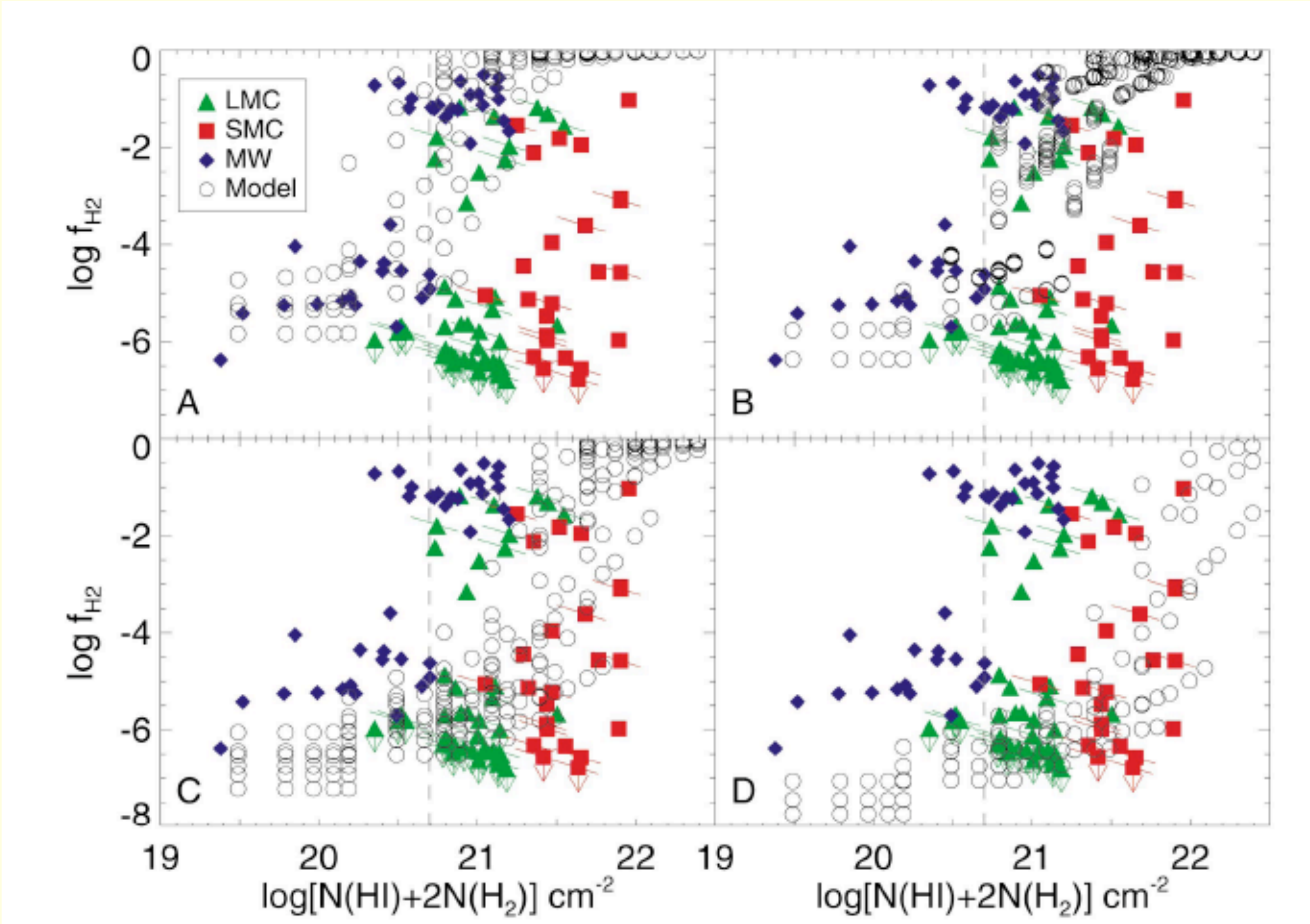

Molecular fraction versus color excess (Tumlinson etal '02)

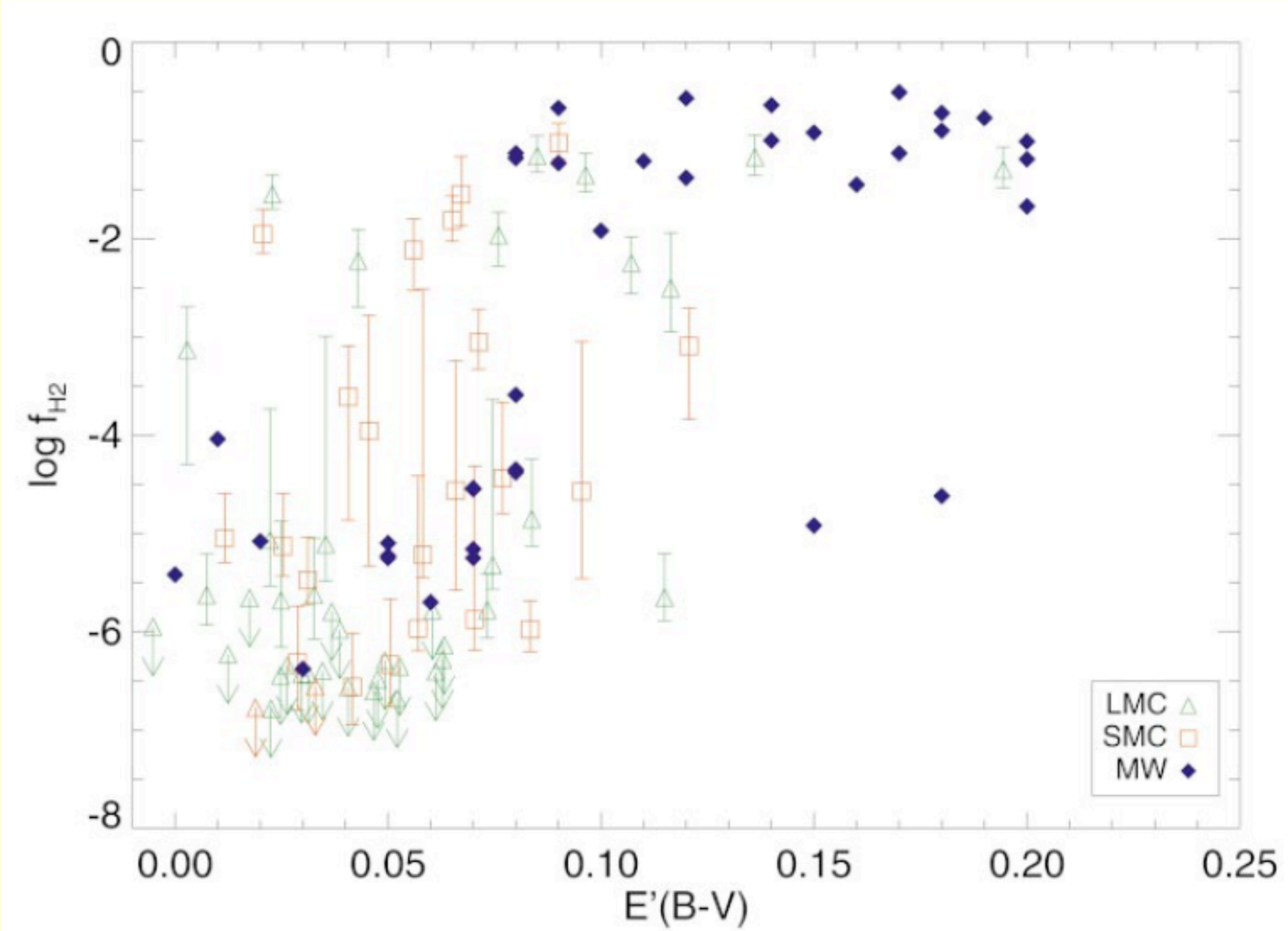

Effect of increasing N_{max}

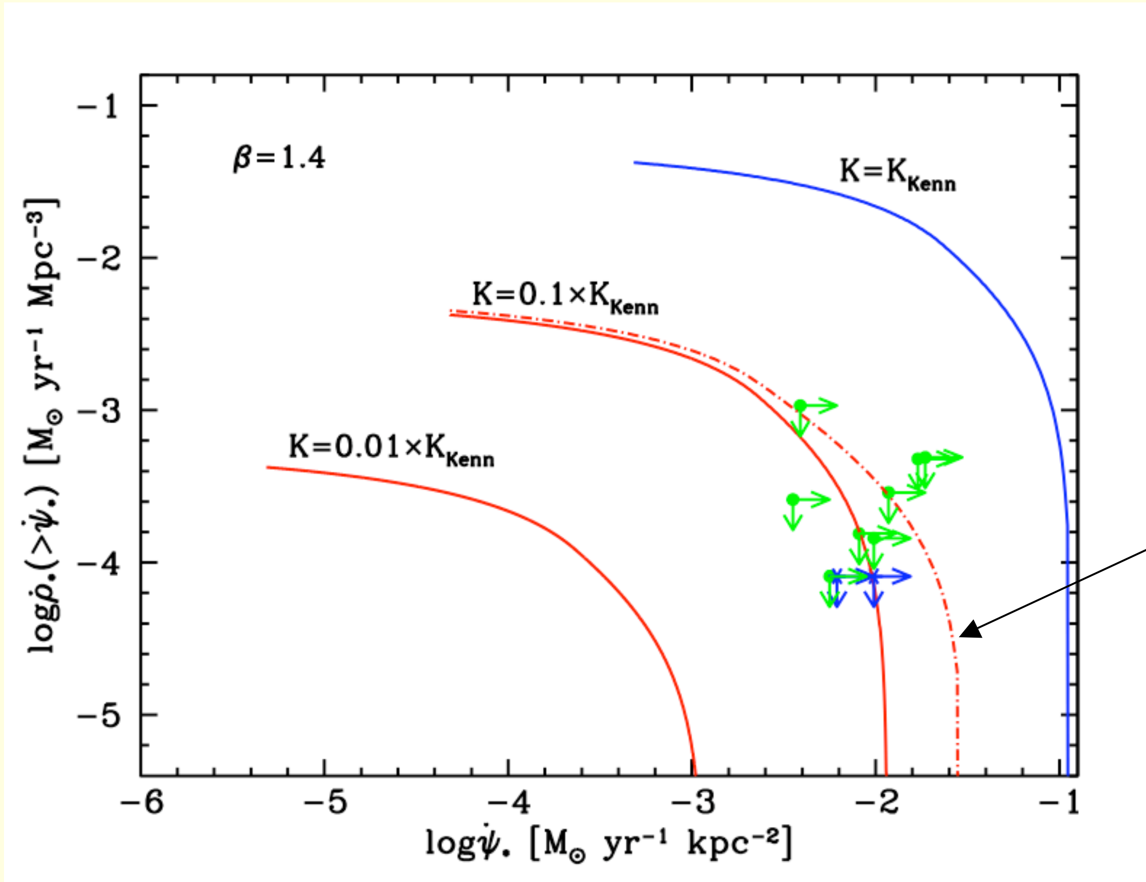

N_{max}= $2x10^{22}$

Examples of Lyman Break Galaxies

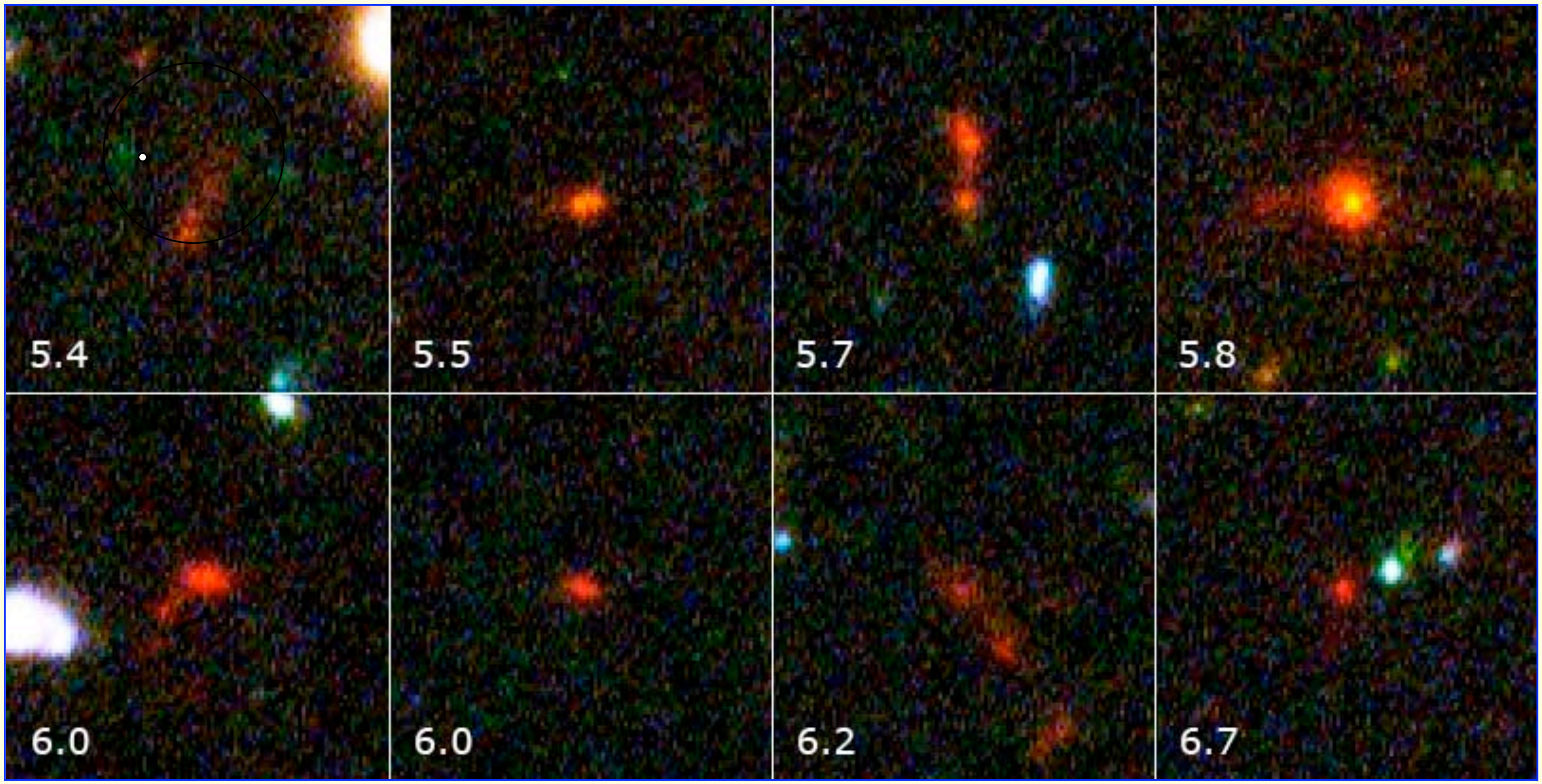

UDF Search with F606W Image

- Central λ matches FUV rest-frame wavelength of 1500Å for z=[2.5,3.5].
- FUV emitted mainly by massive stars, so $L_\nu(t)$ proportional to SFR(t)
- Same technique used to get SFRs for LBGs

- No U-band sensitivity in UDF. Therefore photometric z's unreliable. But technique valuable for obtaining upper limits on comoving SFR densities

SFR or Luminosity per unit Comoving volume

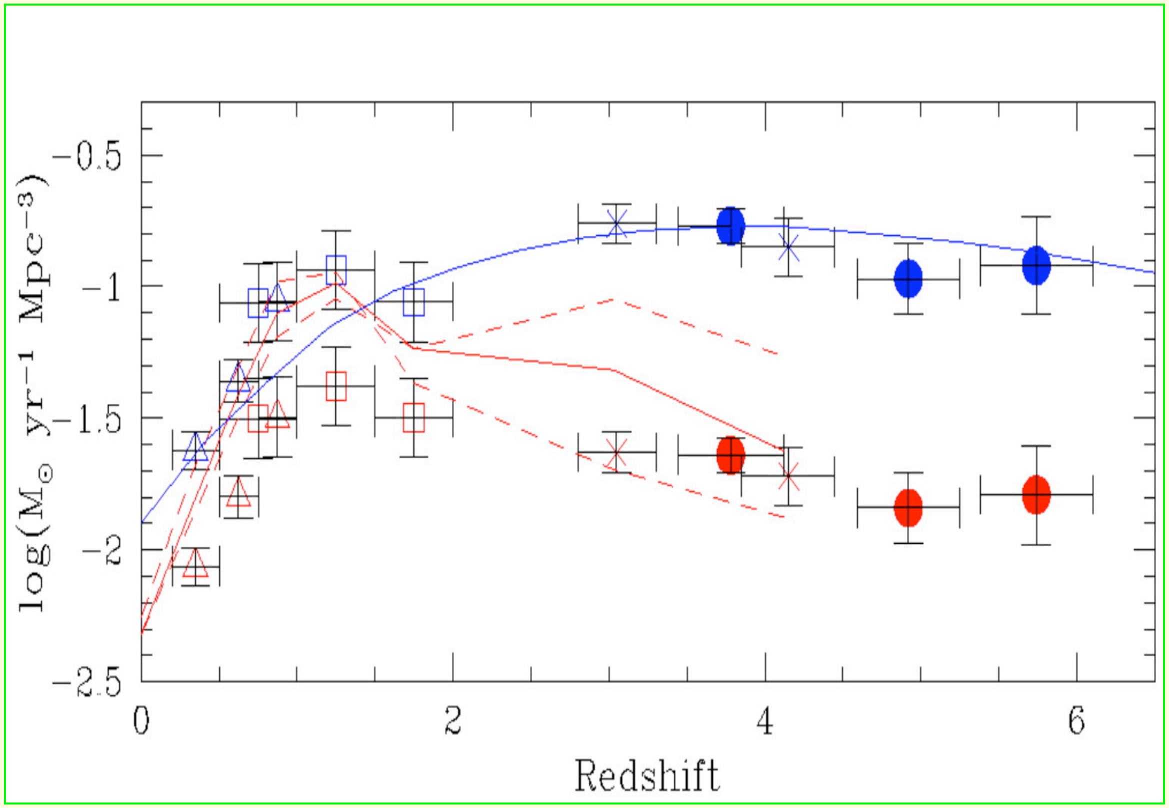

Observed

De-reddened

Consequences

- Known star formation occurs in compact objects
- SFRs higher at large redshifts
- 50 % of current stars and metals produced by z~1
- 10 % of current stars and metals produced by z~3

But This Picture is Incomplete

- At high redshifts most baryons were gas
- Since then cold, neutral gas condensed into stars and C and heavier elements formed.
- How did this happen? Throughout gas?
- SFRs of LBGs imply $\Delta\Omega_{gas} = \Omega_{visible}(z=0)$ consumed between z=5 and z=2
- External Neutral gas reservoirs may be needed

Outline: High-z Neutral Gas Reservoirs

- **Damped Lyα Systems (DLAs)**
- **Evidence for Star Formation in DLA gas**
- **Apply local Kennicutt-Schmidt law for star formation to DLAs**
- **Test predictions by searching for *in situ* star formation in HUDF**
- **DLA-LBG Connection**

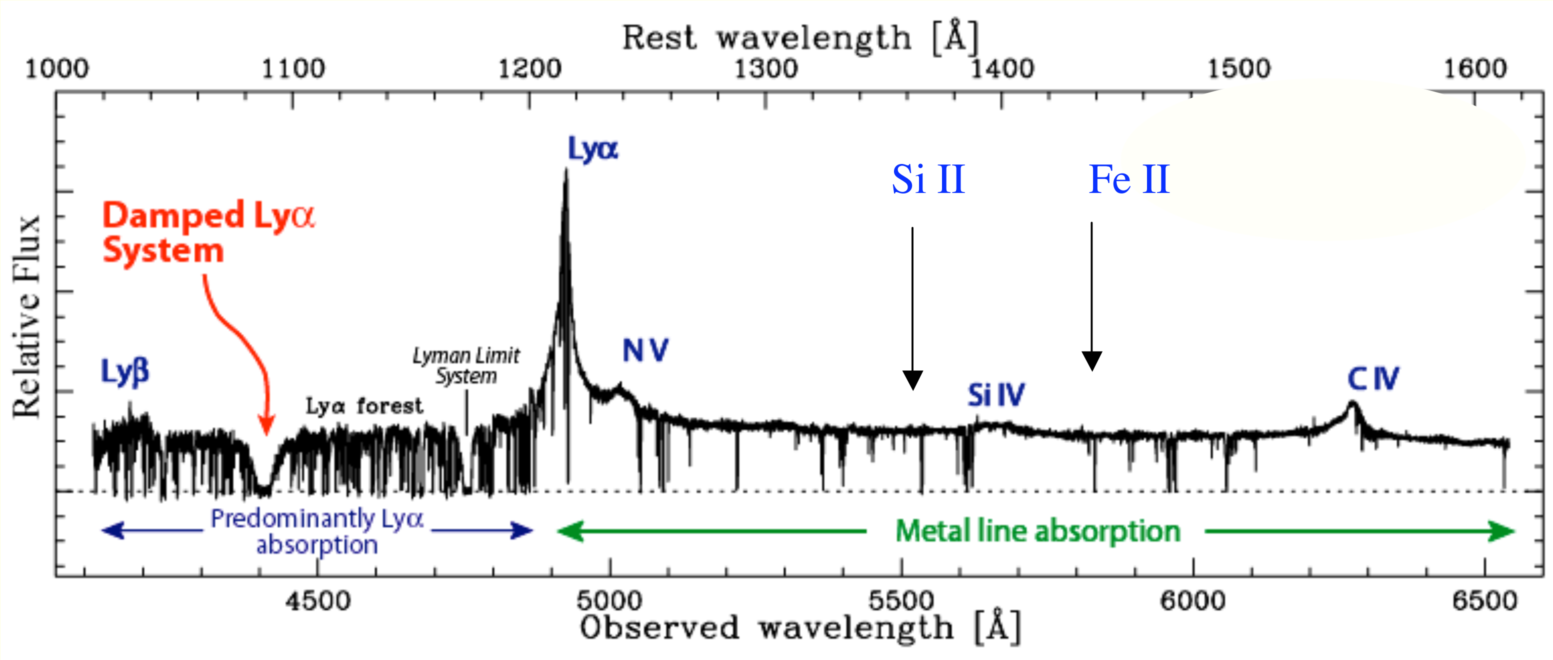

- Definition of Damped Lyα System (DLA): N(HI) > $2x10^{20}$ cm^{-2}

- Distinguishing characteristic of DLAs : Gas is Neutral

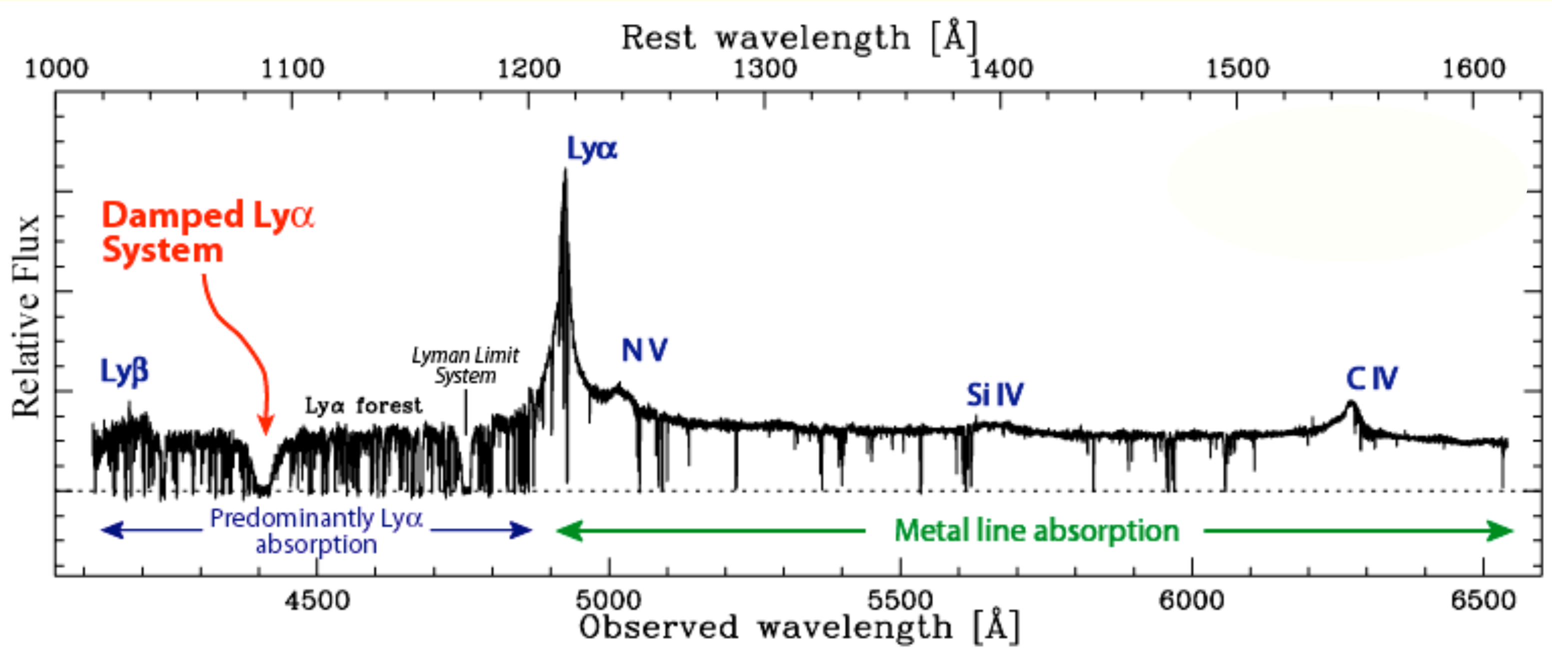

•Definition: N(HI) > 2×10^{20} cm^{-2}

•Distinguishing characteristic of DLAs : Gas is Neutral

How are DLAs heated?

Stars form out of cold gas

Measuring Mass Density of Neutral gas

- $\rho_{gas} = \langle\Sigma\rangle * f_A / L$

- Area covering fraction $f_A = 1/3$ for $z = [2.5, 3.5]$

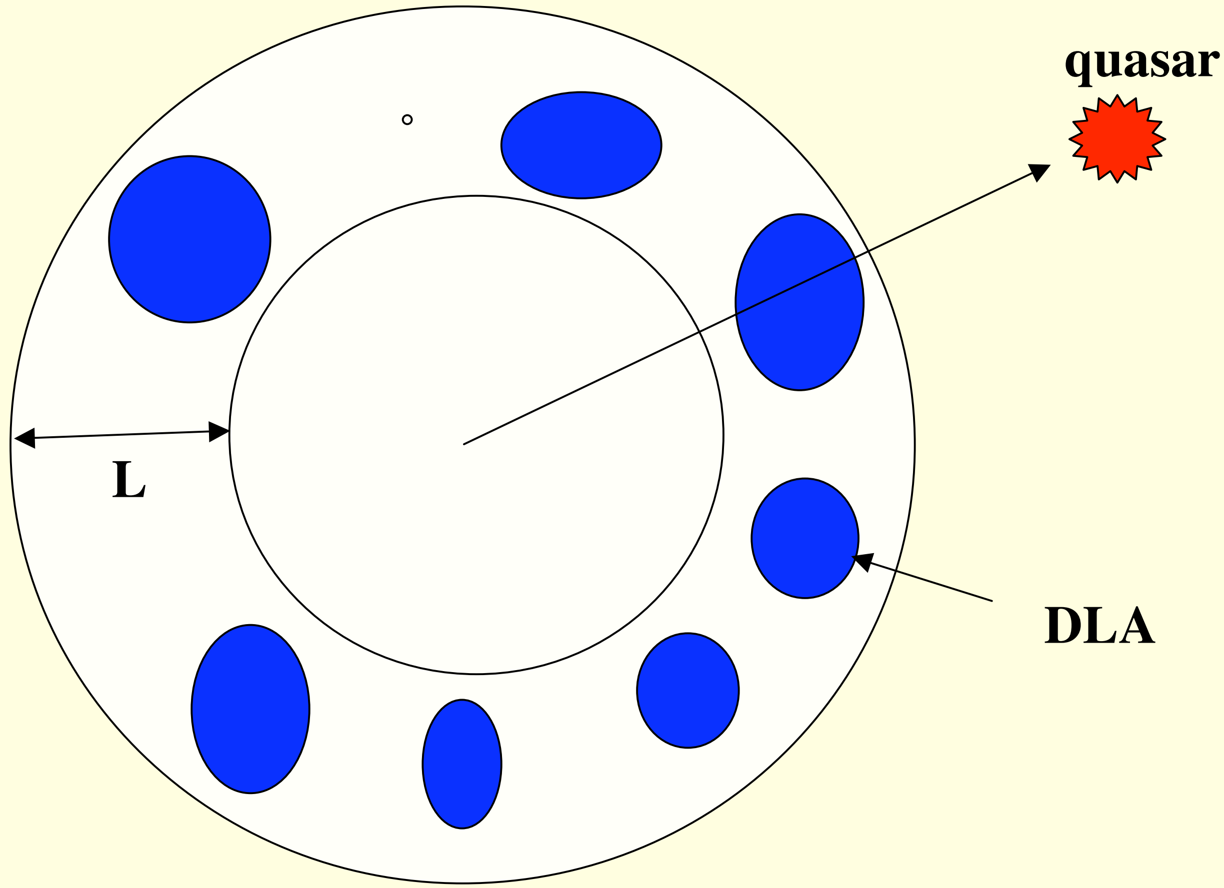

Evidence for Star Formation in DLAs?

- Evidence from Metal Abundances
- Presence of Dust
- Evidence for Starlight

Metals in DLAs

- ***Most accurate Metal abundances at high-z are for DLAs***

Ionization State of Gas is Accurately Known: $H=H^0$
Dominant ions are Si^+, C^+, Fe^+, O^0, etc.

Accurate Measurements of Keck Velocity Profiles

- ***Metals are Byproducts of Star Formation***

- ***Abundance Ratios are Signatures of Star Formation Histories***

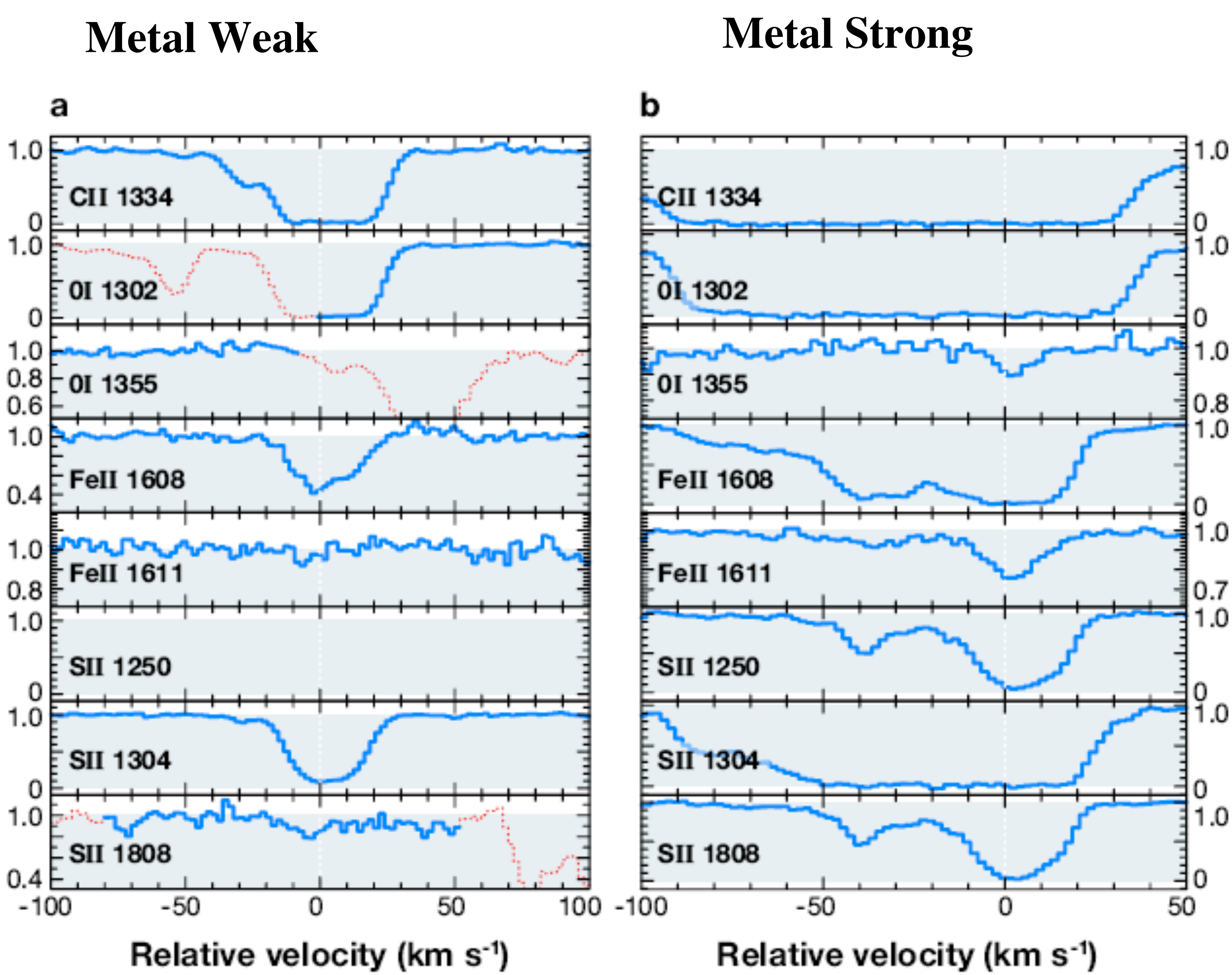

Metal Weak
Metal Strong
a
b
CII 1334
OI 1302
OI 1355
FeII 1608
FeII 1611
SII 1250
SII 1304
SII 1808
Relative velocity (km s-1)
Relative velocity (km s-1)

DLA Age-Metallicity Relationship

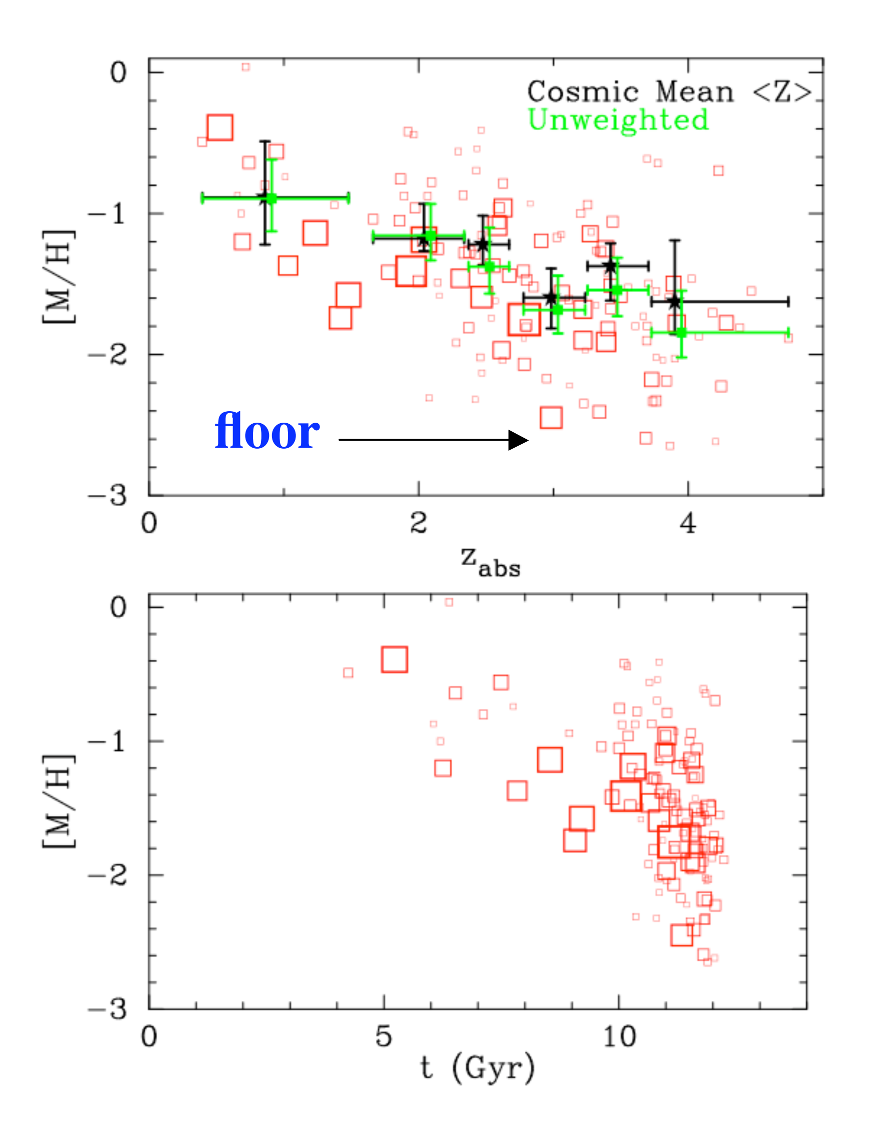

- Sub-solar metals at all z. But [M/H] underestimated at low z due to undersampling.
- Statistically Significant evidence for increase of metals with time
- Most DLAs detected at epochs prior to formation of Milky Way Disk
- But too many metal-poor galaxies would result if high-z gas turned into stars

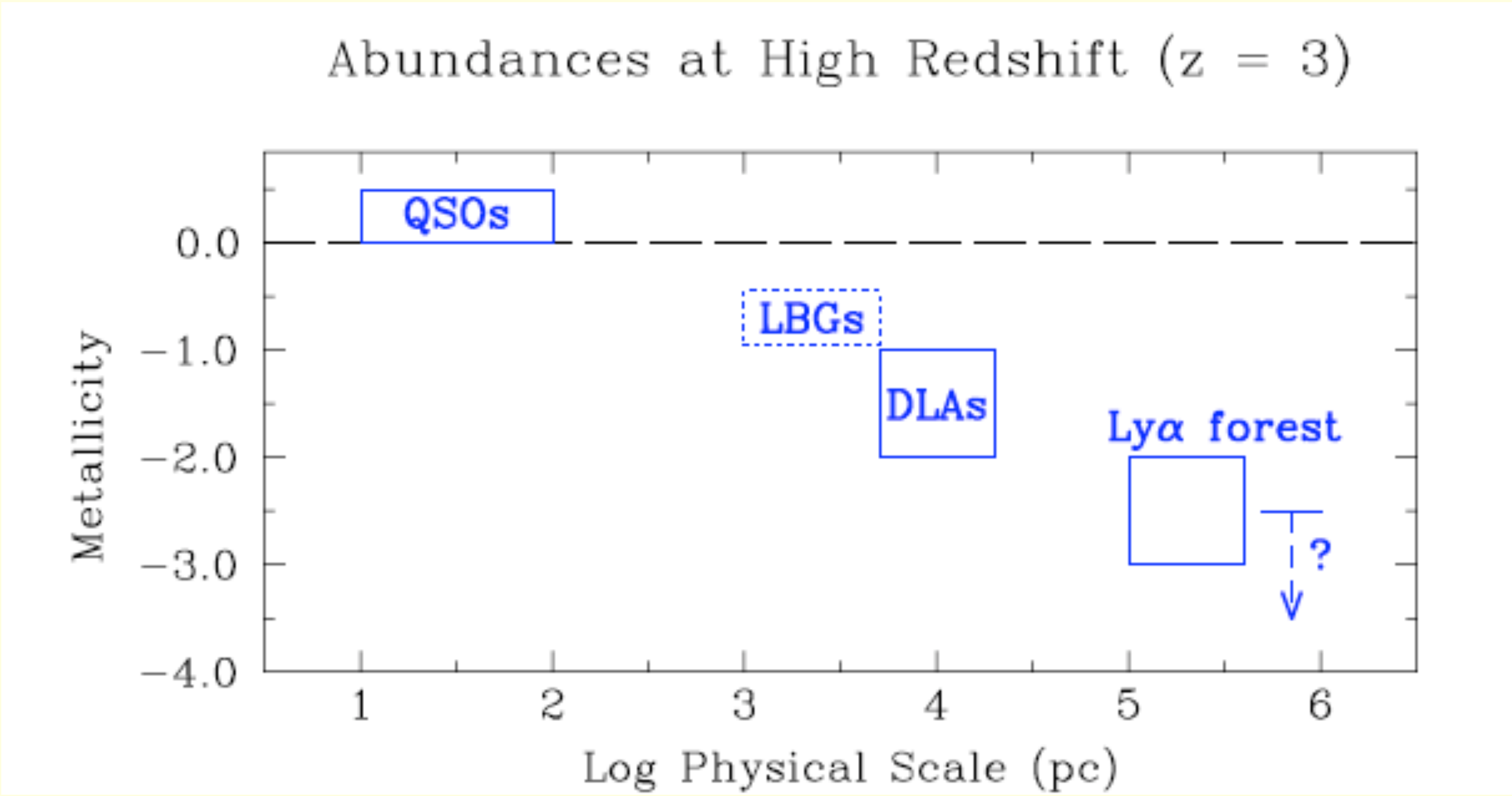
Abundances at High Redshift (z = 3)
QSOs
LBGs
DLAs
Lyα forest
?
0.0
−1.0
−2.0
−3.0
−4.0
Metallicity
1
2
3
4
5
6
Log Physical Scale (pc)

Comoving SFR Density

face-on disks

$$\mathbf{d}\dot{\rho}_* = \mathbf{n_{co}dA_\perp} \times [(\dot{\psi}_*)_\perp] \quad ,$$

$$SFR = dA_\perp \times (\dot{\psi}_*)_\perp$$

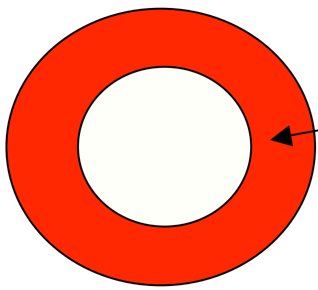

inclined disks

$$\mathbf{d}\dot{\rho}_* = \mathbf{n_{co}dA_\perp cos(i)} \times [(\dot{\psi}_*)_\perp / \mathbf{cos(i)}] \times \mathbf{sin(i)di} \quad ,$$

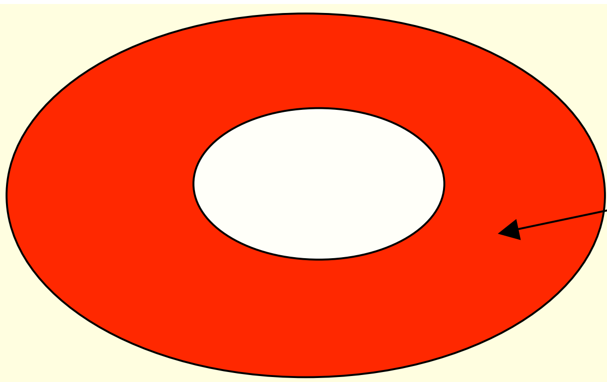

$$SFR = dA_\perp cos(i) \times \frac{(\dot{\psi}_*)_\perp}{cos(i)}$$

$$\mathbf{f_\perp(N_\perp, X) dN_\perp \equiv (c/H_0) n_{co} dA_\perp}$$

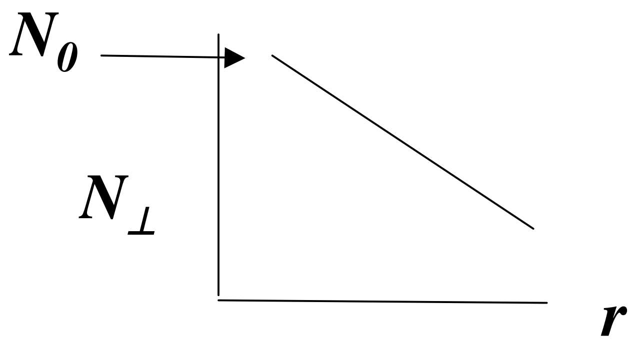

Since $\cos(i) = N_\perp / N$

$$\dot{\rho}_*(\geq N) = \frac{H_0}{c} \int_N^{N_{max}} dN K (N/N_c)^\beta \int_{N_{min}}^{\min(N_0,N)} dN_\perp f_\perp(N_\perp, X)(N_\perp^2/N^3)(N_\perp/N)^{\beta-1}$$

where $f_\perp(N_\perp, X)$ **and** $f(N, X)$ **are related by**

$$f(N, X) = \int_{N_{min}}^{\min(N_0,N)} dN_\perp f_\perp(N_\perp, X)(N_\perp^2/N^3)$$

Observed H I Column-Density Distribution Function

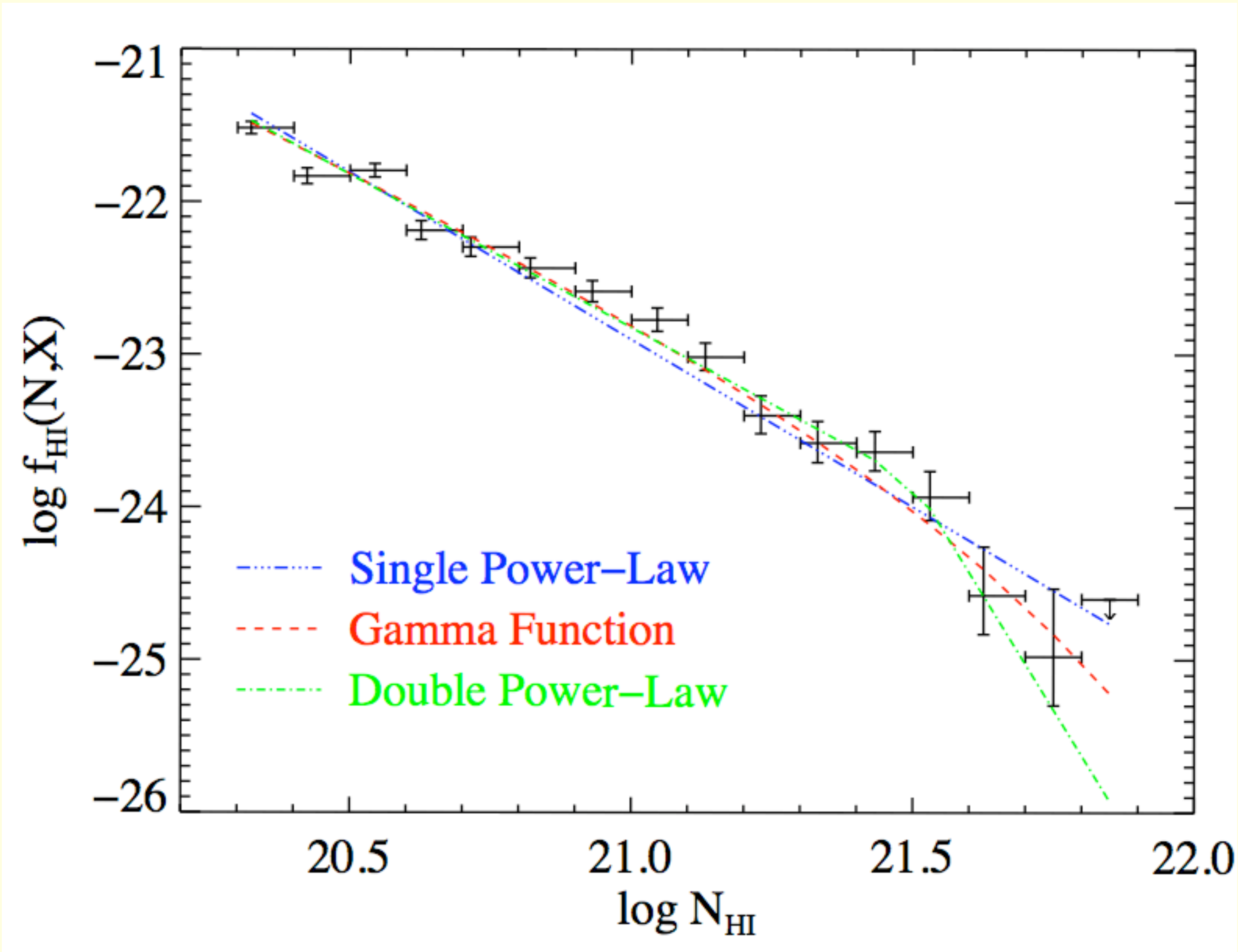

UDF Search with F606W Image

- Central λ matches FUV rest-frame wavelength of 1500Å for z=[2.5,3.5].
- FUV emitted mainly by massive stars, so $L_\nu(t)$ proportional to SFR(t)
- Same technique used to get SFRs for LBGs

- No U-band sensitivity in UDF. Therefore photometric z's unreliable. But technique valuable for obtaining upper limits on comoving SFR densities

Results of UDF Search

- **Unsmoothed Image (θ_{psf}=0.09"):**
  -Found 11,000 objects with V<30.5
  -None satisfied criteria for *in situ* star formation at Kennicutt-rate: i.e. , μ_V > 26 , θ_{dla} > 0.25"
- **Smoothed Images:**
  -Removed HSB objects
  -Smoothed image with Gaussian kernels with FWHM=θ_{kern} to enhance SNR when θ_{kern}=θ_{dla}
  -Let θ_{kern}=0.25" to 4.0" or d_{dla}=1.9 kpc to 31 kpc

Threshold Determinations from Simulations

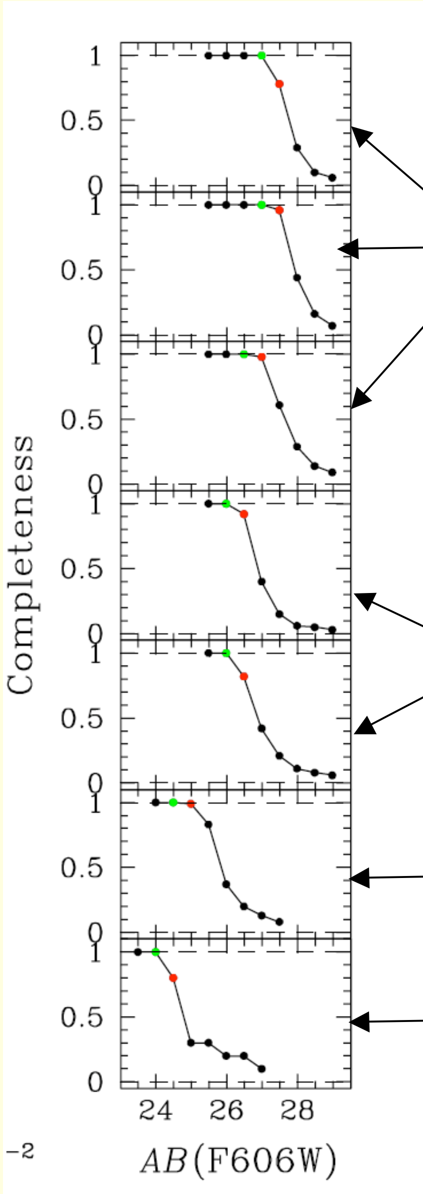

θ_{DLA}

0.5"

1.0"

2.0"

4.0"

1. **Place 10^3 objects with identical V magnitude, θ_{DLA} , on UDF image**

2. **Compute recovery fraction as function of V magnitude**

3. **In principle threshold given by $N_{recover}=N_{95}$**

4. **In practice we used more conservative threshold given by $N_{recover}=200$**

Why is Star Formation Less Efficient at High z ?

1. ***Critical Surface Density Increases with redshift***

   – $\Sigma_{crit}(R_{disk})=(2^{1/2}V_c/R_{disk})\sigma/\pi G$

   -Spherical Collapse Model: $V_c/R_{200}=10H(z)$

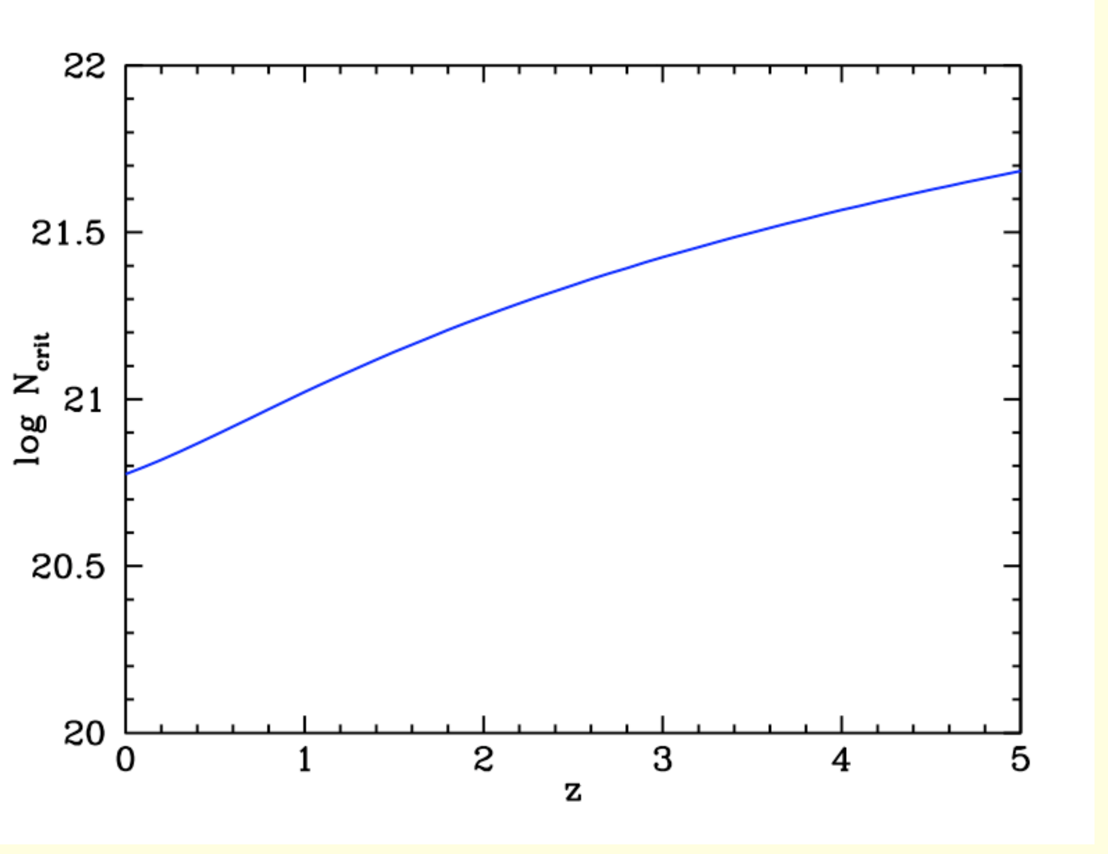

Evidence for Threshold Surface Densities at z=0

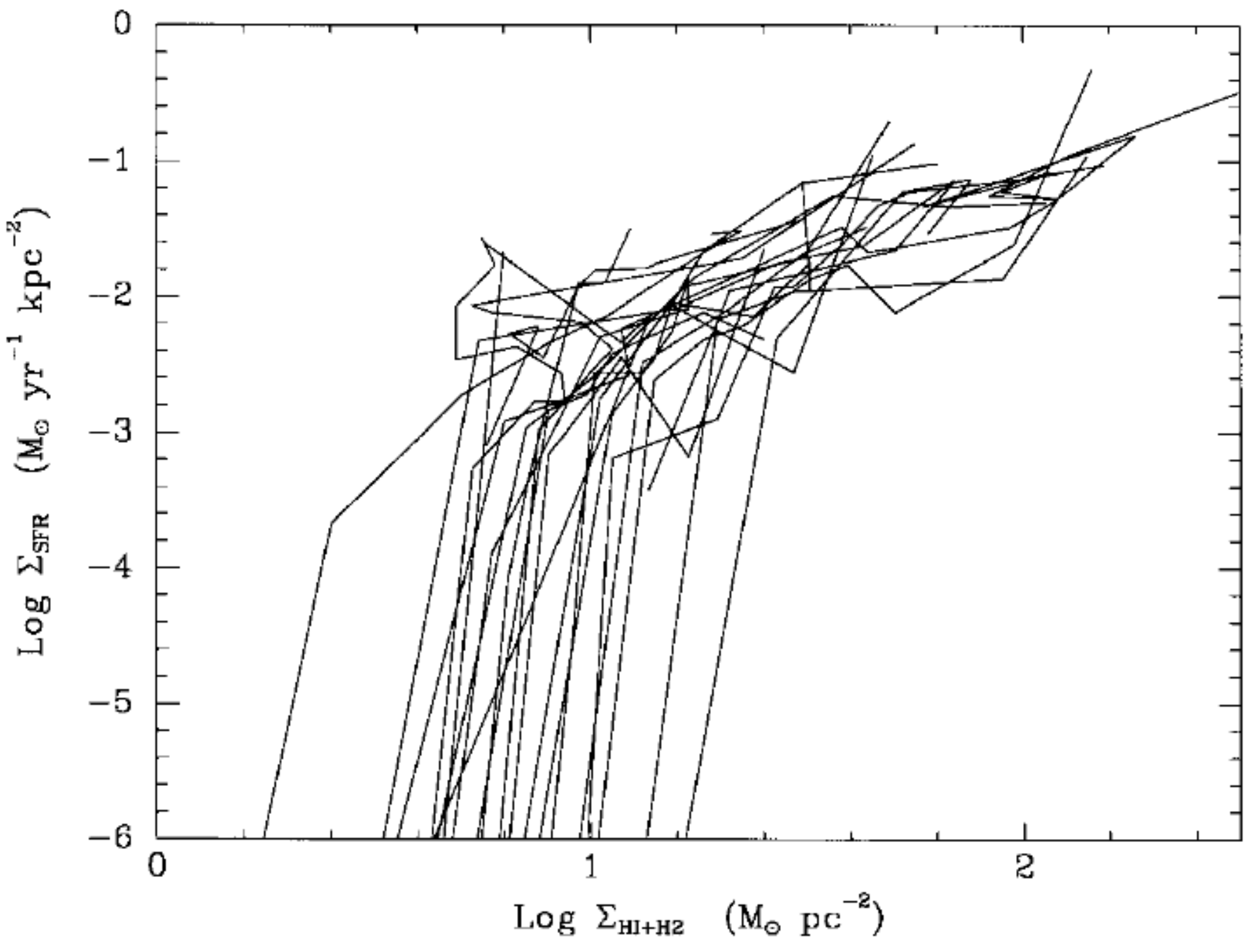

FIG. 3.—Profiles of the azimuthally averaged SFR per unit area as a function of gas density for 21 spirals with spatially resolved Hα data.

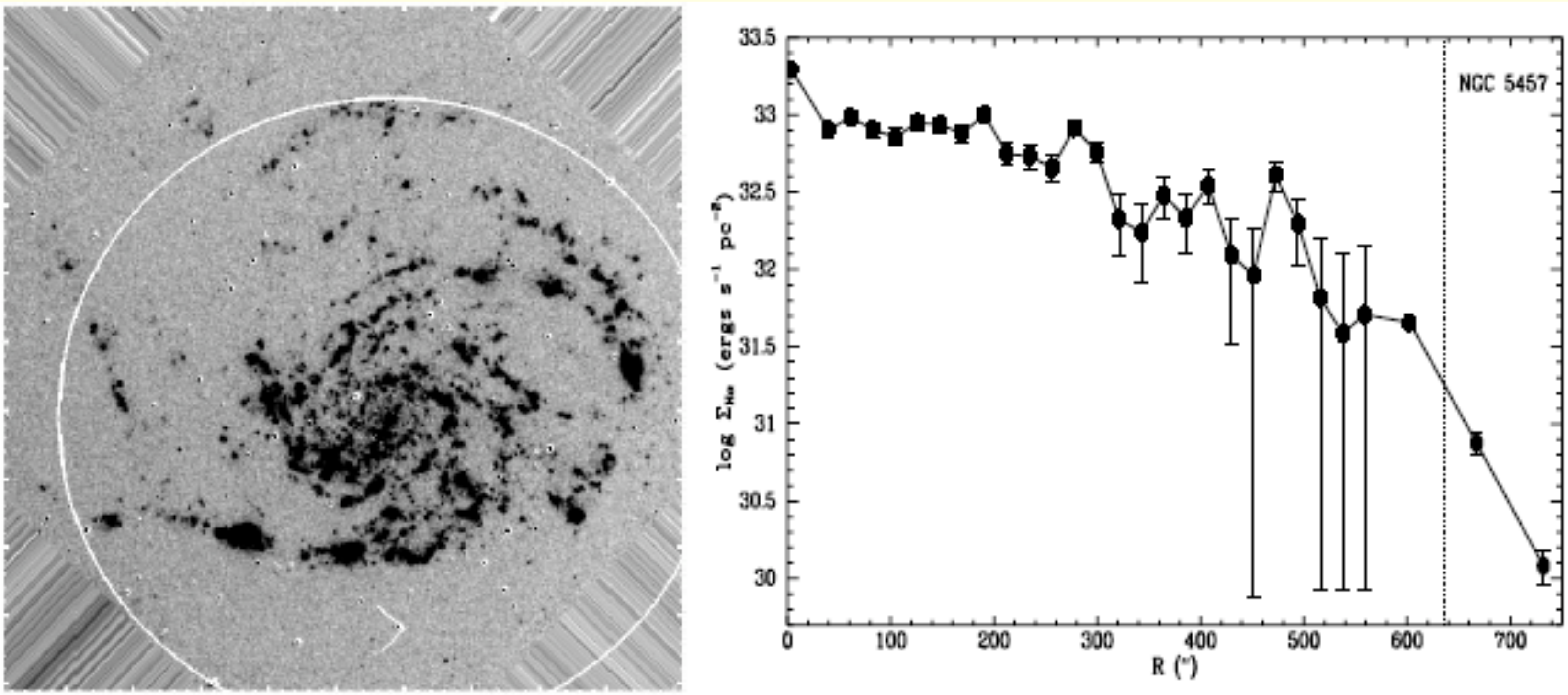

NGC 5457
log $\Sigma_{H\alpha}$ (ergs s^{-1} pc^{-2})
R (")
33.5
33
32.5
32
31.5
31
30.5
30
0
100
200
300
400
500
600
700

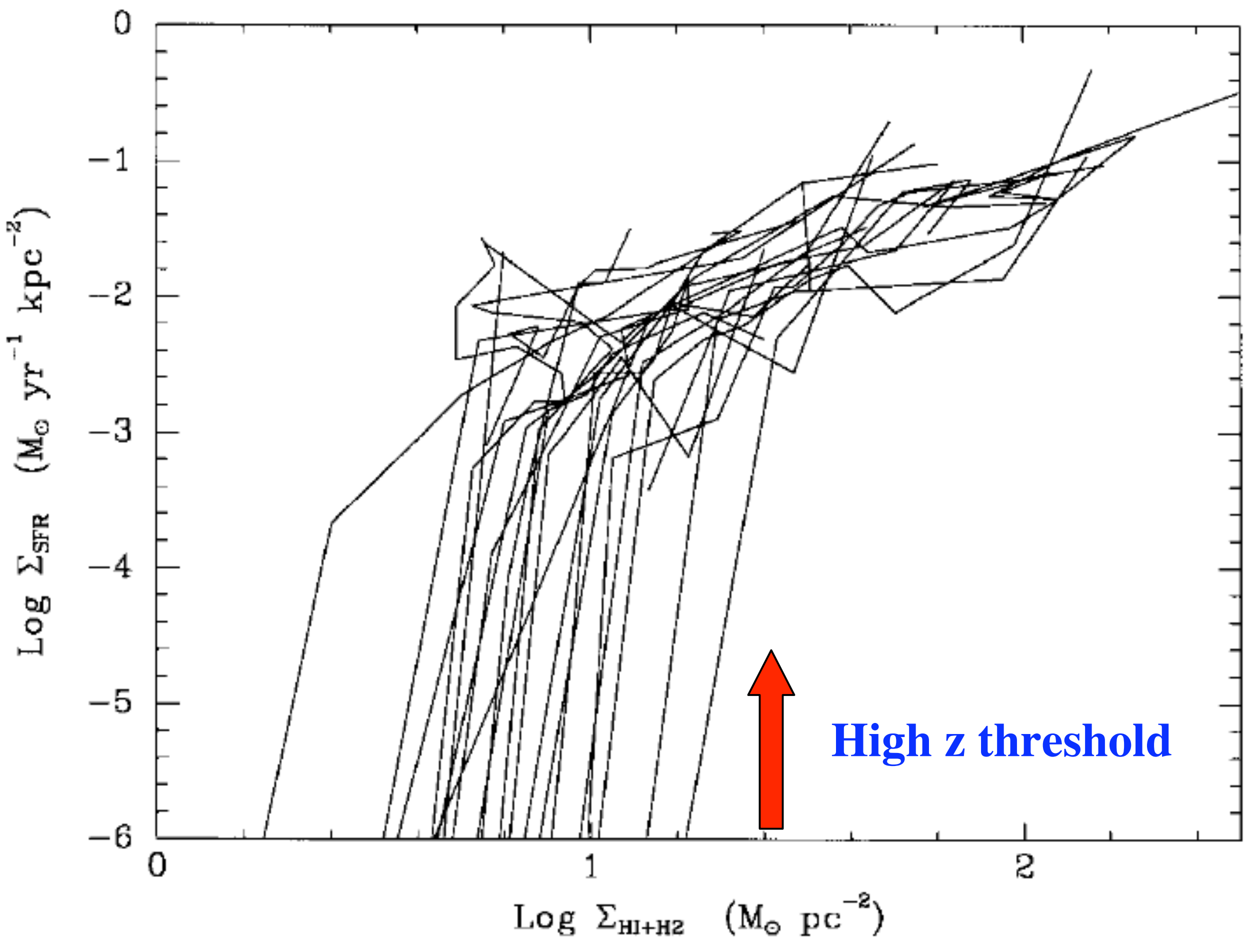

FIG. 3.—Profiles of the azimuthally averaged SFR per unit area as a function of gas density for 21 spirals with spatially resolved Hα data.

2. Does Low Molecular Content of DLAs imply low SFR?

-But R(HII) in Nearby Galaxies is independent of f_{GMC}

-Implication is that gravitational (Toomre) instability of gas is sufficient condition for star formation

3. Lower gas volume densities could suppress SFR

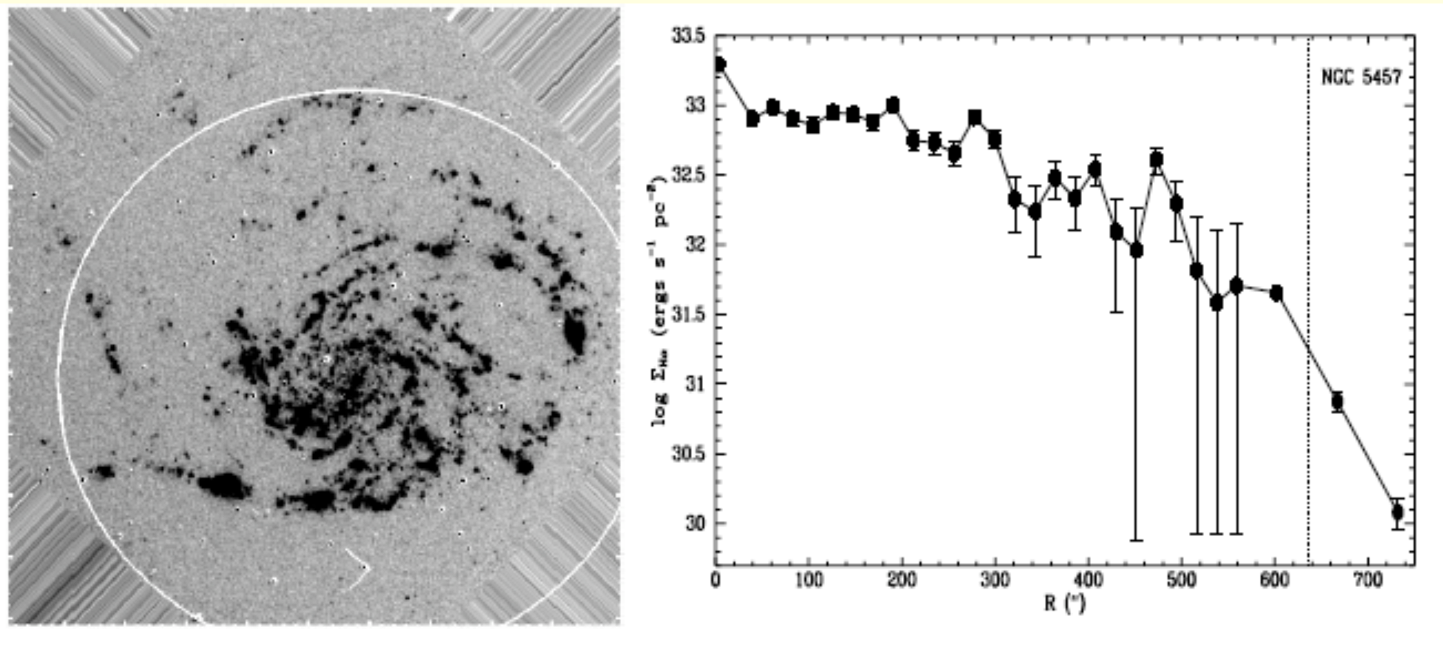
NGC 5457
log $\Sigma_{H\alpha}$ (ergs s^{-1} pc^{-2})
R (")

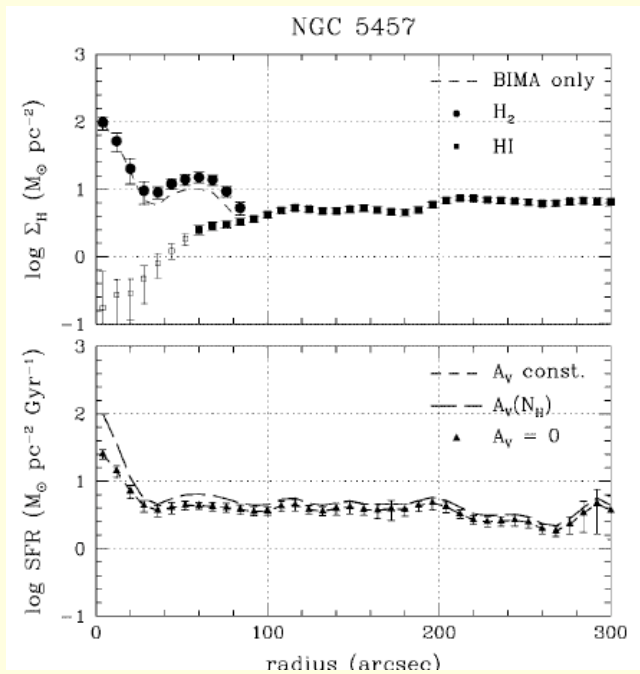
NGC 5457
BIMA only
H_2
HI
log Σ_H ($M_\odot$ pc^{-2})
A_V const.
$A_V(N_H)$
A_V = 0
log SFR ($M_\odot$ pc^{-2} Gyr^{-1})
radius (arcsec)

Consequences of upper limit on comoving SFR density

Upper limit: $d\rho_*/dt < 10^{-2.4}\ M_\odot\ yr^{-1} Mpc^{-3}$

1. ***Limit on Metal Production***

-Predicted [M/H] < -1.9

compared to measured [M/H]=-1.4±0.07

-Source of Observed Metals?

2. ***Limit on Energy Input from stars into neutral gas***

Are DLAs Passive Layers of Gas?

- **Element Abundance "Floor" implies enrichment process exceeding that of Intergalactic Medium**

- **Energy Input into ~50% of Known DLAs exceeds radiative heating rate due to Ultra-Violet and Soft X-ray background radiation**

  - **--Heating Rates inferred from measured cooling rate per H atom.**

  - **--Cooling rates measured by inferring [C II] 158 μm emission**

Does Global Heating Rate Balance Global DLA Cooling Rate?

- **Global Cooling Rate per unit Comoving Volume:**

$$C = \langle l_c \rangle \Omega_{gas} \rho_{crit} / (\mu m_H) = (2 \pm 0.5) \times 10^{38} \text{ ergs s}^{-1} \text{ Mpc}^{-3}$$

- **Global Heating Rate (grain photoelectric effect):**

$$H = 10^{-5} \frac{\kappa \epsilon < N >}{8\pi} [1 + ln(R/h)] \int \phi(L_\nu) L_\nu dL_\nu$$

--κ is the dust-to-gas ratio

--ε is the grain photoelectric heating efficiency

$H_{DLA} < 4 \times 10^{37}$ erg s^{-1}Mpc^{-3}

$H_{LBG} = (3 \pm 2) \times 10^{38}$ ergs s^{-1}Mpc^{-3} (uncorrected for extinction)

Summary of Results

•Application of Kennicutt-Schmidt Law to neutral gas at high z predicts significantly higher comoving SFR densities than observed

•Physical Implications

-SFR Efficiency is lower in high-z neutral gas

-Explanation ?

Increase in critical density with z

lower molecular content of gas

lower volume density

•Astrophysical Implications

-Predicted metal content lower than observed at z~3

-Comoving cooling rate of gas exceeds upper limits on heating rate due to *in situ* star formation in gas

•Suggested Scenario

-DLAs with higher [C II] cooling rates powered by centrally located LBGs, which may also supply required metals

• Star formation mode: central bulge formation at z > 2. Switch to wide spread star formation at lower z's

Emerging Picture

- **At high z, star formation and element production occurs mainly in compact LBGs.**

- **DLAs are neutral gas reservoirs that supply "fuel" for LBG star formation rate.**

- **Questions**

(1) How does DLA gas become chemically enriched?
DLA abundance pattern indicates core-collapse SNe.

(2) Why is star formation suppressed in DLA gas?

(3) Galaxies at $z < 1.5$ exhibit star formation over large areas. What causes shift from compact to diffuse mode?

Search for LBGs Associated With DLAs

Keck R-band Image with 5 U-band dropouts associated With z=2.936 DLA

Δz less than 900 km s^{-1}

10h^{-1} Mpc

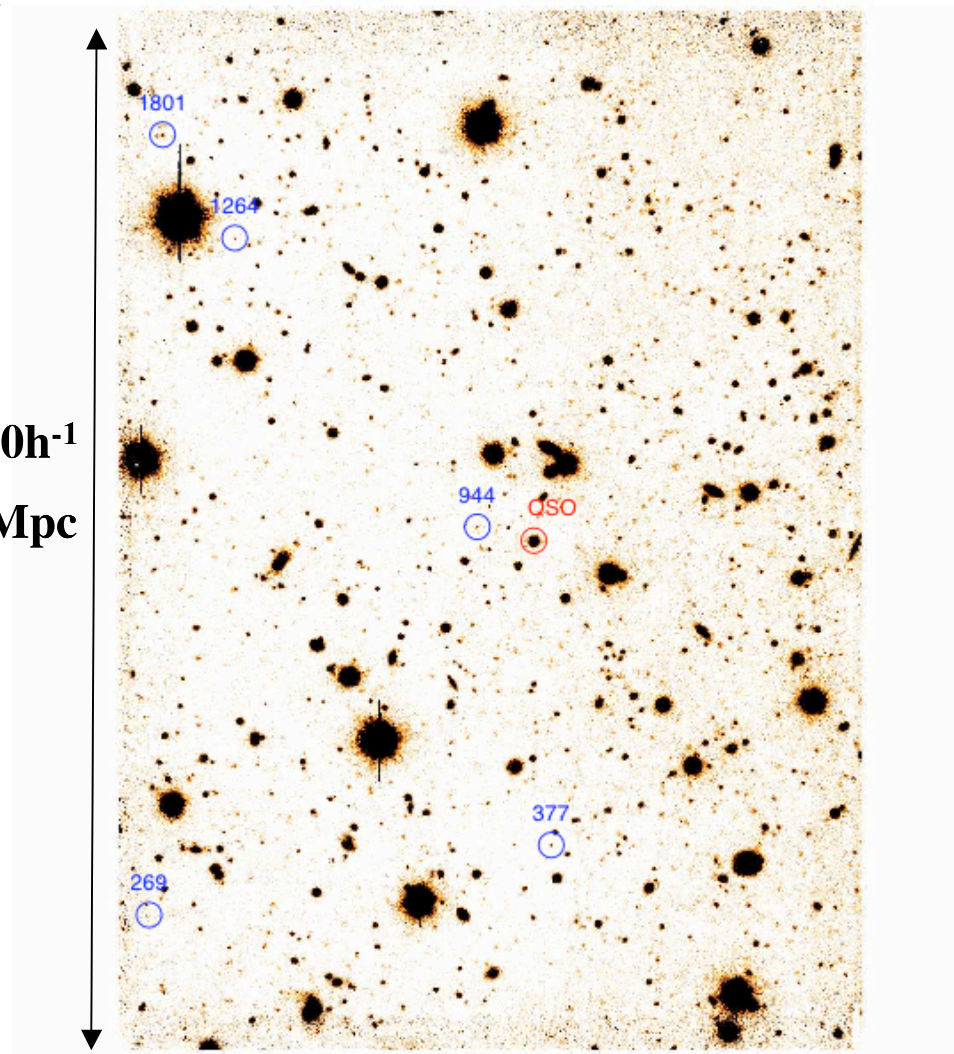

7h^{-1} Mpc

Detection of [C II] 158 μm Emission from DLAs

- Benefits
  - Determine spatial extent of cold gas
  - Determine DM mass from line widths
  - Determine total cooling and heating rates

- Is it possible?
  - Detected in all late-type galaxies
  - ALMA required for high-z detection

[C II] contours superposed on 6.75 μm Image

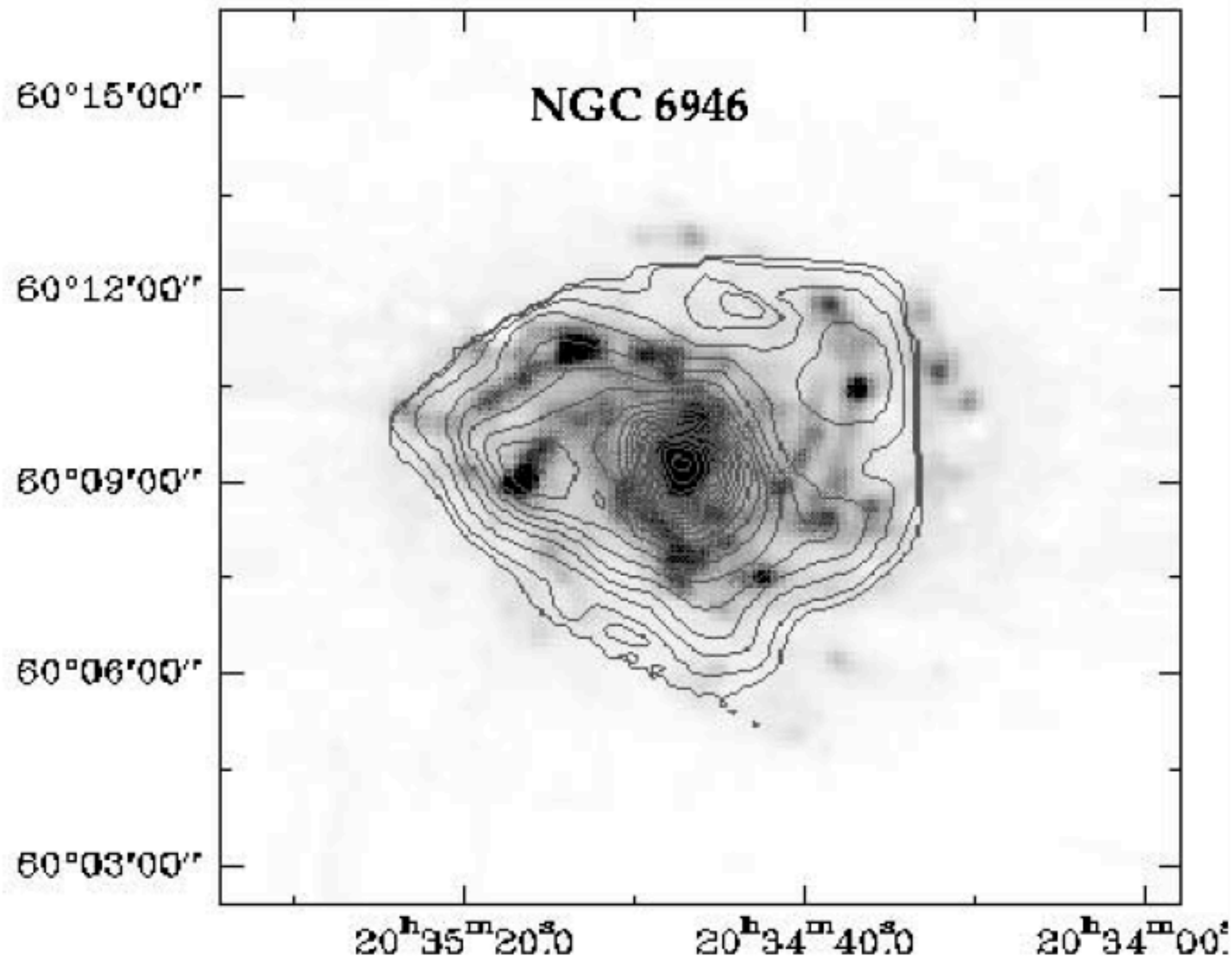

[C II] Flux Densities Predicted for DLAs

Estimate of S_{ν_0} for DLA2206−19A, z=1.92:

$$S_{\nu_0} = 1.35\left(\frac{M_{\rm HI}}{10^{10}M_\odot}\right)\left(\frac{\ell_c}{10^{-26.2}{\rm ergs\ s^{-1}\ H^{-1}}}\right)\left(\frac{100{\rm km\ s^{-1}}}{\Delta v}\right)\ {\rm mJy}$$

Predicted $S_{\nu 0}$ for DLA 2206-19A

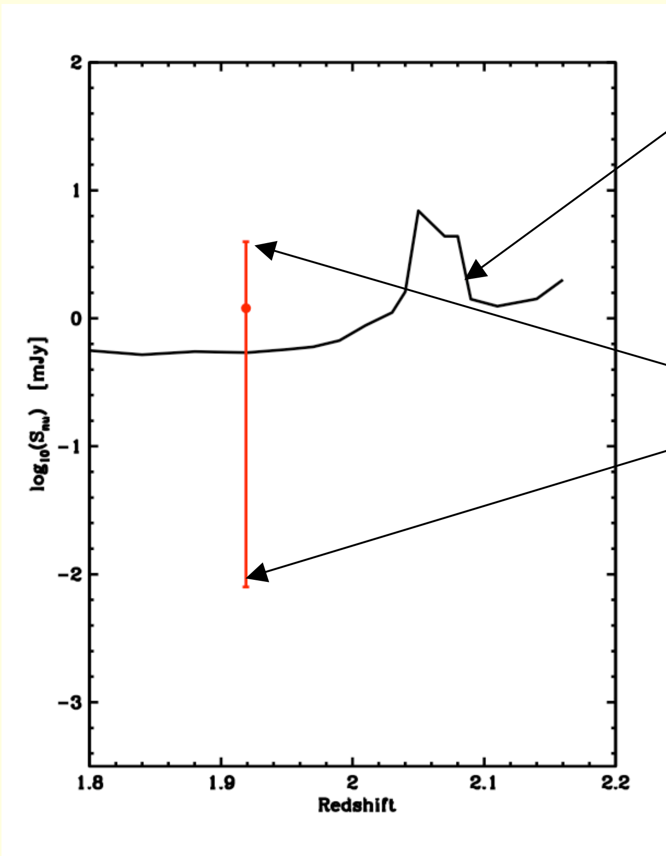

- *3 σ Alma limit for 20 hr integration time*
- *90 % Mass range predicted for CDM Models of DLAs*
- *$M_{H\ I} = m_D M$*

Predicted Distribution of 158 μm Flux Densities (Nagamine etal '06)

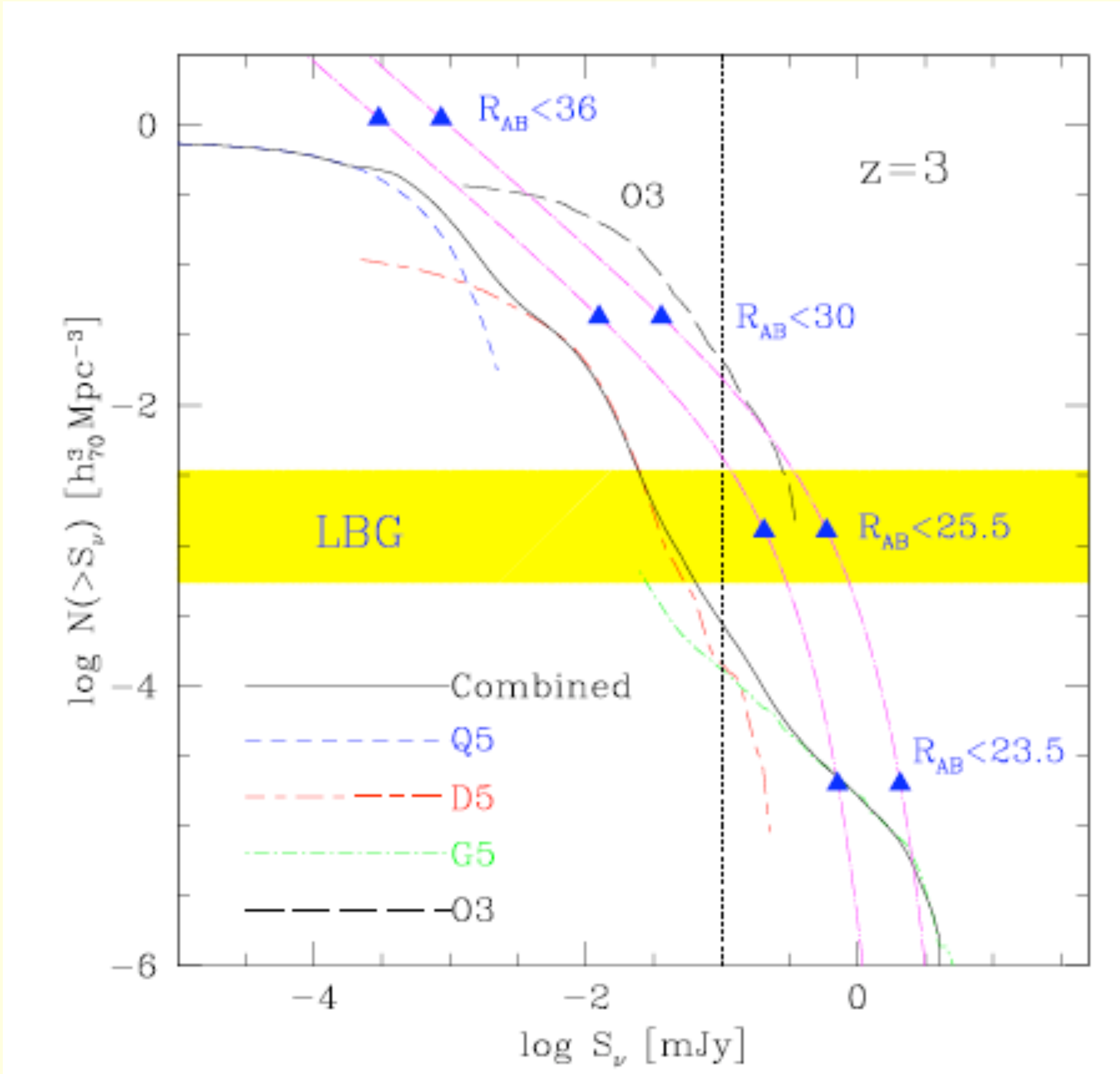

Metal Strong DLA at z=2.6: Probing Nucleosynthesis

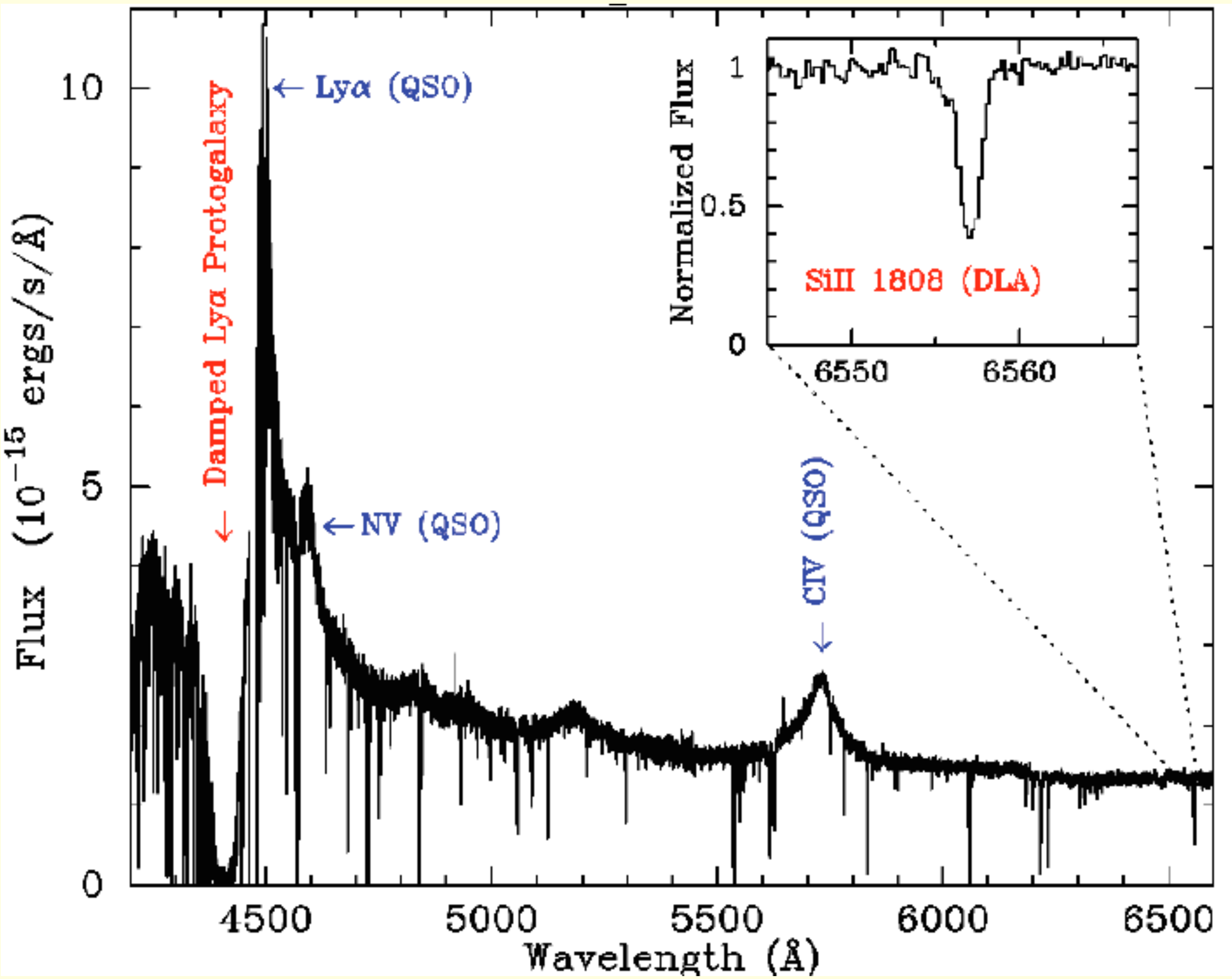

Abundance Pattern at z=2.6

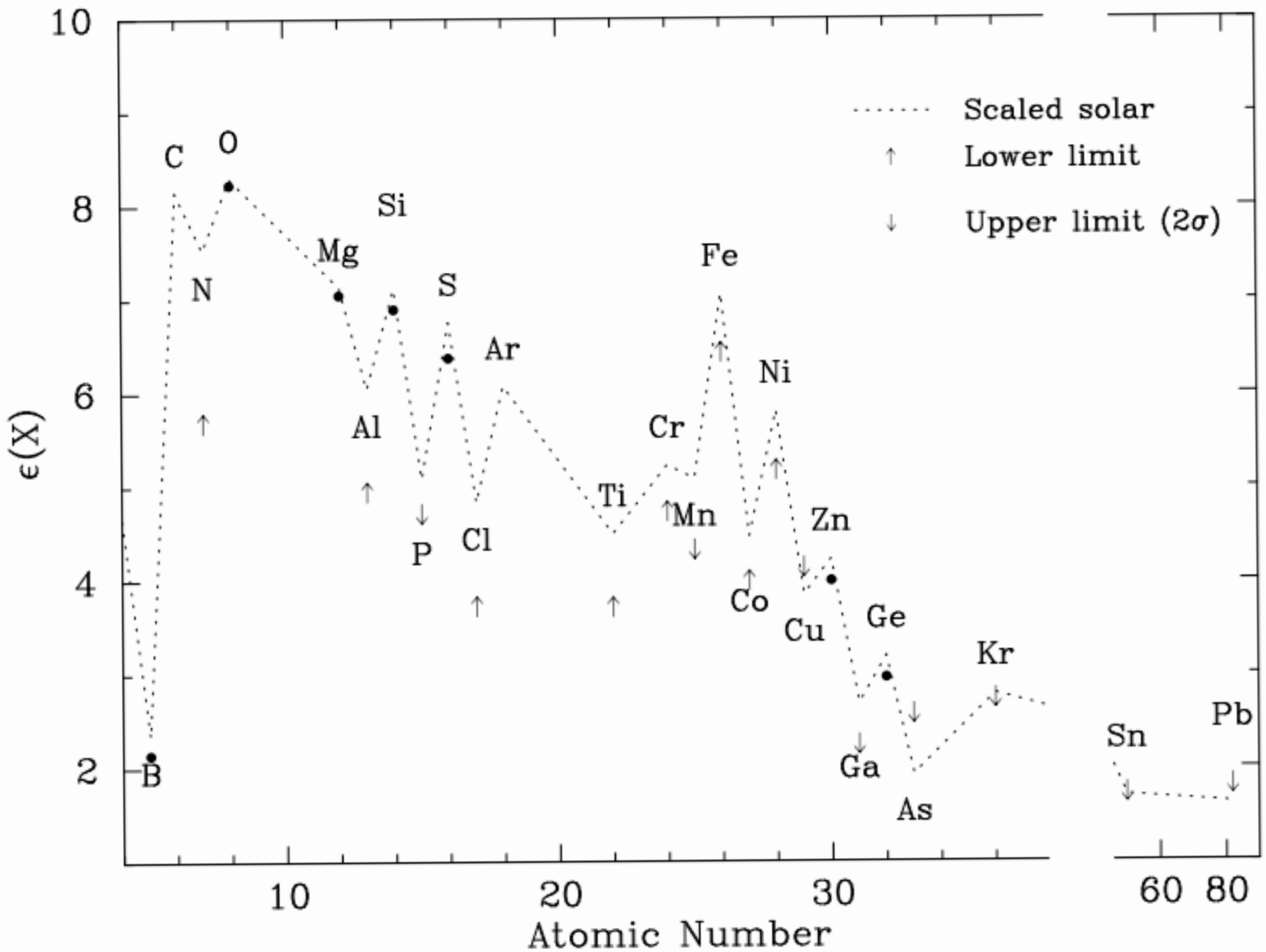

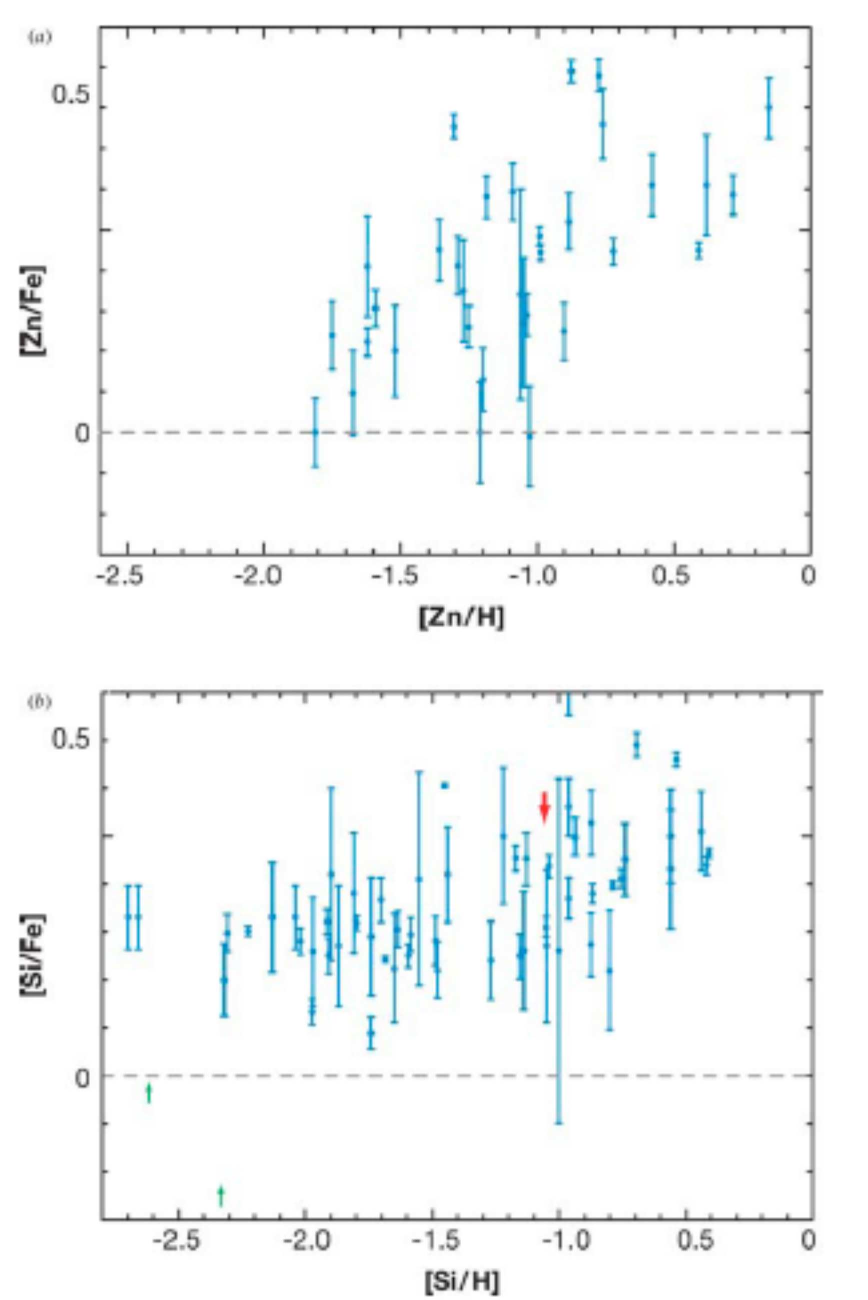
(a)
[Zn/Fe]
0.5
0
-2.5
-2.0
-1.5
-1.0
0.5
0
[Zn/H]
(b)
[Si/Fe]
0.5
0
-2.5
-2.0
-1.5
-1.0
0.5
0
[Si/H]

Grain Photoeletric Heating of Neutral Gas in DLAs

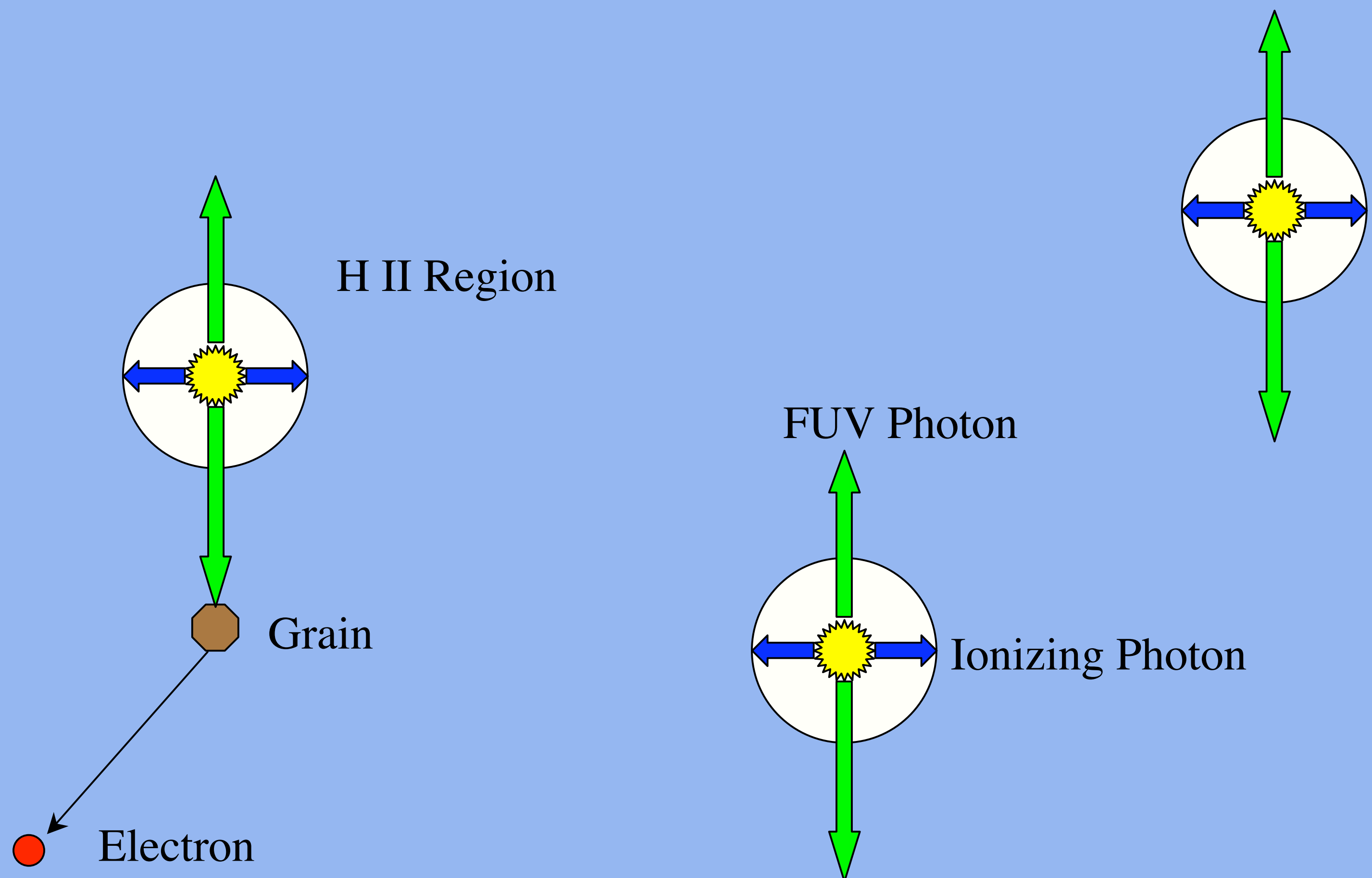

(3) Critical Surface Density Increasing function of *z*

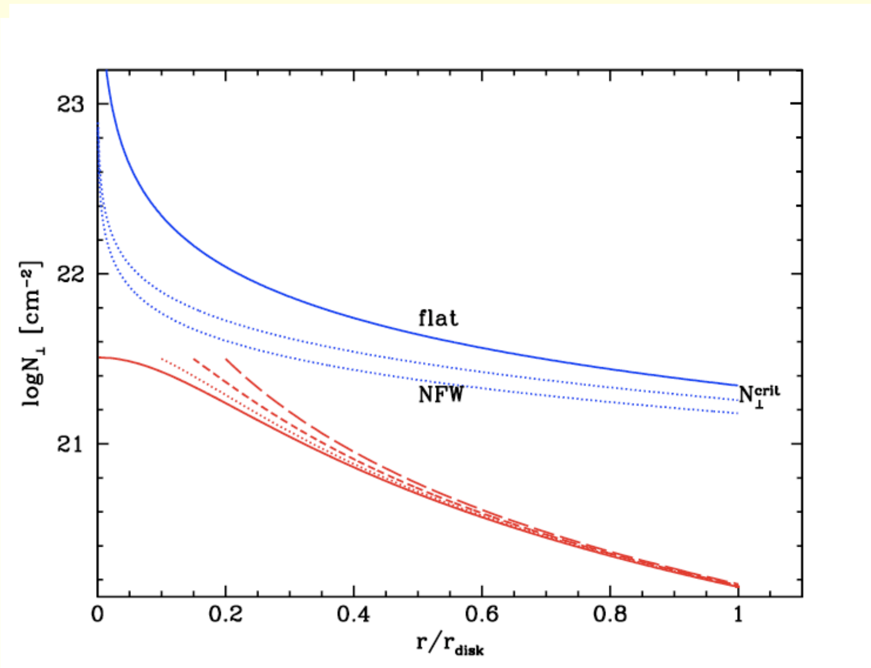

- $N^{crit}_\perp \propto \kappa\sigma$
- $\kappa \propto (G\rho)^{1/2}$ (epicyclic freq.)
- $N^{crit}_\perp \propto (1+z)^{3/2}$
- Neutral Gas Subcritical

(2) But DLA disks may be sub-critical (Toomre stable)

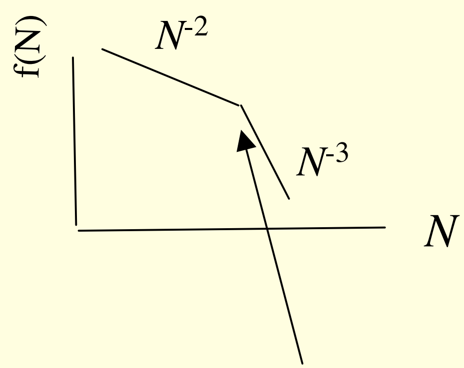

- $f(N)$ exhibits break at $N_{\mathrm{break}}=10^{21.5}\,\mathrm{cm}^{-2}$. If DLAs are randomly oriented disks, N_{break} equals maximum $N_{\perp}$.

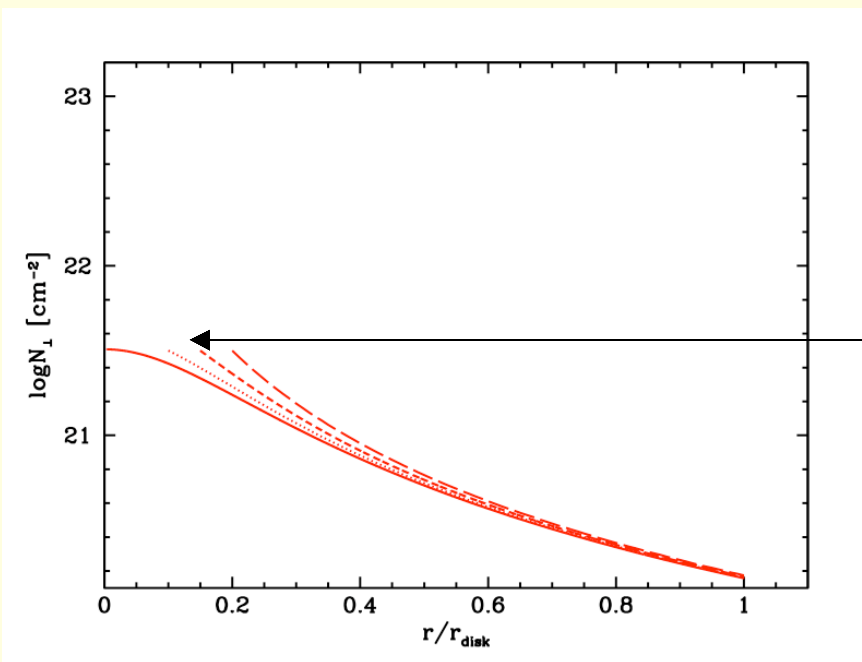

- Infer $N_{\perp}$ versus r from f(N)

N_{break}

Identifying Galactic Gas in Absorption Against Quasars

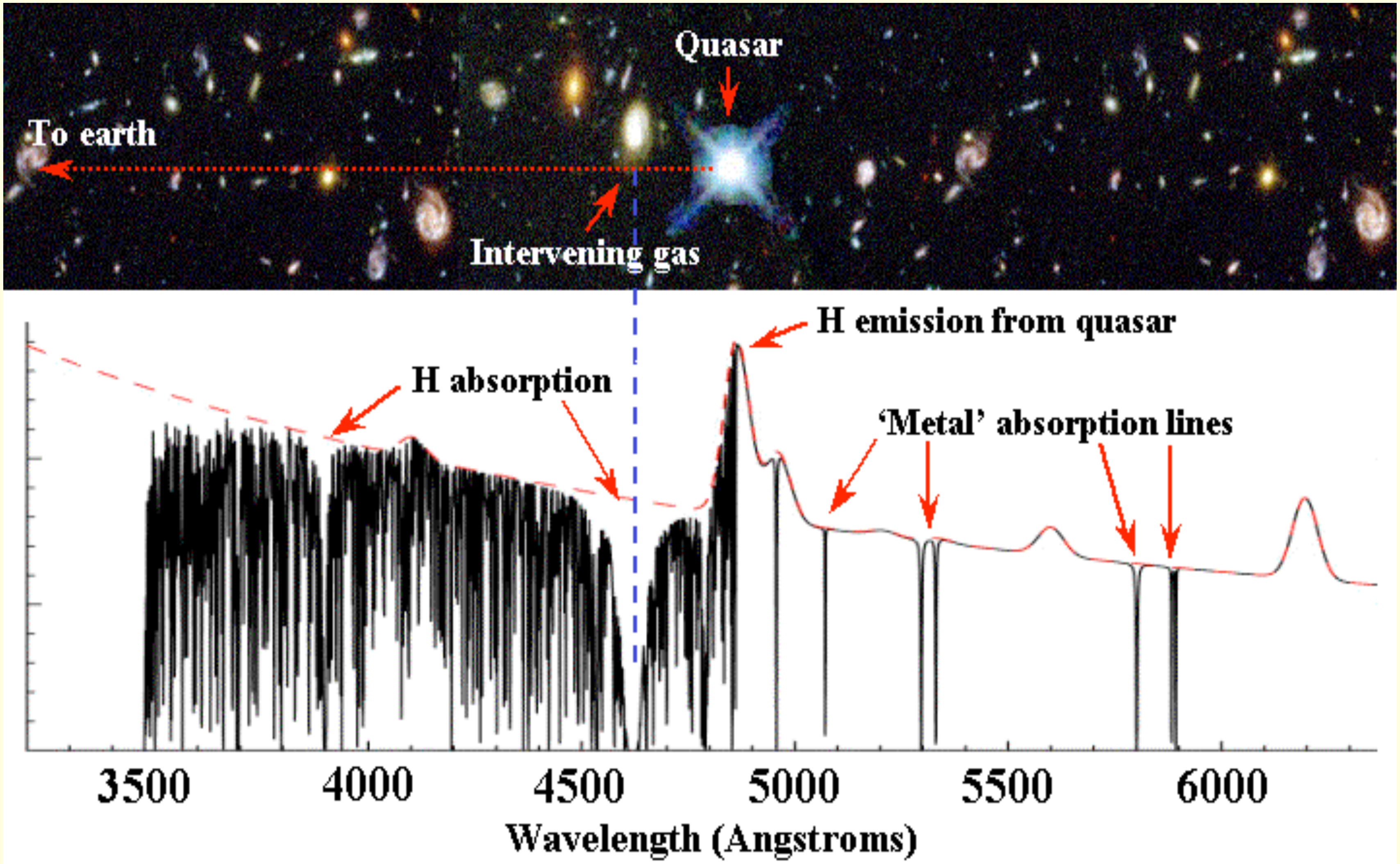

- Absorption-line Strength Independent of Galaxy Luminosity

(2) But DLA disks may be sub-critical (Toomre stable)

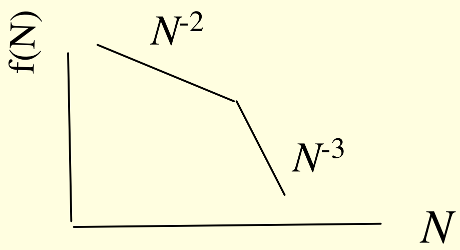

• *f(N)* exhibits break at $N_{break}=10^{21.5}$ cm^{-2} . If DLAs are randomly oriented disks, N_{break} equals maximum $N_{\perp}$.

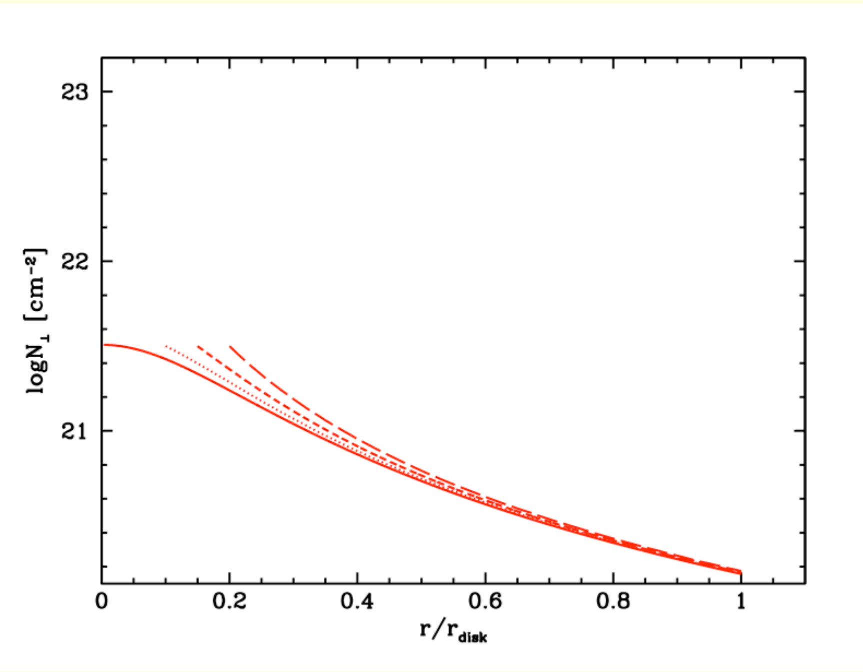

•Infer $N_{\perp}$ versus r from f(N)